Technical Report Documentation Page

1. Report No.	2. Government Accession No.	3. Recipient's Catalog No.
FHWA/TX-05/0-4518-1 Vol. 1		

4. Title and Subtitle	5. Report Date
DESIGN PROCEDURE FOR PAVEMENTS ON EXPANSIVE SOILS: VOLUME 1	October 2004 Resubmitted: August 2005
7. Author(s)	8. Performing Organization Report No.
Robert Lytton, Charles Aubeny, and Rifat Bulut	Report 0-4518-1
9. Performing Organization Name and Address Texas Transportation Institute The Texas A&M University System College Station, Texas 77843-3135	10. Work Unit No. (TRAIS) 11. Contract or Grant No. Project No. 0-4518
12. Sponsoring Agency Name and Address Texas Department of Transportation Research and Technology Implementation Office P. O. Box 5080 Austin, Texas 78763-5080	13. Type of Report and Period Covered Technical Report September 2002 - August 2004 14. Sponsoring Agency Code

15. Supplementary Notes

Research performed in cooperation with the Texas Department of Transportation and the U.S. Department of Transportation, Federal Highway Administration
Research Project Title: Re-evaluate Current Potential Vertical Rise (PVR) Design Procedures

16. Abstract

Swelling and shrinkage of sub-grade soils are critical factors contributing to increases in roughness and degradation of serviceability of highway pavements. Existing procedures for predicting swell are largely based on the potential vertical rise (PVR) procedure developed by McDowell in 1956. While the PVR procedure represents a major development in the design of pavements on expansive soils, instances of apparently over-conservative PVR predictions have led some designers to suggest revision or replacement of the existing procedure. This project reviews the basic assumptions of the existing PVR procedure and identifies the likely sources of the questionable predictions that have arisen in the past. An alternative procedure is presented that features rigorous modeling of both the moisture diffusion process that induces changes in suction within a soil mass and the deformations that occur in response to changes in suction. This alternative procedure includes provisions for measuring and/or estimating soil and environmental input parameters necessary for the predictions. A procedure for predicting the impact of soil deformations on pavement performance is also presented. The proposed procedure is applied to three study sections involving Texas roadways on expansive soils, and parametric studies are presented evaluating the effectiveness of various design measures including moisture barriers, lime treatment, and replacement of in situ sub-grade soils with "inert" soils.

17. Key Words	18. Distribution Statement
Soil Mechanics, Expansive Soils, Pavement Design, Pavement Roughness, Pavement Serviceability	No restrictions. This document is available to the public through NTIS: National Technical Information Service Springfield, Virginia 22161 http://www.ntis.gov

19. Security Classif.(of this report)	20. Security Classif.(of this page)	21. No. of Pages	22. Price
Unclassified	Unclassified	198	

Form DOT F 1700.7 (8-72) **Reproduction of completed page authorize**

DESIGN PROCEDURE FOR PAVEMENTS ON EXPANSIVE SOILS.

by

Robert Lytton
Professor
Texas A&M University

Charles Aubeny
Assistant Professor
Texas A&M University

Rifat Bulut
Post-Doctoral Research Associate
Texas Transportation Institute
Texas A&M University

Report 0-4518-1 Vol. 1
Project Number 0-4518
Research Project Title: Re-evaluate Current Potential Vertical Rise (PVR) Design Procedures

Performed in cooperation with
Texas Department of Transportation
and the
U.S. Department of Transportation
Federal Highway Administration

October 2004
Resubmitted: August 2005

TEXAS TRANSPORTATION INSTITUTE
The Texas A&M University System
College Station, Texas 77843-3135

DISCLAIMER

The contents of this report reflect the views of the authors, who are responsible for the facts and the accuracy of the data presented herein. The contents do not necessarily reflect the official view or policies of the Federal Highway Administration (FHWA) or the Texas Department of Transportation (TxDOT). This report does not constitute a standard, specification, or regulation. The engineer in charge was Robert Lytton, P.E., (Texas, # 27657).

ACKNOWLEDGMENTS

This project was conducted in cooperation with TxDOT and FHWA. The authors would like to express their appreciation to Program Coordinator Elias Rmeili, P.E, and Project Director Richard Williammee, P.E, from the Texas Department of Transportation, for their support and assistance throughout this project. The authors thank the members of the Project Monitoring Committee: Mark McDaniel, Darlene Goehl, P.E, Jamshid Shirali, David Fowler, Andrew Wimsatt, Ph. D., P.E, James Knight, P.E and Gary Williams, P.E. Finally, the authors would like to acknowledge the contributions of Texas A&M University graduate research assistants Gyeong Taek Hong, Xiaoyan Long, Eeshani Sood, and Anshuman Thakur.

TABLE OF CONTENTS

LIST OF FIGURES

Page

LIST OF TABLES

CHAPTER 1:
INTRODUCTION

This research evaluates the existing Texas Department of Transportation (TxDOT) procedure Tex-124-E, "Method for Determining the Potential Vertical Rise, PVR" [1]. The research also highlights the comprehensive framework developed at Texas A&M University (TAMU), for predicting the roughness that is developed in a pavement over a period of time due to swelling and shrinkage of expansive clays. TTI Research Report 1165-2F entitled "Effectiveness of Controlling Pavement Roughness Due to Expansive Clays with Vertical Moisture Barriers" [2] provides much of the groundwork for the TAMU approach. Using the methodology developed, this report compares the predicted values of the vertical movement, calculated using both the existing TxDOT method and the method developed by the studies conducted at Texas A&M.

The Texas Department of Transportation has been a leader in the study and implementation of practical methods of anticipating the roughness that will develop in pavement surfaces due to the change of moisture in the expansive clay subgrade. In a landmark paper that was written by Chester McDowell and published in the Proceedings of the Highway Research Board (HRB) in 1956[3], a method was described by which the total swelling movement of expansive clay profile could be predicted. TxDOT took the results of this paper and built the standard specification Tex-124-E with it, adding several refinements along the way to the present version.

In the original report that was published in 1956, McDowell suggested that these movements could be reduced by moisture control, pre-wetting, or by removing and replacing some of the expansive soils near the surface of the subgrade. The paper and its discussions appeared on pages 754 to 772 of that year's HRB Proceedings [3]. In putting together this method, McDowell made several assumptions, all of which were necessary in order for the method to be implemented in the practical day-to-day operations of the Department. In the text of the paper, he acknowledged some of the limitations of his method. For example, he noted, "vertical volume change of soils in deep cuts and under certain types of structures will be greater than that shown", and he later noted that "... cuts in marls and clays usually heave more than other sections because of their low moisture contents." As a first attempt at putting some rational order into the process of engineered design of pavements on expansive clay, it was recognized by

those who discussed the paper as being a very good synthesis of what was known at the time. Most practical engineers realize that McDowell intended that the Potential Vertical Rise (PVR) procedure should be used as an index of the potential activity of a pavement subgrade and they use it that way.

During the last two decades, significant advances have been made in the method for predicting the swelling and shrinkage of expansive soil. In 1977, Lytton [4] presented a method of estimating the volume change with depth based upon the initial and final suction values, the mean principal stress at all depths, and logarithmic compression coefficients of the soil for changes of both suction and mechanical pressure. Mitchell and Avalle [5] used an approach that had originated in Australia, which used a logarithmic compression coefficient and the change of the logarithm of suction at all depths to estimate the surface movement of the expansive soil. This works only in shallow depths where the overburden pressures do not suppress much of the volume change due to the change of suction. Gay [6] and Jayatilaka [7] both used Lytton's approach in predicting the roughness of pavements on expansive clay. Finally, Lytton summarized all of the developments and presented a complete method of predicting heave and shrinkage vertically and horizontally with time using suction[8,9]. The method presented in this report is the culmination of the nearly two decades of effort by the TxDOT, the Texas Transportation Institute, and various other institutes.

OVERVIEW OF EXISTING PVR PROCEDURE

The current PVR method is based upon the work of McDowell [3] in which he made five assumptions. A proper re-evaluation of the PVR method requires revisiting and reviewing each of the five assumptions.

A summary of these assumptions is listed below.

1. Soil at all depths has access to water in capillary moisture conditions (pp. 755, 756, 764).
2. Vertical swelling strain is one-third of the volume change at all depths (pp. 755, Fig. 1).
3. Remolded and compacted soils adequately represent soils in the field (pp. 757).
4. PVR of 0.5 inch produces unsatisfactory riding quality (pp. 760).
5. Volume change can be predicted by use of the plasticity index alone (P. 763, Fig. 11).

Making use of these assumptions, McDowell worked out the Potential Vertical Rise of several hypothetical soil profiles with different amounts of volumetric swell. The results of these calculations are tabulated below in Table 1 and illustrate the effect of the combination of the five assumptions listed above.

Table 1. PVR of Sites with 18-inch Thick Pavement.

Page	Table	% Volumetric Swell	Depth of Swell (ft)	PVR (in)
758	2	35.0	82.1	24.09
759	3	25.0	58.6	11.77
759	4	22.5	52.8	9.67
760	5	15.0	33.9	3.71
760	6	7.5	16.7	0.77

(Figures in the above table were extracted from McDowell's 1956 HRB paper[3] on the pages and tables cited.)

The above assumptions lead to the conclusion that by following this procedure, soil can be expected to swell to a depth greater than 82 ft, even allowing for the suppression of the swell by the effect of the overburden pressure and the weight of the pavement. This is a direct result of **Assumption 1**, that soil at all depths has access to water under capillary moisture conditions. However, soil at all depths does not have access to moisture in the capillary condition. In a consulting report [10] in and a paper in the 4th International Conference on Expansive Clays [11], Mitchell showed how the diffusion coefficient, alpha, can be measured using undisturbed shelby tube samples and how this value can be used to predict the transient changes of suction beneath a covered area like a pavement or a foundation. The determination of the alpha diffusion coefficient permits an estimate of the rate at which water will move into the soil both vertically and horizontally. It is also used to estimate the depth of the moisture active zone. The relations between the horizontal extent of the moisture zone and the alpha-value are given in the TTI Report 1165-2F [2] on page 58 and will not be repeated here.

In **Assumption 2,** vertical swelling strain is assumed to be one-third of the volume change at all depths. This assumption is unrealistic, especially at greater depths, due to high confining pressure. At these depths, the vertical swelling strain can be as high as the volumetric strain. If it were not for Assumption 2, the PVR figures would be three times higher than those in the table above. This leads to questions of the effects of Assumptions 3, 4, and 5.

Assumption 3 is that remolded and compacted soils adequately represent soils in the field. However, from actual observation it is found that the volume change characteristics of

undisturbed soils are distinctively different than the remolded and compacted soils used by McDowell in developing his method. There is a very large database of such characteristics for over 100,000 soil samples from all over the United States that was developed over the last three decades by the U.S. Department of Agriculture's Natural Resources Conservation Service. A set of volume change coefficient charts was developed from this database and published in a paper by Covar and Lytton in ASCE Geotechnical Special Publication No. 115 [12], which is a written record of the presentation that was made at the Houston National ASCE Convention in October 2001[13]. The data are for undisturbed clods of soil taken from the ground and tested in their natural state with all of the cracks, roots, and wormholes as occur in the field. It turns out that accurate estimates of the volume change coefficient requires measurements of the liquid limit (LL), the plasticity index (PI), the percent of soil particles passing the #200 sieve, and the percentage of soil particles finer than 2 microns. All of these are standard geotechnical tests. In the process of constructing these charts, the work of Covar and Lytton confirmed the earlier work of Professor Casagrande [14], who located where the expansive minerals would fall on the plasticity chart. Some of these minerals have PI less than 15, namely chlorite and halloysite. This finding implies that **Assumption 5** is inadequate.

Concerning **Assumption 4,** the multiple year study of the roughness of pavements on expansive clay subgrade that researchers conducted at the Texas Transportation Institute showed that the sum of the *shrinking* and *swelling* movements at a point beneath a pavement surface is related not to the pavement roughness, but to the *rate* at which roughness develops. Because this conclusion is based upon monitoring pavements all over Texas for periods ranging from 3 to 15 years, the result is not in doubt. These results were reported in TTI Research Report 0-1165-2F (Jayatilaka, Gay, Lytton, and Wray) titled "Effectiveness of Controlling Pavement Roughness Due to Expansive Clays with Vertical Moisture Barriers" [2]. In the process, the researchers developed a way to both measure and predict the maximum bump height on the pavement that was based on the thousands of pavement profile data points that were collected and analyzed in the monitoring process. Both the measured and predicted bump height for serviceability indexes between 2.5 and 4.0 was in the range between 0.5 and 1.0 inch (12 to 25 mm) for all pavements. A bump is not the total movement, such as PVR, but instead is a *differential* movement and it is this movement that causes pavement roughness.

In reviewing the assumptions that underlie the PVR method, it is seen that Assumptions 1 and 2, which form the core of the PVR method of Tex-124-E, are not realistic as they are not based on sound analytical principal. Furthermore, Assumptions 3, 4, and 5 cannot be supported by subsequent findings on actual Texas pavements and on the soils of the United States. Therefore, it is suggested that Tex-124-E "Method for Determining the Potential Vertical Rise, PVR" [1] be replaced by a more robust method based on sound rational principal such as the one developed at Texas A&M University.

OVERVIEW OF TAMU SUCTION BASED PROCEDURE

The prediction of movement in expansive soil is important principally for the purpose of designing foundations and other ground supported structural elements such as pavements. In design, the principal interest is in making an accurate estimate of the range of movements that must be sustained by the foundation. It is for this reason that envelopes of maximum heave or shrinkage are important for design purpose.

There are three categories of methods of predicting movements in expansive clays: oedometer, empirical, and suction methods. The oedometer methods basically use the consolidation theory in reverse and are based on determining a swelling property of the soil by one of two tests: the constant volume or swell-pressure test and the consolidation-swell test. Objective studies of these methods (e.g., Osman and Sharief, 1987 [15] and Dhowian et al., 1987 [16]) show that the oedometer methods always overpredict the in situ heave except in those rare cases where the capillary moisture conditions are met in the field as in the case where high water tables are present on the site.

The empirical or semi-empirical methods are based on a correlation between laboratory or field measurements and soil indices such as the liquid limit, plasticity index, and clay content. There are large numbers of these empirical relations in the literature, but all are hampered by having been developed locally and, thus, are not applicable except in their locale of origin. McDowell's method, which has been incorporated into the Tex-124-E specification, is another empirical method and the discussion presented above shows its shortcomings. In general, empirical relations all suffer from the same limitations of being confined to their locale of origin and having to rely upon an assumed final moisture condition. These limitations apply to both laboratory samples and to field measurements.

The methods using soil suction have the distinct advantage of using the moisture energy for predicting the heave and shrinkage of soil. Movements in expansive soils are generated by change of suction that is brought about by entry or loss of moisture. The volume change depends upon the total stress states that surround the soil. The following section details the philosophy behind the method and then outlines the comprehensive framework developed at Texas A&M University for predicting the movement of expansive soil based on changes of suction.

CONSTITUTIVE EQUATIONS FOR VOLUME CHANGE IN EXPANSIVE SOIL

The comprehensive framework developed at Texas A&M University for predicting the differential movement of expansive soil based on change of suction finds its roots in the early work carried out by Juarez-Badillo [17, 18]. It may be mentioned that Juarez-Badillo successfully predicted the expansion and settlement characteristics of highly compressible Mexico City clays based on his theory of natural limits.

The natural limits in this process are mean principal stress, suction, and volume (Figure 1). Under conditions of zero mechanical pressure and suction, the soil reaches its maximum volume, Vo; under conditions of zero suction and infinite mechanical mean principal stress, the soil volume compresses to the volume of the solids alone, Vs; and under conditions of zero mean principal stress and infinite suction, the soil volume compresses to the dry volume, Vd, in which the dry soil contains a volume of air-filled voids. For small increments of volume change on the volume–mean principle stress-suction surface (Figure 2), $\Delta V/V$ is linearly related to the logarithms of the mechanical pressure and suction components.

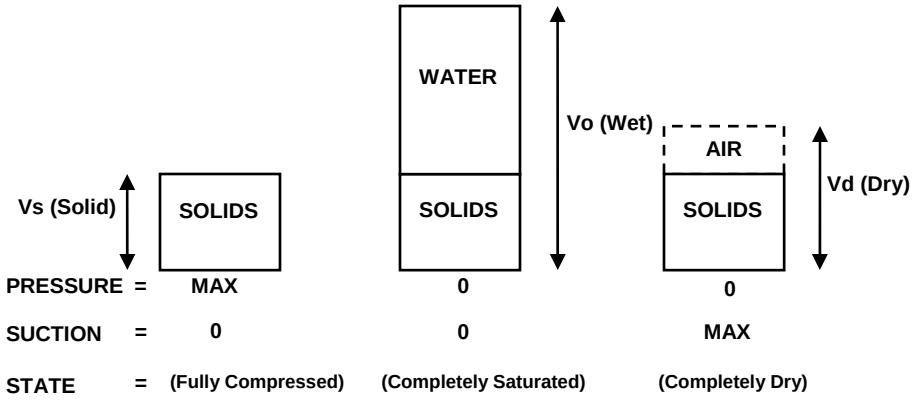

Figure 1. Natural Limits of Volume Change Process in Unsaturated Soils.

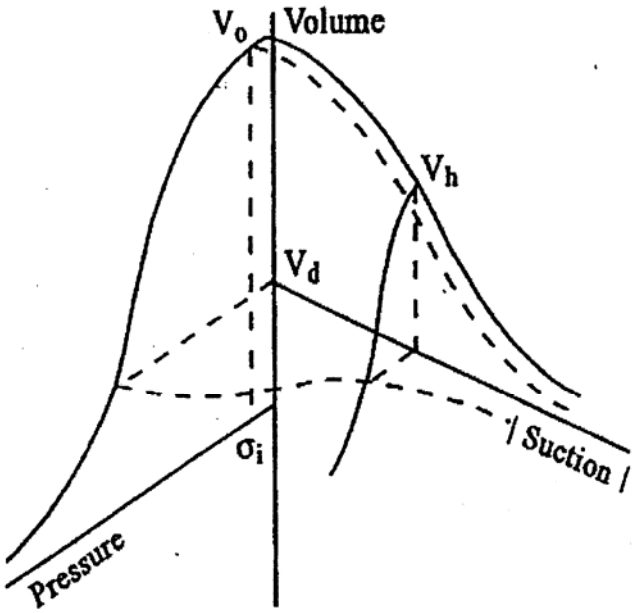

Figure 2. The Volume–Mean Principal Stress-Suction Surface.

In general, the relation between these components and a change in osmotic suction, π is:

$$\frac{\Delta V}{V} = -\gamma_h \log_{10}\left(\frac{h_f}{h_i}\right) - \gamma_\sigma \log_{10}\left(\frac{\sigma_f}{\sigma_i}\right) - \gamma_\pi \log_{10}\left(\frac{\pi_f}{\pi_i}\right) \qquad (1)$$

where:

$\frac{\Delta V}{V}$ = the volume strain

h_i, h_f = the initial and the final values of matric suction

σ_i, σ_f = the initial and the final values of mean principal stress

π_i, π_f = the initial and the final values of osmotic suction

γ_h = the matric suction compression index

γ_σ = the mean principal stress compression index

γ_π = the osmotic suction compression index

The mean principal stress compression index, γ_σ, is related to the commonly used compression index, C_c, by:

$$\gamma_\sigma = \frac{C_c}{1+e_o} \quad \left(\text{refer to } \frac{\Delta \mathrm{V}}{\mathrm{V}} = \frac{C_c}{1+e} \log \frac{\sigma_f}{\sigma_i} = \gamma_\sigma \log \frac{\sigma_f}{\sigma_i} \right) \tag{2}$$

where:

e_o = the void ratio

In order to predict the total movement in a soil mass, initial and final values of the matric suction, osmotic suction, and mean principle stress profiles with depth must be known.

It is the change of matric suction that generates the heave and shrinkage, while osmotic suction rarely changes appreciably, and the mean principal stress increases only slightly in the shallow zones where most of the volume change takes place. It is commonly sufficient to compute the final mean principal stress, σ_f, from the overburden, surcharge, and foundation pressure and treat the initial mean principal stress, σ_i, as a constant corresponding to the stress-free suction-versus-volume strain line. Because there is no zero on a logarithmic scale, σ_i may be regarded as a material property, i.e., a stress level below which no correction for overburden pressure must be made in order to estimate the volume strain. It has been found to correspond to the mean principal stress at a depth of 80 cm.

The mean principal stress is estimated by:

$$\sigma = \frac{1+2K_o}{3}\sigma_z \tag{3}$$

where:

σ_z = the vertical stress at a point below the surface in the soil mass

K_0 = the lateral earth pressure coefficient

The lateral earth pressure coefficient, K_0, is given by:

$$K_0 = e\left(\frac{1-\sin\phi'}{1+\sin\phi'}\right)\left(\frac{1+d\sin\phi'}{1-k\sin\phi'}\right)^n \tag{4}$$

Values of the coefficients e, d, k, and n for different soil conditions are given in Table 2. With an active soil, which can crack itself in shrinking and generate large confining pressures in swelling, the lateral earth pressure coefficient, K_o, can vary between 0.0 and passive earth pressure levels. Typical values that have been back-calculated from field observations of heave and shrinkage are given in Table 2:

Table 2. Typical Values of Lateral Earth Pressure Coefficient for Several Different Conditions.

Conditions	K_o	e	d	k	n
Cracked	0	0	0	0	1
Drying (Active)	1/3	1	0	0	1
Equilibrium (at rest)	1/2	1	1	0	1
Wetting (within movement active zone)	2/3	1	1	0.5	1
Wetting (below movement active zone)	1	1	1	1	1
Swelling near surface (passive earth pressure)	3	1	1	1	2

The regression equation between the angle of internal friction, ϕ', and plastic index, PI, based on the empirical correlation (Figure 3) from the triaxial compression tests is given by:

$$\phi' = 0.0016PI^2 - 0.3021PI + 36.208 \tag{5}$$

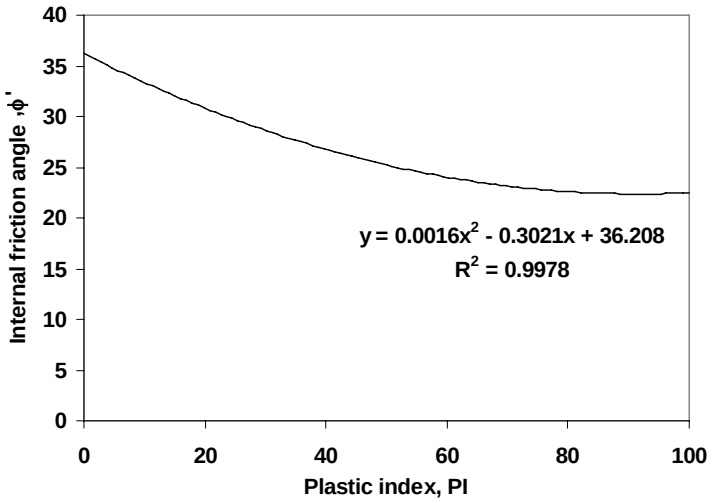

Figure 3. The Regression Equation based on the Relation on the Empirical Correlation between ϕ' and PI. (after Holtz and Kovacs, 1981 [19])

The vertical strain is estimated from the volume strain by using a crack fabric factor *f*:

$$\frac{\Delta H}{H} = f\left(\frac{\Delta V}{V}\right) \tag{6}$$

where:

$\frac{\Delta H}{H}$ = the vertical strain

$f = 0.67 - 0.33\,\Delta pF$ ($\Delta pF =$ the change of suction, $1/3 \le f \le 1.0$)

Back-calculated general values of *f* are 0.5 when the soil is drying and 0.8 when the soil is wetting. The level to which the lateral pressure rises is limited by the Gibbs free energy (suction) released by the water; the level to which it drops on shrinking is limited by the ability of the water phase to store released strain energy. The total heave or shrinkage in a soil mass is the sum of the products of the vertical strains and the increment of depth to which they apply, Δz_i.

$$\Delta H = \sum_{i=1}^{n} f\left(\frac{\Delta V}{V}\right)_i \Delta z_i \tag{7}$$

where:

$$
\begin{aligned}
n &= \text{the number of depth increments} \\
\Delta z_i &= \text{the i}^{\text{th}}\text{ depth increment} \\
f &= \text{the crack fabric factor} \\
\left(\frac{\Delta \mathrm{V}}{\mathrm{V}}\right)_{i,swelling} &= -\gamma_h \log\left(\frac{h_f}{h_i}\right) - \gamma_\sigma \log\left(\frac{\sigma_f}{\sigma_i}\right) \\
\left(\frac{\Delta \mathrm{V}}{\mathrm{V}}\right)_{i,shrinkage} &= -\gamma_h \log\left(\frac{h_f}{h_i}\right) + \gamma_\sigma \log\left(\frac{\sigma_f}{\sigma_i}\right)
\end{aligned}
$$

ESTIMATING SOIL SWELLING PARAMETERS FROM INDEX PROPERTIES

The principal material property needed to compute the vertical movement is the suction compression index, γ_h. Historically, this has been estimated with the chart developed by McKeen (1981) [20], shown in Figure 4. The two axes are given by the activity ratio, A_c, and the cation exchange activity ratio, CEA_c, which are defined as follows:

$$A_c = \frac{PI\%}{\frac{\%-2micron}{\%-No.200sieve}\times 100} \tag{8}$$

where:

$PI\%$ = the plastic index in percent

$$CEA_c = \frac{CEC\,\frac{milli\,equivalents}{100gm\,of\ dry\,soil}}{\frac{\%-No.2\,micron}{\%-No.200\,sieve}\times 100} \tag{9}$$

where:

CEC = the cation exchange capacity in milliequivalents per 100 gm of dry soil

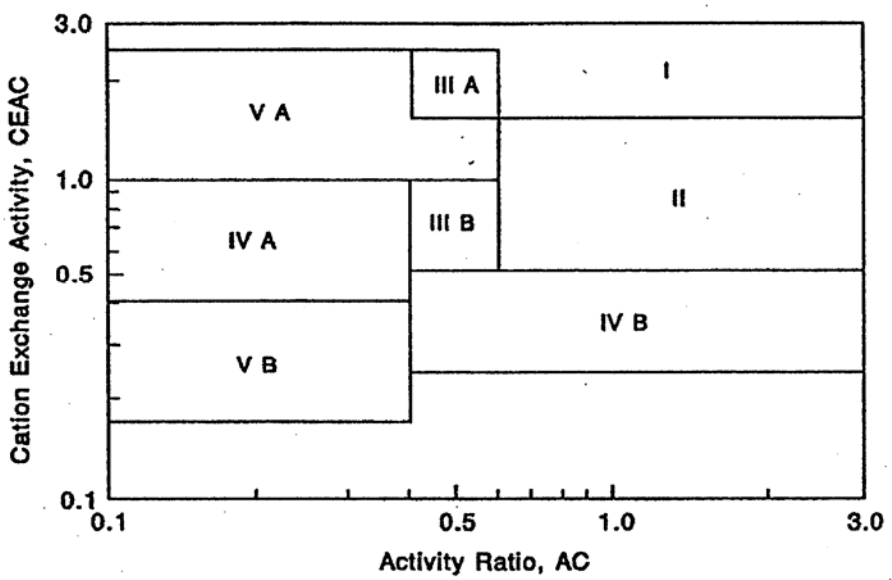

Figure 4. Chart for Prediction of Suction Compression Index Guide Number. (Mckeen, 1981[20])

The denominator of both activity ratios is known as the "percent fine clay" and represents that percent of the portion of the soil which passes the No. 200 sieve and is finer than 2 microns.

The cation exchange capacity (CEC) may be measured with a spectrophotometer or it may be estimated with sufficient accuracy by the following equation that was developed by Mojeckwu [21].

$$CEC \cong (LL\%)^{0.912} \tag{10}$$

The regions on the chart each have a volume change guide number corresponding to the suction compression index of a soil with 100 percent fine clay. Values of the guide numbers are given in Table 3. The actual suction compression index is proportional to the actual percent of fine clay in the soil. Thus, the actual γ_h is:

$$\gamma_h = \gamma_o \times \left[\frac{\%-2\,micron}{\%-No.200\,sieve} \right] \tag{11}$$

Table 3. Values for a Soil with 100% Fine Clay Content.

Region	Volume Change γ_0 Guide Number
I	0.220
II	0.163
IIIA	0.096
IIIB	0.061
IVB	0.061
VA	0.033
VB	0.033

The mean principal stress compression index, γ_σ, is related to γ_h by the following equation:

$$\gamma_\sigma = \gamma_h \frac{1}{1 + \frac{h}{\theta\left(\frac{\partial h}{\partial \theta}\right)}} \tag{12}$$

where:

θ = the volumetric water content

$\frac{\partial h}{\partial \theta}$ = the slope of the suction-versus-volumetric water content curve (Figure 5)

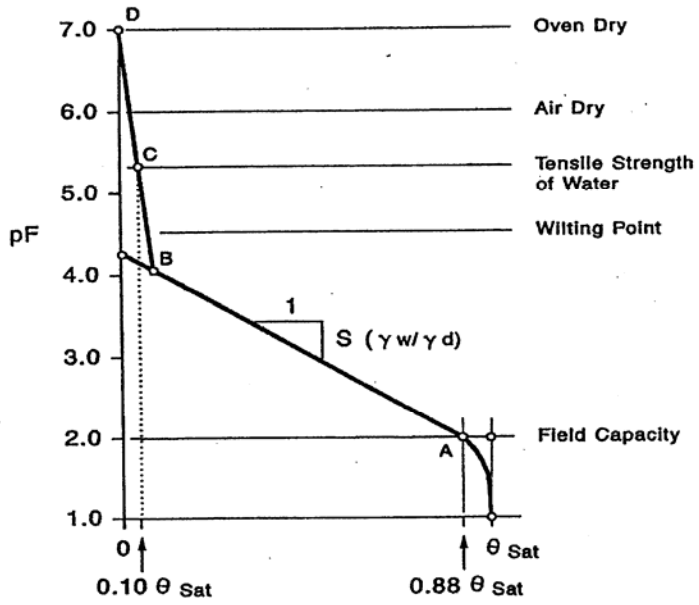

Figure 5. Suction-versus-Volumetric Water Content Curve.

The slope of the suction-versus-volumetric water content curve is given by:

$$\left[\frac{\partial h}{\partial \theta}\right] = \frac{1}{0.4343}\frac{S\gamma_w}{\gamma_d}h \tag{13}$$

The value of S is negative and can be estimated from:

$$S = -20.29 + 0.1555(LL) - 0.117(PI) + 0.0684(-\#200) \tag{14}$$

where:

LL = the liquid limit in percent

PI = the plasticity index in percent

$-\#200$ = the percent of soil passing the #200 sieve.

Because both S and h are negative, the slope is inherently positive. The correction term in the relation between γ_h and γ_σ given in Equation (11) is found by:

$$\frac{h}{\theta\left[\frac{\partial h}{\partial \theta}\right]} = \frac{0.4343}{Sw} \tag{15}$$

where:

w = the gravimetric water content

Because S is negative, so is the correction term. An approximate suction (pF)-versus-volumetric water content curve can be constructed with the empirical relationships given above and the saturated volumetric water contents given in Table 4. The construction is illustrated in Figure 5. First, point A is located at the intersection of the field capacity volumetric water content ($=0.88\theta_{sat}$) and a pF of 2.0. Second, a line with a slope of $S\left(\gamma_w/\gamma_d\right)$ is drawn from point A to its intersection with the vertical axis. Third, point C is located at a volumetric water content of $0.10\theta_{sat}$ and the tensile strength of water (pF=5.3 or 200 atmospheres). Fourth, point D is located at zero water content and a pF of 7.0, corresponding to oven dry. Fifth, a straight line is drawn between points C and D to its intersection with the first line.

This construction makes it possible to estimate water contents once the computed suction profiles are known. This allows measured water contents to be compared with the predicted values.

Table 4. Range of Saturated Volumetric Water Content by Unified Soil Classification System. (Mason et al., 1986) [22]

Unified Class	Ranges of θ_{sat}
GW	0.31-0.42
GP	0.20
GM	0.21-0.38
GM-GC	0.30
SW	0.28-0.40
SP	0.37-0.45
SM	0.28-0.68
SW-SP	0.30
SP-SM	0.37
SM-SC	0.40
ML	0.38-0.68
CL	0.29-0.54
ML-CL	0.39-0.41
ML-OL	0.47-0.63
CH	0.50
θ_{sat} = n (porosity)	

ESTIMATING SOIL SWELLING PARAMETERS BASED ON LL AND PI

The method developed herein represents a refinement of earlier methods. The method builds on these earlier methods in that it is consistent in the use of low cost and easily available testing methods (Atterberg limits and soil particle size distributions) to predict soils properties and behavior. It has been published in the ASCE Geotechnical Special Publication No. 115 (Covar and Lytton) [12].

This method was developed based on the soil data of the Soil Survey Laboratory (SSL) of the National Soil Survey Center. Most of the data in the present database were obtained over the last 40 years with approximately 75 percent of the data being obtained in the last 25 years. The SSL database may be accessed online at http://www.statlab.iastate.edu/soils/ssl. The database is also available on CD-ROM from the SSL.

For this study, the researchers filtered the SSL database to retain only those records that contained non-null results for the following tests:

- liquid limit,
- coefficient of linear extensibility,
- plasticity index,
- percent passing 2 micron,
- plastic limit,
- percent passing No. 200 sieve,
- cation exchange capacity.

This data filtering produced a subset of the data containing approximately 6500 records (Figure 6). Next, the data records were partitioned based on Casagrande [14] and the Holtz and Kovacs [19] mineral classification (Figure 7). This partitioning step resulted in eight separate data groups, each representing a group with some mineralogical similarity.

The method is “stable” in the sense that each mineralogical zone or group is explicitly defined; thus, no arbitrary distinctions can affect the results. Within each group, the practitioner needs only the liquid limit, plasticity index, and the fine clay fraction (%) to get an estimate of the soil compression index (Figure 8 to 15). The soil compression index can then be explicitly entered into Equation (2) to calculate shrink and swell behavior. Small changes in soil index properties result in small changes in the derived soil compression index within each

mineralogical based group. The proposed method, therefore, provides a quick and stable prediction of an important soil property using low cost and commonly available soil test procedures.

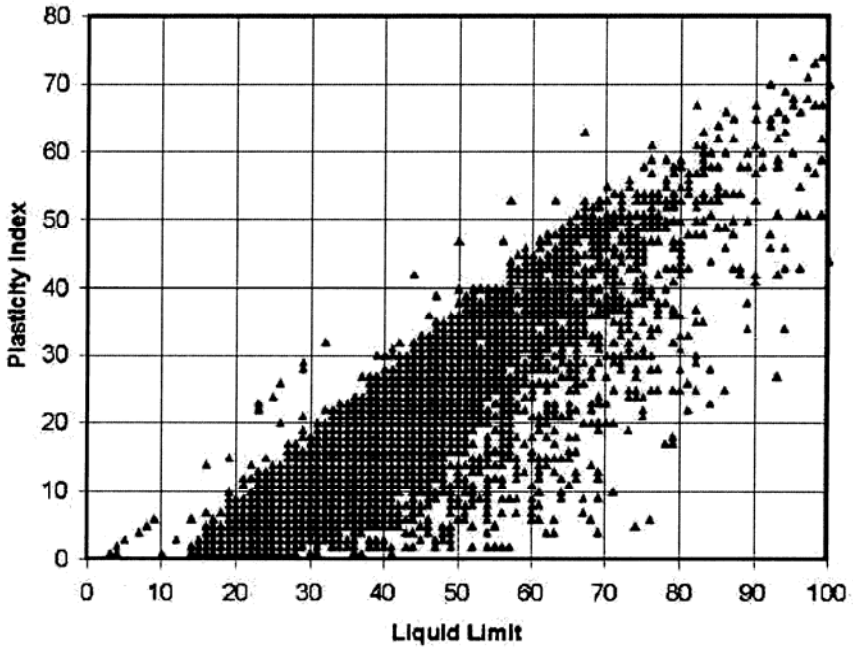

Figure 6. Data Set (6500 records) for Soil Compression Index Calculations.

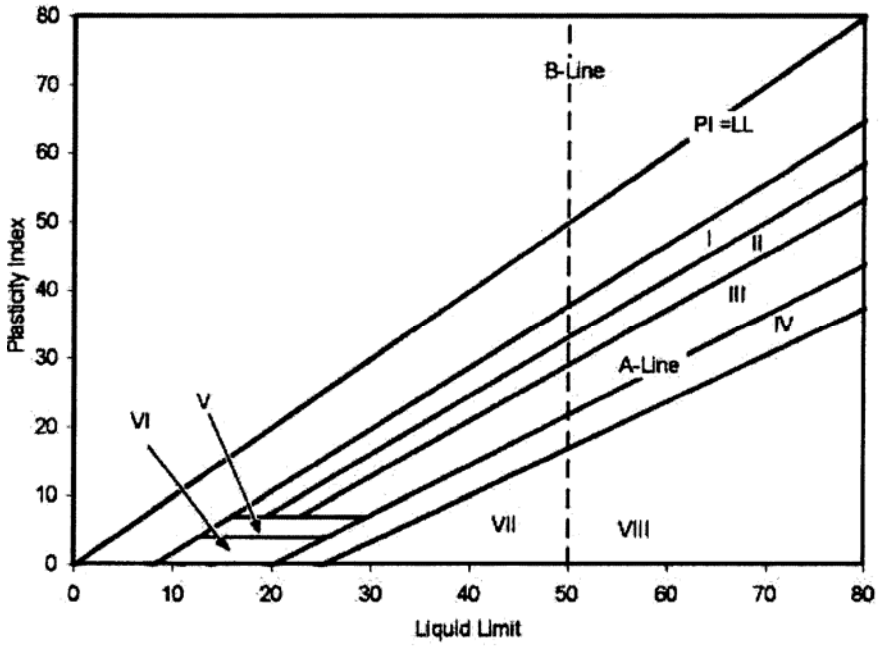

Figure 7. Data Filter for Partitioning Database on Mineralogical Types. (after Casagrande (1948) and Holtz and Kovacs (1981) [14, 19]).

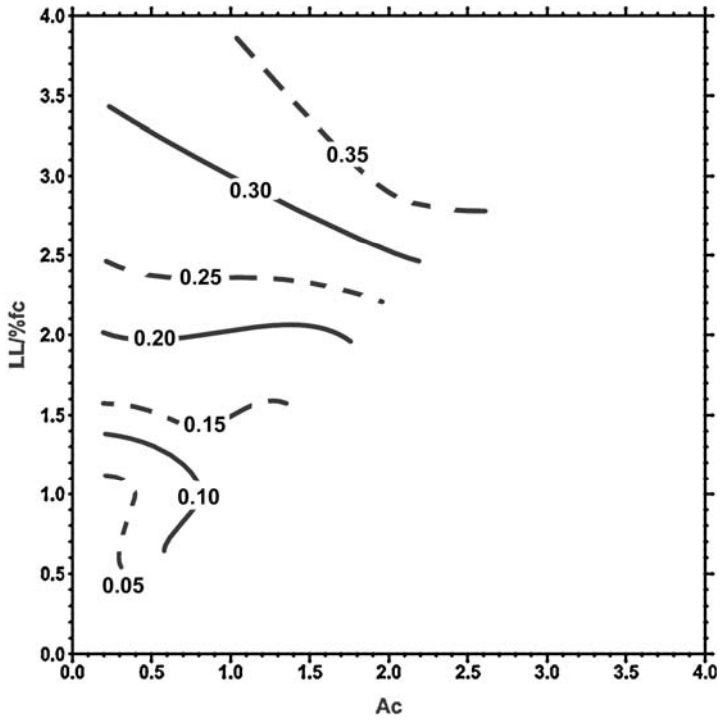

Figure 8. Zone I Chart for Determining γ_o. (Covar and Lytton, 2001).[12]

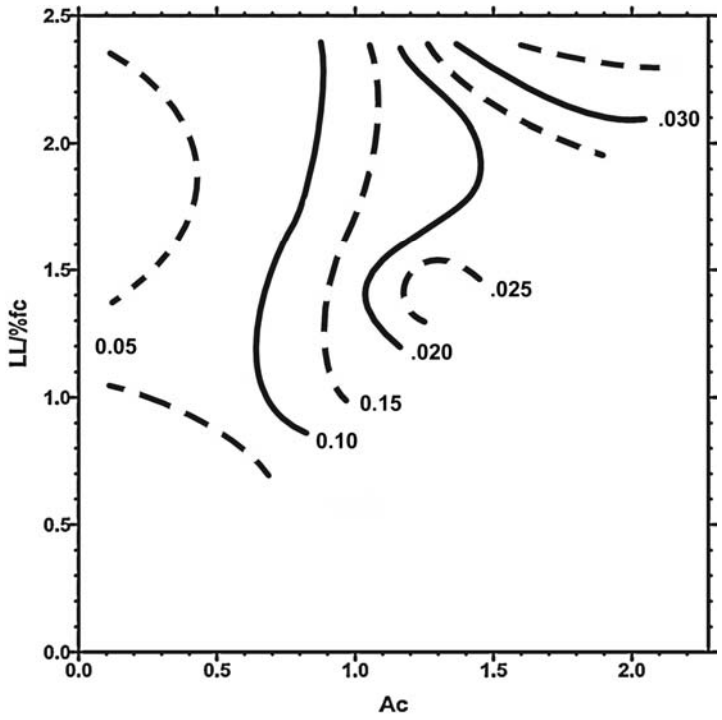

Figure 9. Zone II Chart for Determining γ_o. (Covar and Lytton, 2001).[12]

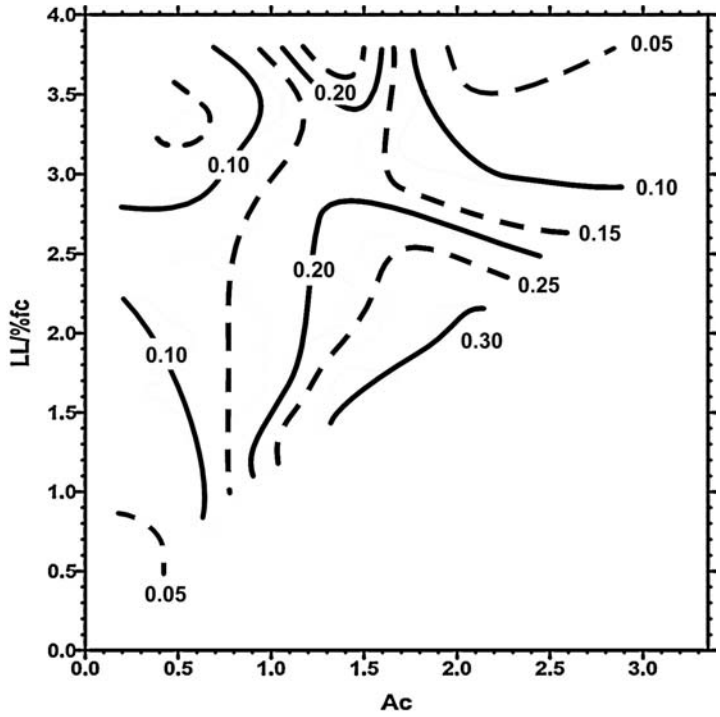

Figure 10. Zone III Chart for Determining γ_o. (Covar and Lytton, 2001).[12]

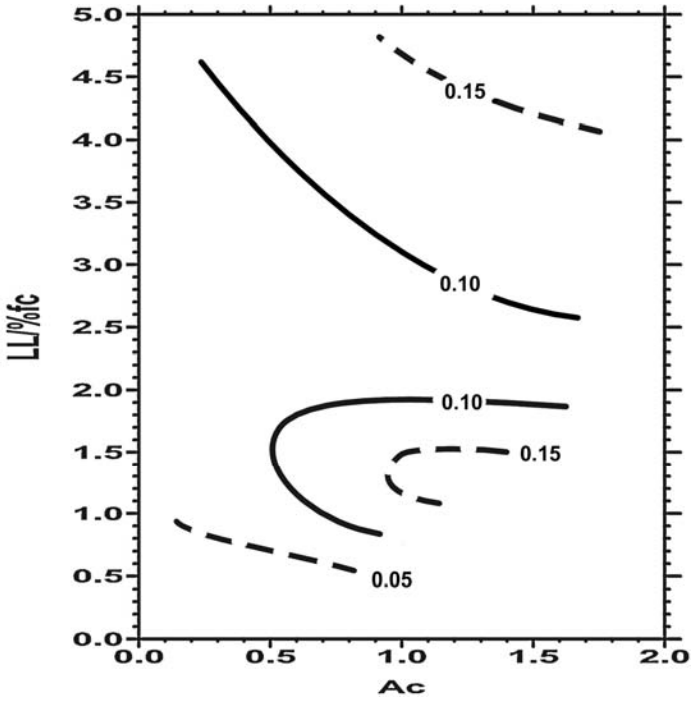

Figure 11. Zone IV Chart for Determining γ_o. (Covar and Lytton, 2001).[12]

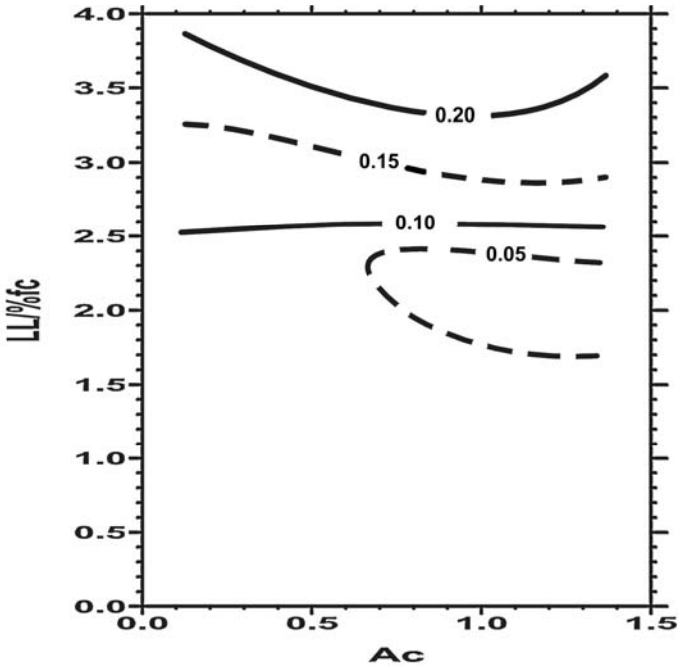

Figure 12. Zone V Chart for Determining γ_o. (Covar and Lytton, 2001).[12]

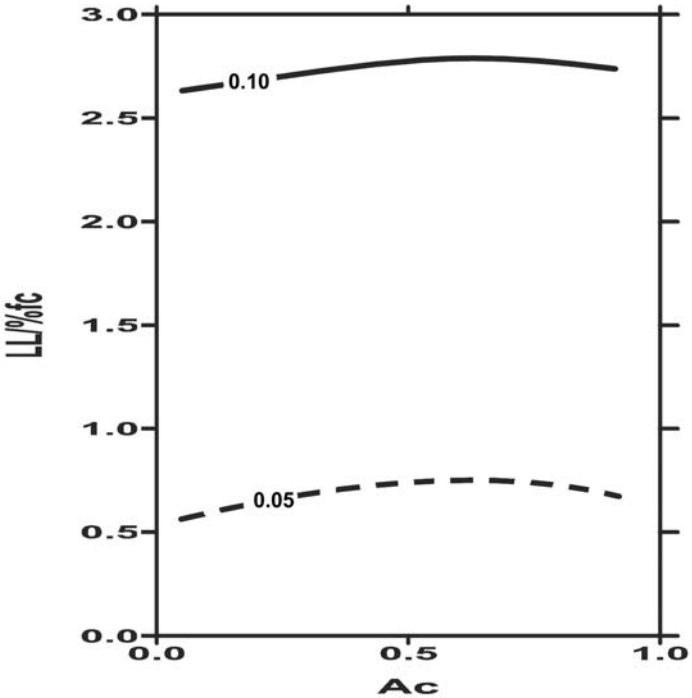

Figure 13. Zone VI Chart for Determining γ_o. (Covar and Lytton, 2001).[12]

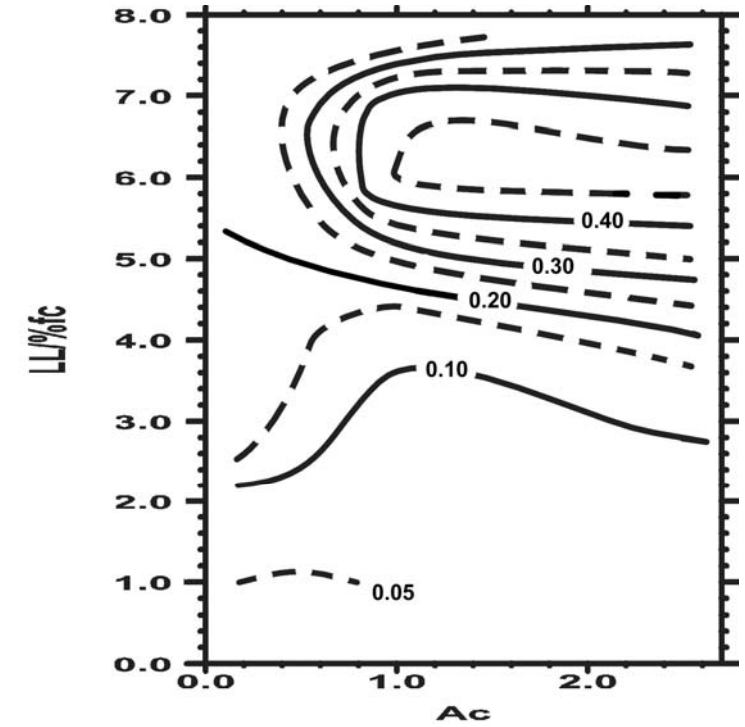

Figure 14. Zone VII Chart for Determining γ_o. (Covar and Lytton, 2001).[12]

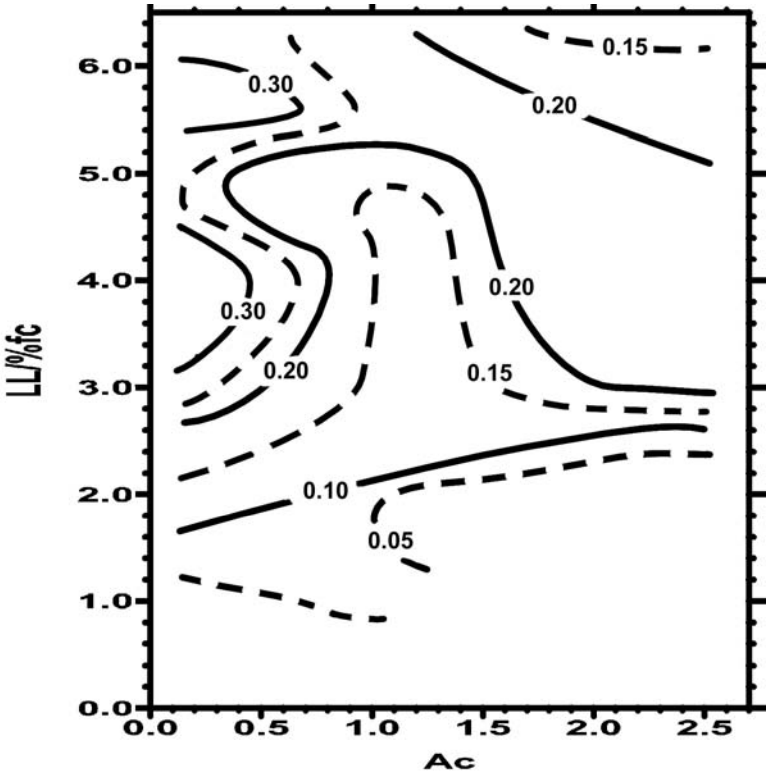

Figure 15. Zone VIII Chart for Determining γ_o. (Covar and Lytton, 2001).[12]

The suction compression index obtained from Equation (11) is corrected to compensate for the different initial volume of soil mass during a wetting or drying process.

$$\gamma_{h(swelling)} = \gamma_h e^{\gamma_h} \tag{16}$$

$$\gamma_{h(shrinkage)} = \gamma_h e^{-\gamma_h} \tag{17}$$

A suction compression index for stabilized soil can be estimated using Atterberg limits, soil particle size distribution of the natural soil to be stabilized, and the percent of stabilizing material such as lime or cement.

If lime is used as a stabilizing material,

$$\mathrm{PI}_{\text{stabilized}} = \mathrm{PI}_{\text{unstabilized}} \left(\frac{9 - \%\,\text{lime}}{9} \right) \tag{18}$$

$$LL_{stabilized} = \frac{PI_{stabilized}}{a} + b \tag{19}$$

If cement is used as a stabilizing material,

$$\mathrm{PI}_{\text{stabilized}} = \mathrm{PI}_{\text{unstabilized}} \left(\frac{8 - \%\,\text{cement}}{8} \right) \tag{20}$$

$$LL_{stabilized} = \frac{PI_{stabilized}}{a} + b \tag{21}$$

The parameters *a* and *b* can be determined using the mineral classification chart (Figure 7) for untreated soil. Typical values of these parameters are shown in Table 5.

Table 5. Determination of Parameters a and b Corresponding to Mineral Classification.

Group	a	b
I	0.85	11
II	0.81	14
III	0.73	20
IV	0.68	25
V	0.68	25
VI	0.68	25

The empirical suction-versus-volumetric water content curve for natural, inert, and stabilized soil can be constructed as in Figures 16, 17 and, 18, respectively.

Suction-versus-Volumetric Water Content Curve for Clay Soil

The suction-versus-volumetric water content curve for clay soil is generated using the following process:

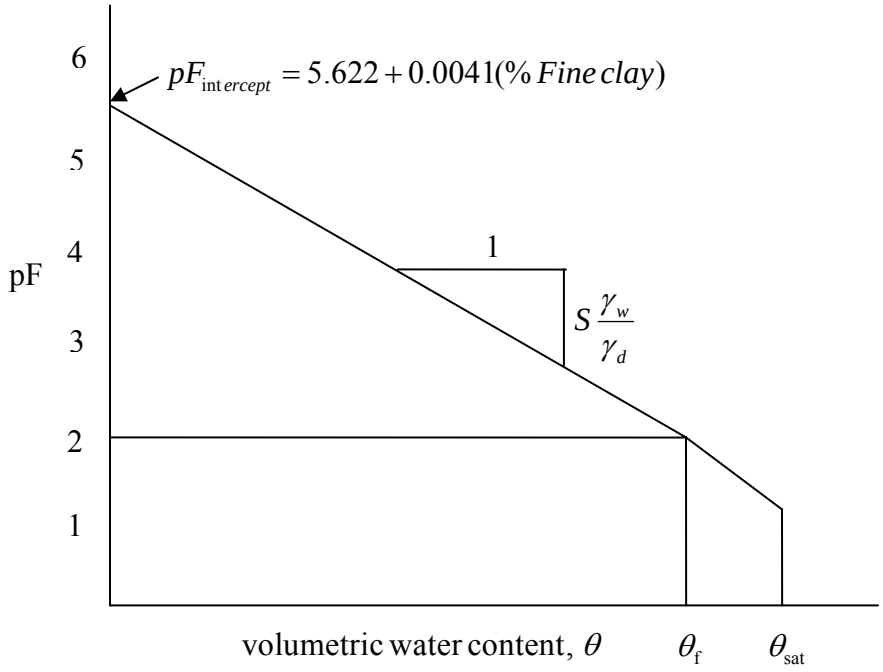

Figure 16. Suction-versus-Volumetric Water Content Curve for Clay Soil.

The slope of suction-versus-gravimetric water content, S, is estimated by:

$$S = -20.29 + 0.1555(LL\%) - 0.117(PI\%) + 0.0684(\% - \#200) \tag{22}$$

From the geometric relation in Figure 16, the relation of volumetric water content to the pF is:

$$\frac{\theta}{1.0} = \frac{pF_{\text{int}} - pF}{|S|\frac{\gamma_w}{\gamma_d}} \tag{23}$$

From rearranging the Equation (23), the volumetric water content is:

$$\theta = \frac{pF_{\text{int}} - pF}{|S|\frac{\gamma_w}{\gamma_d}} \tag{24}$$

Gravimetric water content is given by:

$$w = \frac{pF_{\text{int}} - pF}{|S|} \tag{25}$$

Suction-versus-Volumetric Water Content Curve for Inert Soil

The suction-versus-volumetric water content curve for inert soil is generated using the following process:

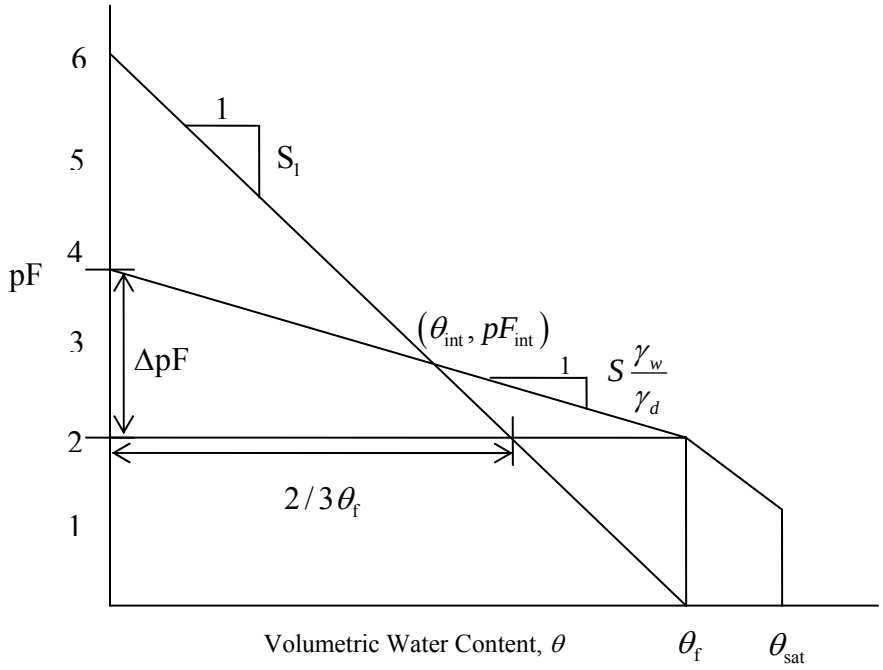

Figure 17. Suction-versus-Volumetric Water Content Curve for Inert Soil.

where:

S_1 = the slope from zero to the volumetric water content at the intersection

θ_{int} = the volumetric water content at the intersection

pF_{int} = the suction value at the intersection

The first slope, S_1, using the geometric relation in Figure 17 is as follows:

$$\frac{6.0 - 2.0}{\frac{2}{3}\theta_f} = \frac{|S_1|}{1.0} \tag{26}$$

From rearranging Equation (26):

$$|S_1| = \frac{6.0}{\theta_f} \tag{27}$$

where:

$$\theta_f = 1 - \frac{\gamma_d}{G_s \gamma_w} (\text{assuming } G_s = 2.70) \tag{28}$$

Using the second slope, $S\frac{\gamma_w}{\gamma_d}$, ΔpF can be estimated as follows:

$$\frac{\theta_f}{\Delta pF} = \frac{1}{|S|\frac{\gamma_w}{\gamma_d}} \tag{29}$$

$$\Delta pF = \theta_f |S| \frac{\gamma_w}{\gamma_d} \tag{30}$$

The suction at the intersection, pF_{int}, can be expressed by:

$$pF_{\text{int}} = (2.0 + \Delta pF) - |S| \frac{\gamma_w}{\gamma_d} \theta_{\text{int}} \tag{31}$$

$$pF_{\text{int}} = 6.0 - |S_1| \theta_{\text{int}} \tag{32}$$

From Equations (31) and (32):

$$\theta_{\text{int}} = \frac{\Delta pF - 4.0}{|S| \frac{\gamma_w}{\gamma_d} - |S_1|} \tag{33}$$

$$pF_{\text{int}} = 6 - |S_1| \theta_{\text{int}} \tag{34}$$

Therefore, the volumetric water content on the two lines is given by:

$$\theta = \frac{6.0 - pF}{|S_1|} \qquad (0.0 \le \theta \le \theta_{\text{int}}) \tag{35}$$

$$\theta = \frac{pF_{\text{int}} - pF}{|S_1| \frac{\gamma_w}{\gamma_d}} \qquad (\theta_{\text{int}} \le \theta \le \theta_f) \tag{36}$$

And the gravimetric water content is given by:

$$w = \frac{6.0 - pF}{|S_1|} \frac{\gamma_w}{\gamma_d} \qquad \left(0.0 \le \theta \le \theta_{\text{int}}\right) \tag{37}$$

$$w = \frac{pF_{\text{int}} - pF}{|S|} \qquad \left(\theta_{\text{int}} \le \theta \le \theta_f\right) \tag{38}$$

Suction-versus-Volumetric Water Content Curve for Stabilized Soil

The suction-versus-volumetric water content curve for stabilized soil is generated with the following process:

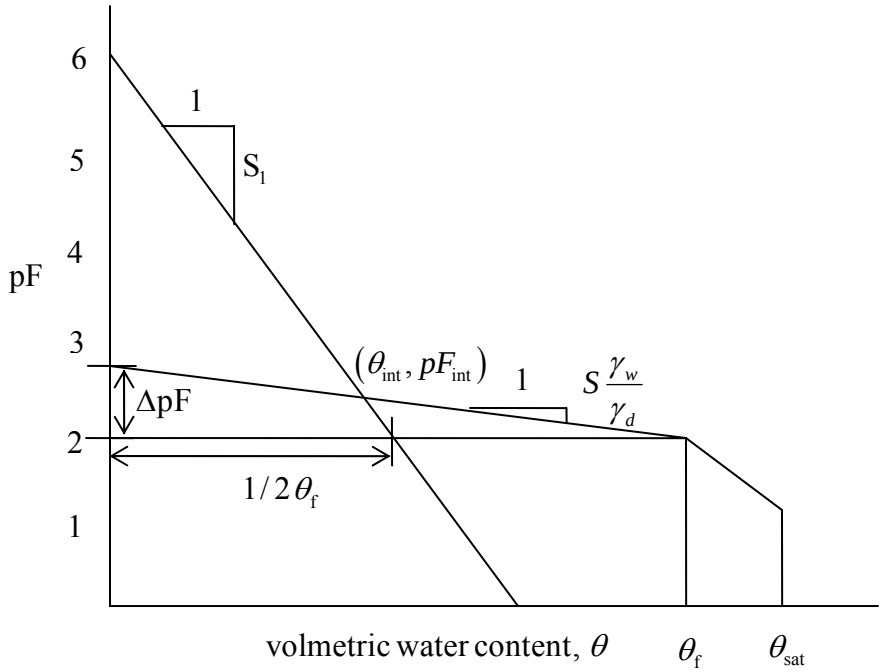

Figure 18. Suction-versus-Volumetric Water Content Curve for Stabilized Soil.

where:

S_1 = the slope from zero to the volumetric water content at the intersection

θ_{int} = the volumetric water content at the intersection

pF_{int} = the suction value at the intersection

The first slope, S_1, using a geometric relation in Figure 18 follows:

$$\frac{6.0-2.0}{\frac{1}{2}\theta_f}=\frac{|S_1|}{1.0} \tag{39}$$

From rearranging Equation (37):

$$|S_1|=\frac{8.0}{\theta_f} \tag{40}$$

where:

$$\theta_f=1-\frac{\gamma_d}{G_s\gamma_w}\ \text{(assuming } G_s=2.70) \tag{41}$$

Using the second slope, $S\frac{\gamma_w}{\gamma_d}$, ΔpF, can be estimated as follows:

$$\frac{\theta_f}{\Delta pF}=\frac{1}{\frac{1}{2}|S|\frac{\gamma_w}{\gamma_d}} \tag{42}$$

$$\Delta pF=\theta_f\frac{1}{2}|S|\frac{\gamma_w}{\gamma_d} \tag{43}$$

The suction at the intersection, pF_{int} can be expressed by:

$$pF_{\text{int}}=\left(2.0+\Delta pF\right)-\frac{1}{2}|S|\frac{\gamma_w}{\gamma_d}\theta_{\text{int}} \tag{44}$$

$$pF_{\text{int}}=6.0-|S_1|\theta_{\text{int}} \tag{45}$$

From Equations (44) and (45):

$$\theta_{\text{int}}=\frac{\Delta pF-4.0}{\frac{1}{2}|S|\frac{\gamma_w}{\gamma_d}-|S_1|} \tag{46}$$

$$pF_{\text{int}}=6-|S_1|\theta_{\text{int}} \tag{47}$$

Therefore, the volumetric water content on the two lines is given by:

$$\theta=\frac{6.0-pF}{|S_1|}\qquad\left(0.0\le\theta\le\theta_{\text{int}}\right) \tag{48}$$

$$\theta = \frac{pF_{\text{int}} - pF}{\frac{1}{2}|S|\frac{\gamma_w}{\gamma_d}} \qquad \left(\theta_{\text{int}} \le \theta \le \theta_f\right) \tag{49}$$

And then the gravimetric water content is given by:

$$w = \frac{6.0 - pF}{|S_1|}\frac{\gamma_w}{\gamma_d} \qquad \left(0.0 \le \theta \le \theta_{\text{int}}\right) \tag{50}$$

$$w = \frac{pF_{\text{int}} - pF}{\frac{1}{2}|S|} \qquad \left(\theta_{\text{int}} \le \theta \le \theta_f\right) \tag{51}$$

These characteristics of the natural soil, inert soil, and stabilized soil are integrated into two separate programs: FLODEF, a finite element transient analysis method, and WinPRES, a program used to design both flexible and rigid pavements on expansive soils. Both of these programs are described in detail in subsequent chapters.

ESTIMATION OF SUCTION PROFILE

For design purposes, it is desirable to compute the total heave that occurs between two steady state suction profiles, one given by constant velocity of water entering the profile (low suction due to wetting) and the other given by constant velocity of water leaving the profile (high suction level due to drying).

The suction profile for two transient states can be predicted approximately using:

$$U(Z,t) = U_e + U_o \exp\left(-\sqrt{\frac{n\pi}{\alpha}}Z\right)\cos\left(2\pi nt - \sqrt{\frac{n\pi}{\alpha}}Z\right) \tag{52}$$

where:

Z = depth

U_e = the equilibrium value of suction expressed as pF

U_o = the amplitude of pF (suction) change at the ground surface

n = the number of suction cycles per second (1 year=31.5×10^6seconds)

α = the soil diffusion coefficient using Mitchell's unsaturated permeability (ranges between 10^5 and 10^3 cm^2/sec)

t = time in seconds

Tables of values of U_e and U_o for clay soils with different levels of Mitchell's unsaturated permeability have been found using a trial and error procedure. The dry suction profile has a U_e value of 4.5 and a U_0 value of 0.0. The wet suction profile has U_e and U_0 values that vary with the soil type and Thornthwaite moisture index. Typical values are shown in Table The value of α can be estimated from:

$$\alpha = 0.0029 - 0.000162(S) - 0.0122(\gamma_h) \quad (53)$$

Table 6. Wet Suction Profile Values.

Thornthwaite Moisture Index	Mitchell Unsaturated Permeability cm^2/sec	U_e (pF)	U_0 (pF)
−46.5	5×10^{-5} 10^{-3}	4.43 4.27	0.25 0.09
−11.3	5×10^{-5} 10^{-3}	3.84 2.83	1.84 0.83
26.8	5×10^{-5} 10^{-3}	3.47 2.79	1.47 0.79

OVERVIEW OF METHODS FOR CONTROLLING PAVEMENT ROUGHNESS

This section gives an overview of the TTI Research Report 0-1165-2F [2]. The objective of this project was to predict the vertical movement and roughness development in highway pavements in different climatic regions. TTI researchers estimated the vertical movement and roughness measures such as serviceability index, international roughness index, and maximum expected bump height for different conditions that are expected in highway pavements. The different conditions considered for this project are:

1. soil type (cracked or highly permeable, tightly closed cracks or minimally permeable, and medium cracked or moderately permeable),
2. drainage type (normal, ponded, and slope),
3. root depth (4 ft or shallow root zone, and 8 ft or deep root zone),
4. sodded and paved medians, and
5. roadways with and without vertical moisture barriers.

The three different drainage conditions considered for this study cover almost all of the drainage conditions that can be expected in a highway pavement. The "normal", "slope," and "ponded" drainage conditions occur in pavements built on a flat terrain, on a sloping terrain, and in a valley area, respectively. The locations considered for this project were EI Paso, San Antonio, Dallas, Houston, and Port Arthur. The project was carried out in the following steps:

1. Estimate mean, dry, and wet moisture depths for the five different locations.
2. Select a function describing surface suction variation with time for the exposed soil on the side slopes of the pavement.
3. Estimate equilibrium, dry, and wet suction profiles.
4. Estimate maximum vertical movement that is expected in a pavement.
5. Estimate roughness measures.
6. Compare measured and predicted roughness measures.

MINIMUM EXPECTED VERTICAL MOVEMENT

The extreme dry and wet suction profiles and surface suction distribution over time were developed and used in the FLODEF program to estimate the maximum expected vertical movement in a highway pavement. For this analysis, a two-lane roadway with two 12-ft-wide travel way lanes and 2-ft-wide paved shoulders on either side of the roadway was considered. The analysis was carried forward for a period of four and one-half years. The expected vertical movements in the outside wheel path of the roadway for both dry and wet initial conditions were estimated separately and added together to obtain the maximum vertical movement that should be expected during the lifetime of the pavement. The outside wheel path was considered to be at a distance of 10 ft from the center line of the pavement.

The maximum expected vertical movement was estimated for roadways with and without vertical moisture barriers. The different barrier depths considered were 3 ft, 5 ft, and 8 ft. The different conditions considered for this project were:

1. soil type (cracked or high permeable, tight or low permeable, and medium cracked),
2. drainage type (normal, ponded, and slope),
3. root depth (4 ft or shallow root zone, and 8 ft or deep root zone), and
4. median type (sodded and paved).

The pavement section considered for this project consisted of a 1.5 ft deep combined subbase and surface layer and one 15 ft deep subgrade soil layer. The vertical moisture barrier consisted of a 0.33 ft wide fabric and a 1.0 ft wide backfill adjacent to the fabric. The finite element mesh used for the analysis is shown in Figure 19.

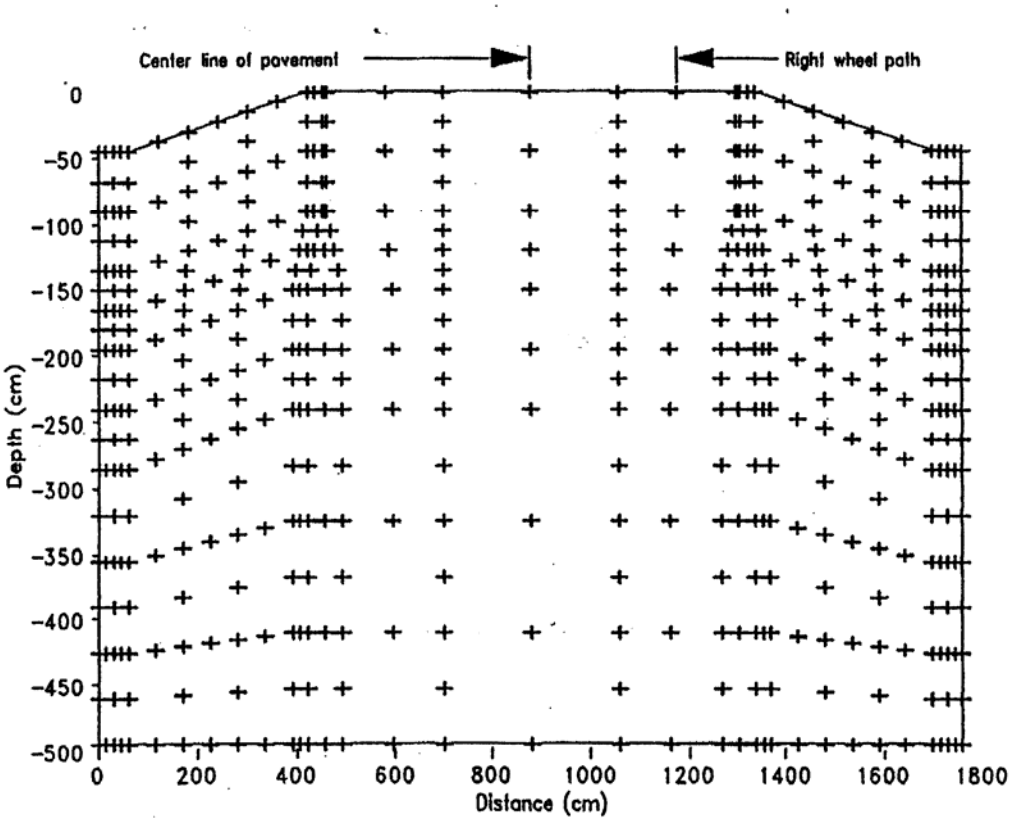

Figure 19. Finite Element Mesh Used for Estimation of Vertical Movement.

The estimated vertical movements were plotted against the Thornthwaite moisture index (TMI). These results show that the maximum vertical movements occur in sites where the mean TMI is approximately -10 and the vertical movements decrease for values of TMI greater or lesser than -10. Also, the vertical movements in "slope" drainage conditions are lower than those in the "normal" drainage conditions in sites where there is a mean TMI of approximately -20 or higher. For the cracked soils with deep roots and tight soils with shallow roots, the vertical movements in "ponded" drainage conditions are higher than those in the "normal" drainage conditions in sites below the mean TMI of +10 and are lower in sites above that level of mean

TMI. The same trend is observed for the medium cracked soils with deep roots; however, the breaking point, in this case, is at the TMI of approximately +24.

Moreover, the results show that the vertical movements increase with the increase of unsaturated permeability. Generally, the increase in moisture barrier depth decreases the vertical movement; however, in some cases of tight soil with shallow roots, this trend has been reversed. Of the three soil types, the highest decrease in vertical movement with an introduction of a vertical moisture barrier is observed in the medium cracked soils. The decrease in vertical movement is negligible in tight soils. The decrease in vertical movement is not significant in dry climates such as EI Paso (mean TMI = -46.5) under the "normal" and "slope" drainage condition; however, this is significant in the "ponded" drainage condition. There is not an appreciable difference in vertical movements in the outside wheel path between the pavements with paved and sodded medians. However, the paving of a median may reduce the vertical movement in the inside wheel path or in inside lanes.

PREDICTION OF ROUGHNESS DEVELOPMENT

The following roughness prediction models developed through the regression analysis of the rates of roughness development (*dR/dt*) and the expected value of vertical movement (ΔH) were used for the prediction of roughness measures for the different cases studied in the previous sections of this chapter.

Serviceability Index (SI)

The change in SI/year, dR/dt is given by:

$$\frac{dR}{dt} = \beta_1(\Delta H) + \beta_2 \tag{54}$$

where for category

A Moisture barriers with paved medians

$\beta_1 = 0.02176 \quad \beta_2 = 0.03226$

B Moisture barriers with sodded medians

$\beta_1 = 0.03430 \quad \beta_2 = 0.07269$

C Control sections with and without medians

$\beta_1 = 0.04418 \quad \beta_2 = 0.12461$

International Roughness Index (IRI)

The mean rate of change of IRI (in/mile/year), dR/dt is given by:

$$\frac{dR}{dt} = \beta_1(\Delta H) + \beta_2 \tag{55}$$

where for category

A Moisture barriers with paved medians

$\beta_1 = 0.61939 \quad \beta_2 = 1.2954$

B Moisture barriers with sodded medians

$\beta_1 = 1.5825 \quad \beta_2 = 2.0105$

C Control sections with and without medians

$\beta_1 = 2.7014 \quad \beta_2 = 4.0146$

Minimum expected bump height (BH)

$$\frac{dR}{dt} = \beta_1 + \beta_2 \exp(\beta_3 \Delta H) \tag{56}$$

where for category

A Moisture barriers with paved medians

$\beta_1 = 0.011 \quad \beta_2 = 0.012 \quad \beta_3 = 0.216$

B Moisture barriers with sodded medians

$\beta_1 = 0.010 \quad \beta_2 = 0.011 \quad \beta_3 = 0.305$

C Control sections with and without medians

$\beta_1 = 0.000 \quad \beta_2 = 0.018 \quad \beta_3 = 0.302$

In the development of these models, the expected vertical movement was estimated by integrating over depth the changes in vertical movement as a function of the change in matrix suction between the expected wet and dry suction profiles. The results were plotted against the Thornthwaite moisture index.

These results indicate that the presence of a vertical moisture barrier significantly reduces the development of roughness in pavements on expansive soils. However, the development of roughness in pavements on tight subgrade soils is generally low even without a moisture barrier. Therefore, a vertical moisture barrier may not be useful in pavements on tight soils. Vertical moisture barriers can be effective in controlling pavement roughness in some circumstances. The conditions under which they can and cannot be expected to perform satisfactorily are discussed in detail in pages 195 t0 205 of TTI Research Report 1165-2F, dated May, 1993.

Based on the results of this project, the following conclusions can be made.

1. Vertical moisture barriers are effective in reducing the development of roughness in pavements on expansive soils under certain circumstances. They are not effective in extremely dry climates such as in EI Paso when the pavement is subjected to “normal” and “slope” drainage conditions. Also, they are not effective in tight subgrade soils.
2. In extremely dry climates, the vertical moisture barriers are effective in “ponded” drainage conditions.
3. In cracked or medium cracked soils, the vertical moisture barriers are effective in reducing the development of roughness in all climates except for the extremely dry climates and under all drainage conditions.
4. Depth of barrier should be greater than or at least equal to the depth of the root zone.

CHAPTER 2:
CASE STUDY SITES

This chapter presents the case study sites. It gives an overview of the location and topography of the sites undertaken for study in this project. The soil samples from three locations, Fort Worth, Atlanta, and Austin, were analyzed. Test data are presented and discussed in Chapter 3.

FORT WORTH NORTH LOOP IH 820

Location

This site is located in Tarrant County, north of Fort Worth on North Loop IH 820. The problem associated with this site was the expansion of fill. Figure 20 shows the site location.

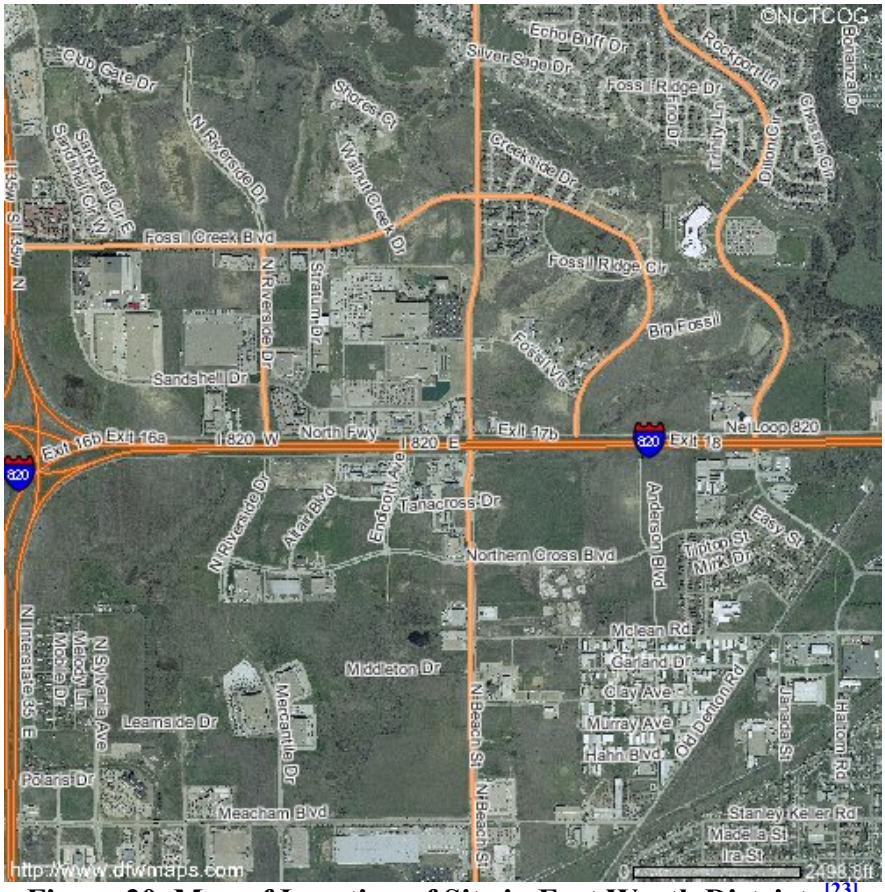

Figure 20. Map of Location of Site in Fort Worth District. [23]

Site Description

Borings were made along three alignments designated as areas A, B, and C. Each area contains five borings. The locations of areas A, B, and C are designated in the aerial photographs in Figures 21, 22, and 23, respectively.

Area A

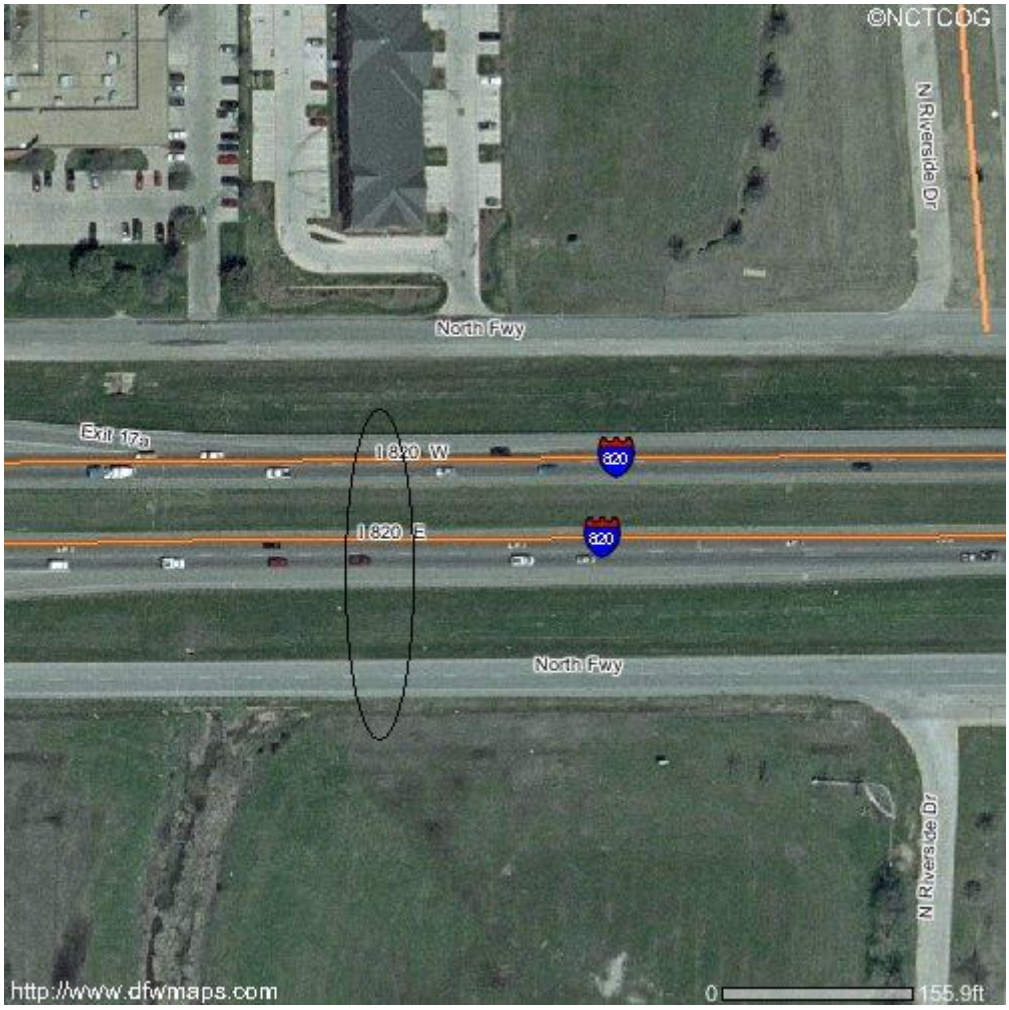

Figure 21. Location of Cross Section A on the Loop 820.[23]

The five boreholes in area A are A1, A2, A3, A4, and A5 are located on a line oriented perpendicular to the highway alignment. Boreholes A1 and A5 are located near the frontage road, A3 is in the median ditch, and A2 and A4 are at the outside shoulders of the pavement. The boreholes were taken in the soil past the pavement edges. The area encircled in Figure 21 shows the approximate location of area A.

Area B

Figure 22. Location of Cross Section B on the Loop 820.[23]

Area B contains boreholes B1 through B5 located on a line oriented perpendicular to the highway alignment. Boreholes B1 and B5 are located near the frontage road, B3 is in the median ditch, and B2 and B4 are at the outside shoulders of the pavement. The boreholes were taken in the soil past the pavement edges. The area encircled in Figure 22 shows the approximate location of area B.

Area C

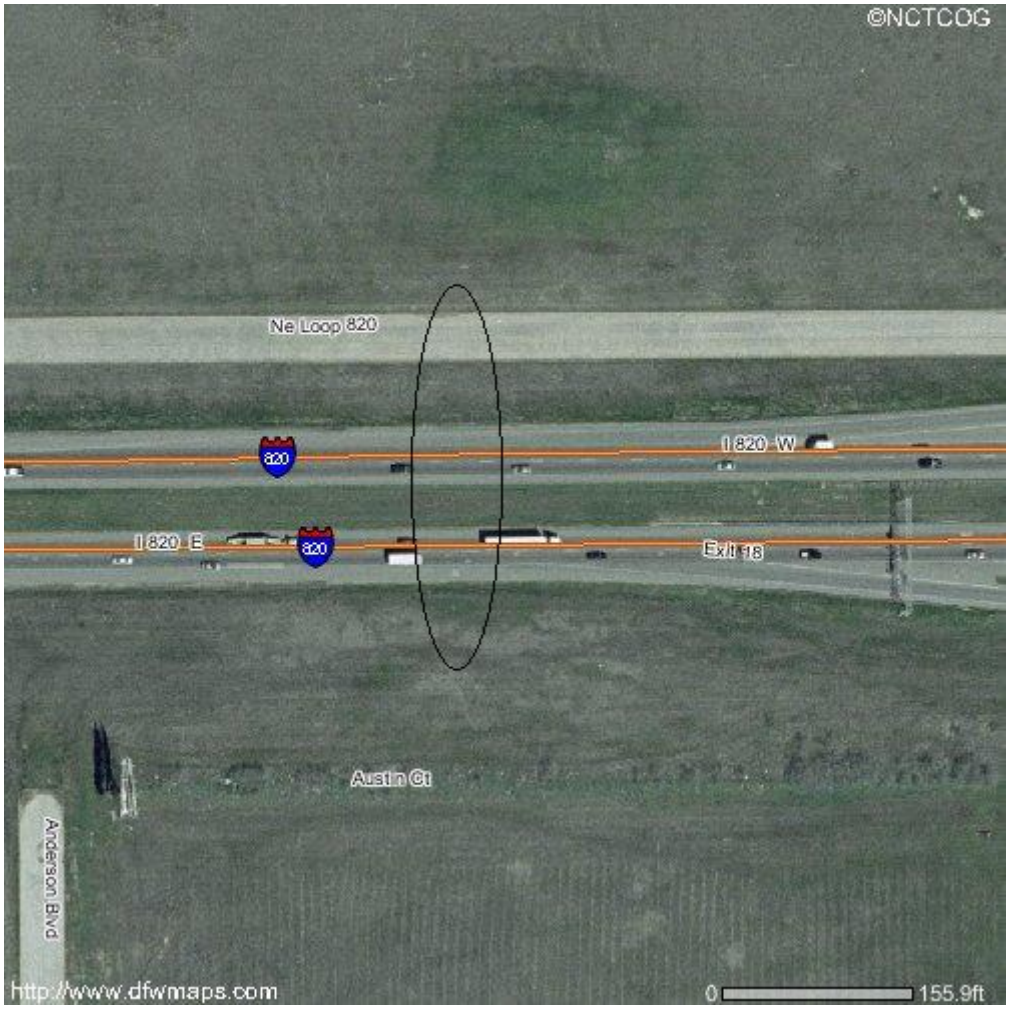

Figure 23. Location of Cross Section C on the Loop 820. [23]

Area C contains boreholes C1 through C5 located on a line oriented perpendicular to the highway alignments. C1 and C5 are located near the frontage road, C3 is in the median ditch, and C2 and C4 are at the outside shoulders of the pavement. The boreholes were taken in the soil past the pavement edges. The area encircled in Figure 23 shows the approximate location of area C.

Geologic Sections

Area A

Figure 24 shows the cross-sectional view of Fort Worth North Loop IH 820, area A (section A1, A2, A3, A4, A5). Figures 25 and 26 shows the detailed description of the boreholes, A1, A3, and A5 and A2, A3, and A4, respectively. The data presented are on the basis of borehole logs provided by TxDOT and the laboratory tests. Figures 25 and 26 contain only the vertical scale. Horizontal distance can be located approximately from Figure 24.

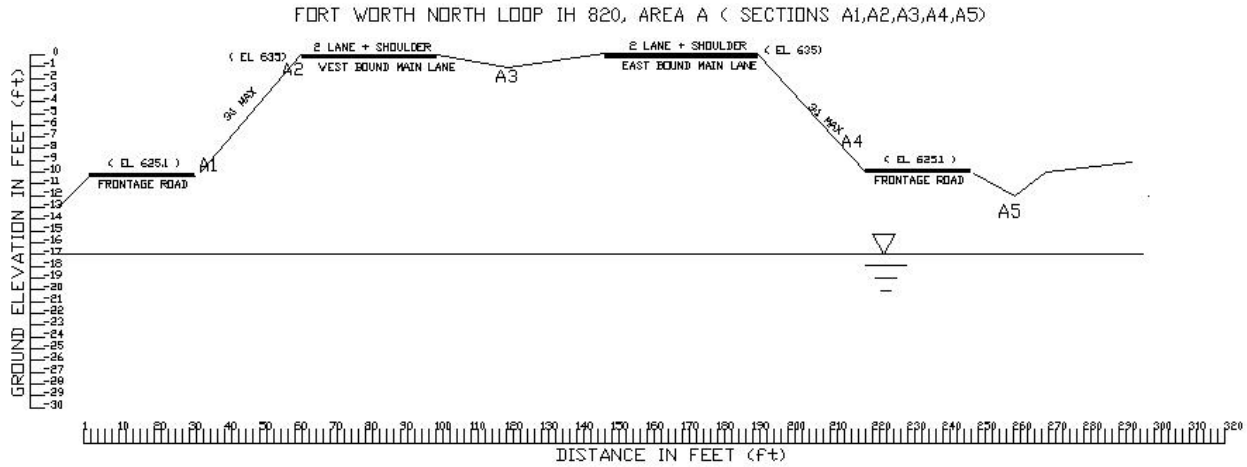

Figure 24. Cross-Sectional View of Area A.

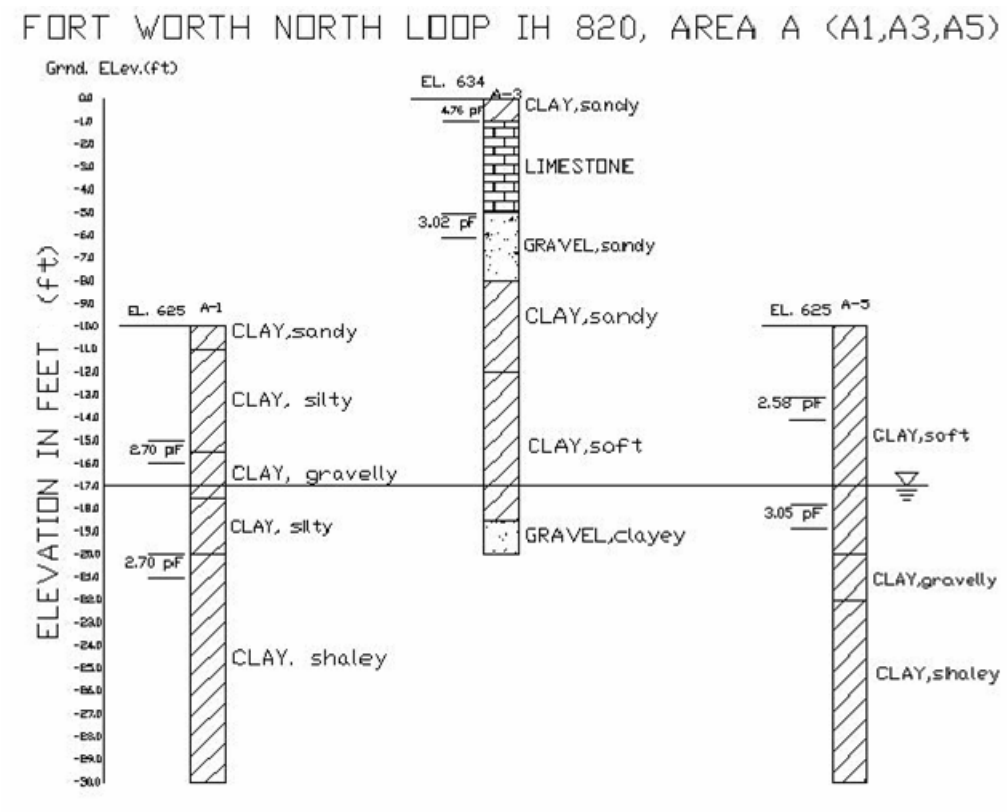

Figure 25. Cross-Sectional View at Boreholes A1, A3, and A5.

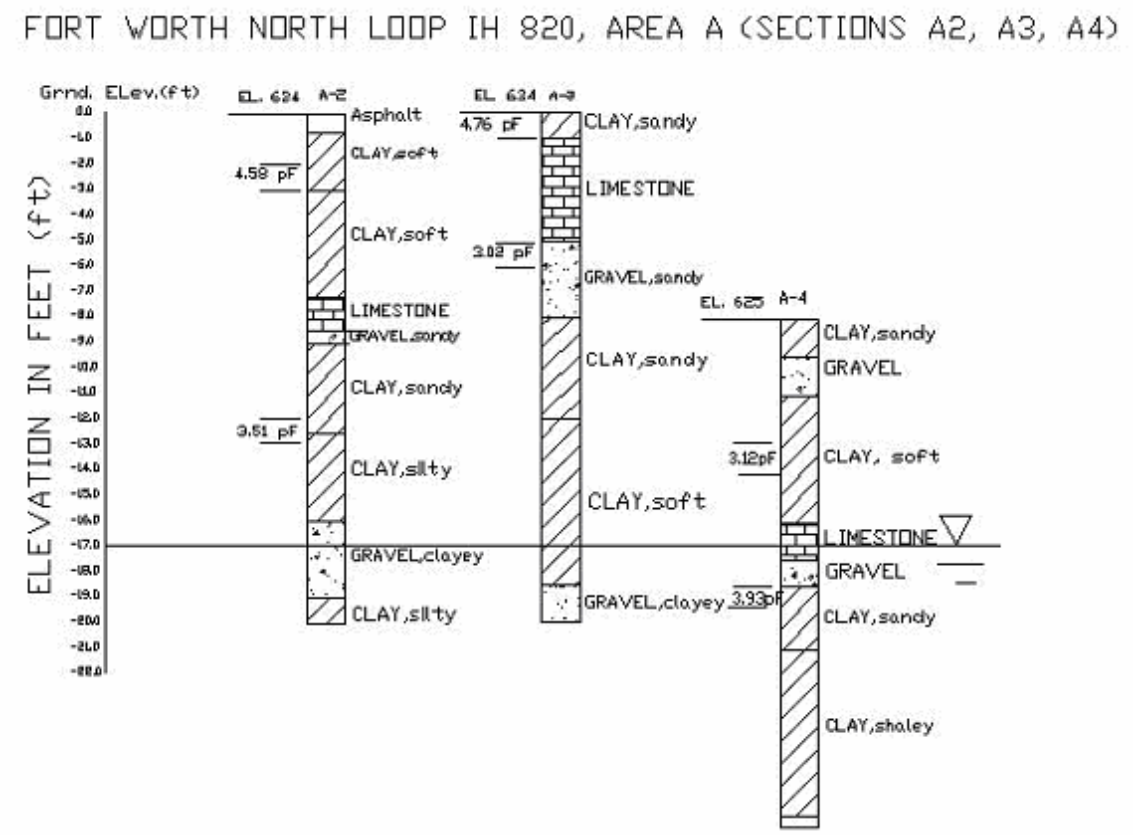

Figure 26. Cross-Sectional View at Boreholes A2, A3,and A4

Area B

Figure 27 shows the cross-sectional view of Fort Worth North Loop IH 820, area B. The locations of boreholes B1 through B5 have been approximated on the basis of the data provided by TxDOT. The cross-sectional detail at each borehole can be seen in Figure 28. These data have been compiled in the pictorial format from the data obtained by laboratory testing and borehole logs of the Forth Worth District provided by TxDOT.

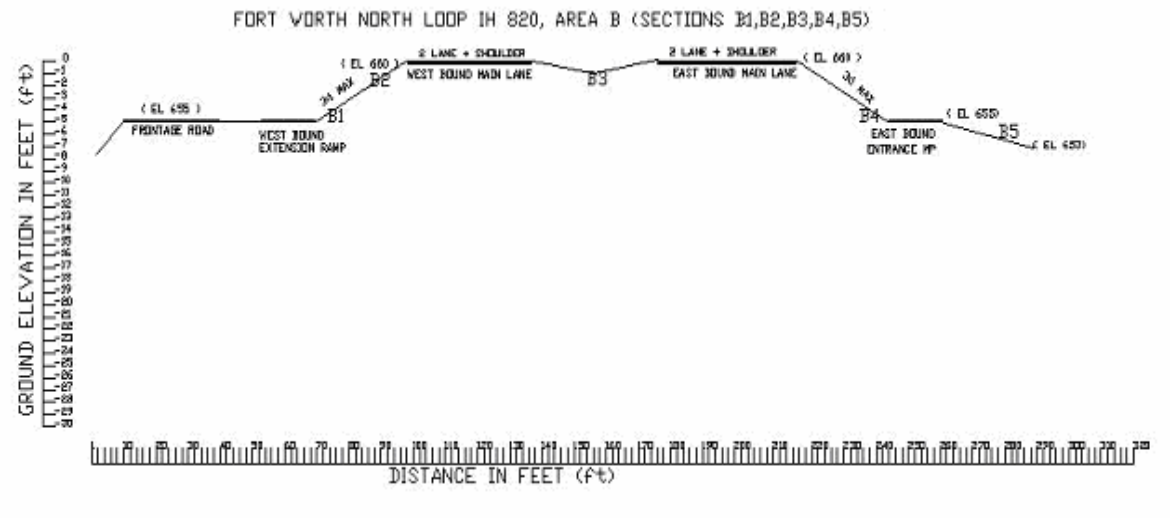

Figure 27. Cross-Sectional View of Area B.

Horizontal distance between boreholes B1 through B5 shown in Figure 28 can be obtained from Figure 27.

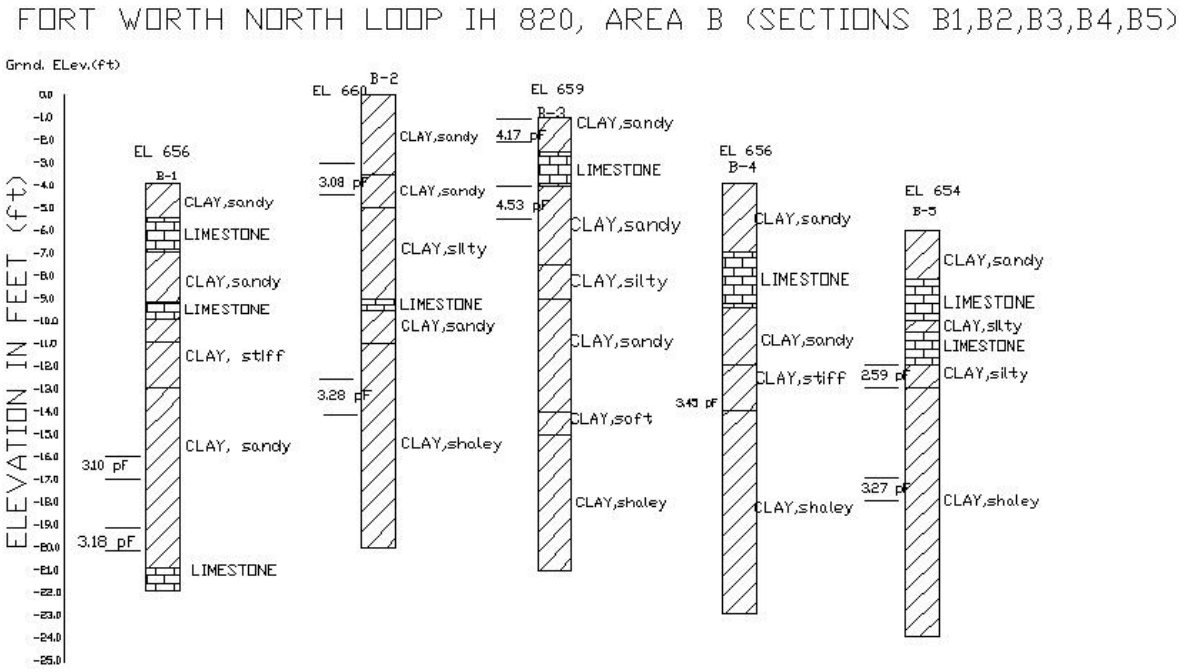

Figure 28. Cross-Sectional View at Boreholes B1, B2, B3, B4, and B5.

Area C

Figure 29 shows the cross-sectional view of Fort Worth North Loop IH 820, area C. The profile of boreholes from C1 through C5 can be seen in Figure 30. This profile has been drawn on the basis of laboratory testing and borehole logs of the Fort Worth District provided by TxDOT.

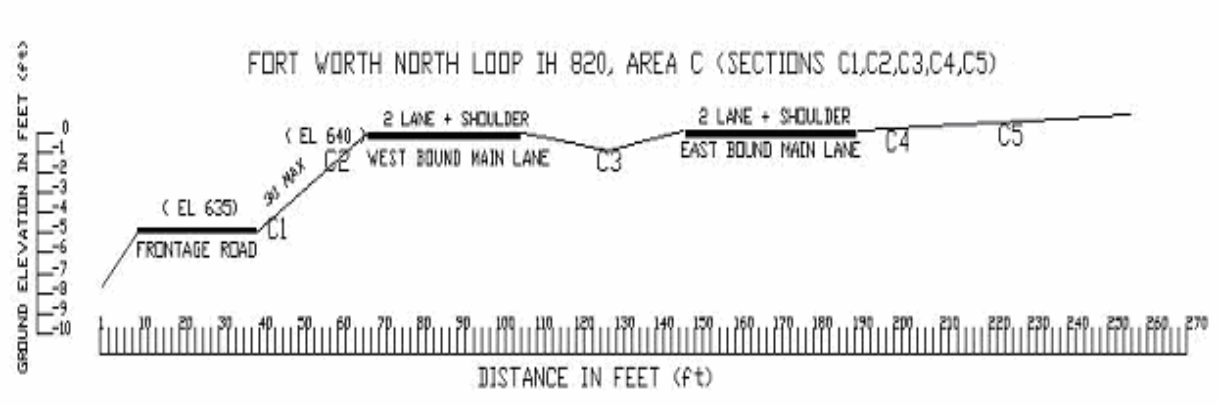

Figure 29. Cross-Sectional View of Area C.

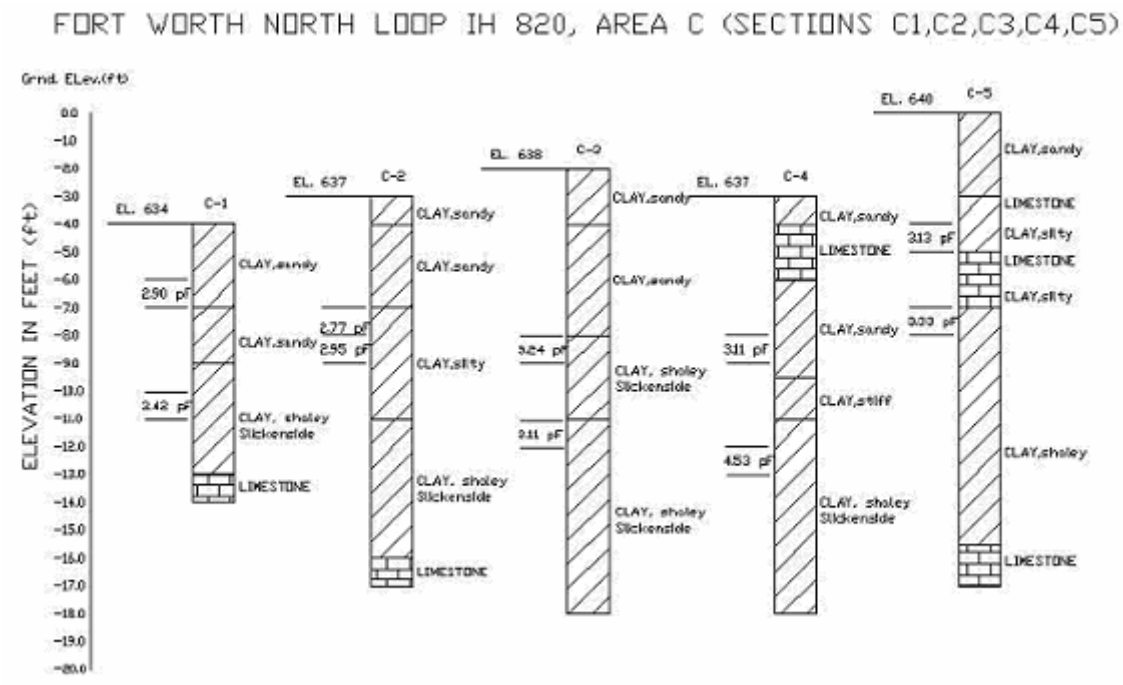

Figure 30. Cross-Sectional View at Boreholes C1, C2, C3, C4, and C5.

ATLANTA US 271

Location

This site is located in Titus County, in the northeast part of Texas near Talco. The problem associated with this site was the drying/shrinkage cracking due to trees. Figure 31 shows the site location. The arrow shows Highway US 271 for convenience.

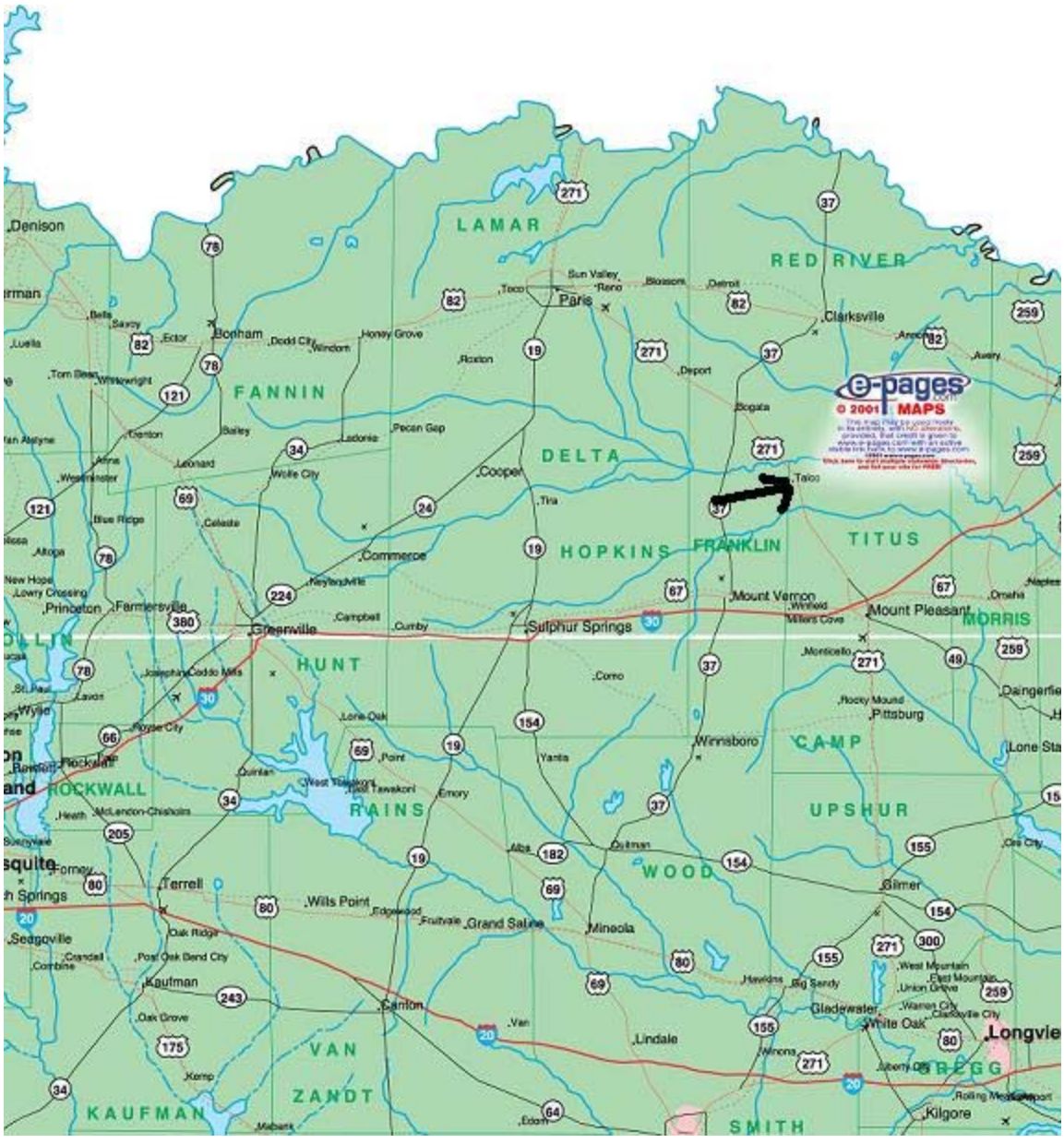

Figure 31. Map of Location of Site in Atlanta District Showing US 271. [24]

Site exploration entailed three boreholes, designated A, B, and C, located on a line oriented perpendicular to the roadway.

Site Description

Figure 32 shows a plan view of the US 271 site. The figure shows measured location of two post oak tree trunks and their associated drip line.

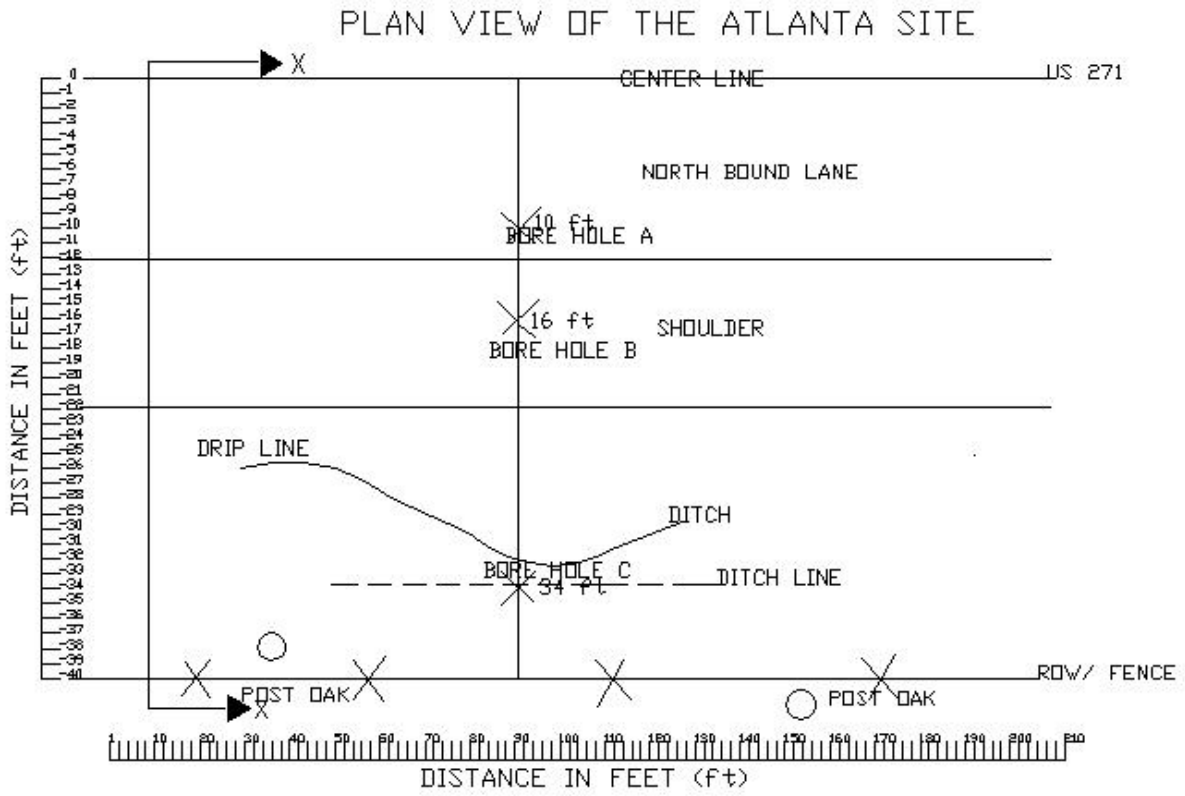

Figure 32. Plan View of the Atlanta Site.

Figure 33 shows a cross-section view at X-X with the locations of boreholes A, B, and C relative to a post oak tree trunk and the tree drip line.

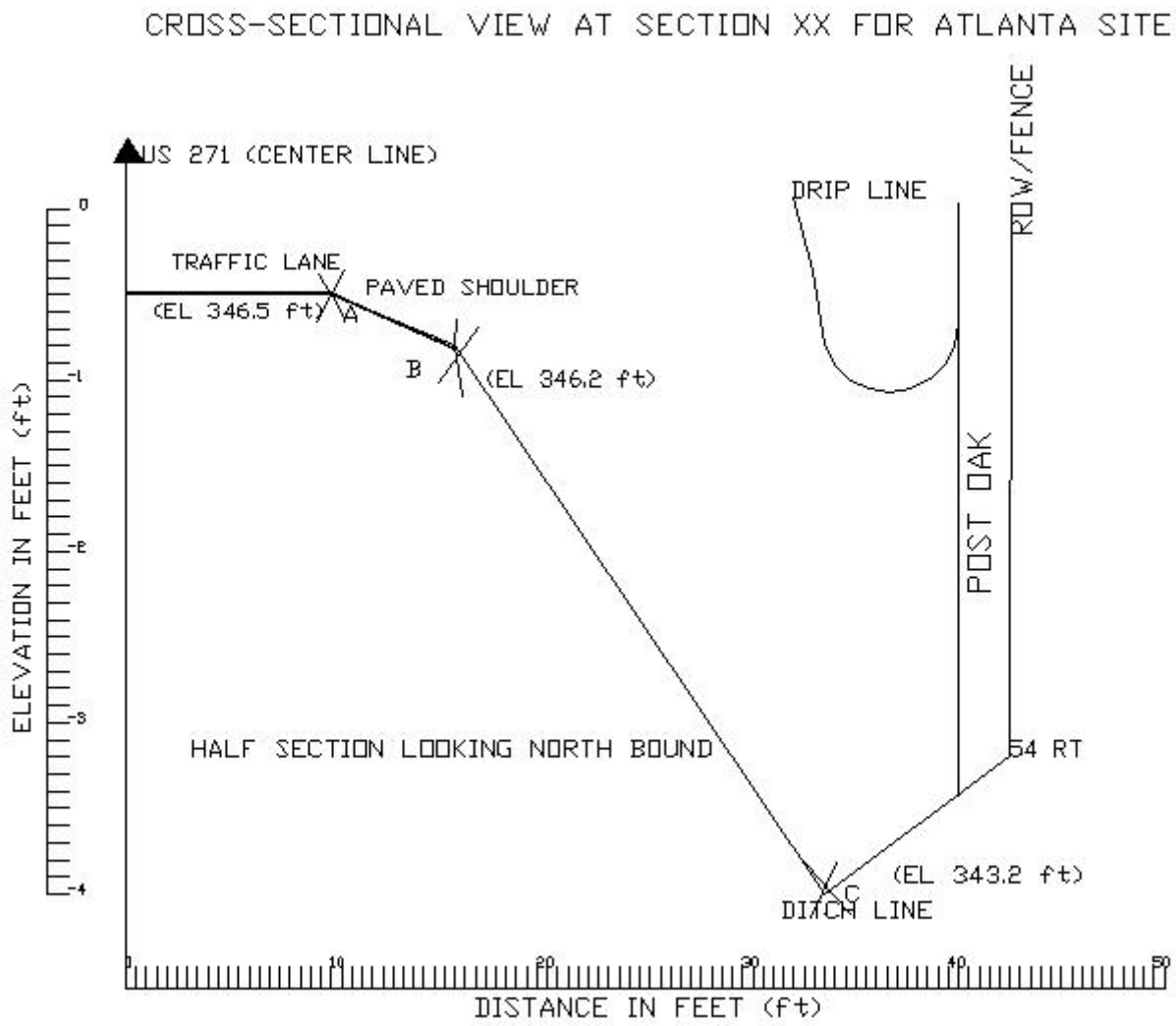

Figure 33. Borehole Location at the Site in Atlanta District.

Geologic Sections

Figure 34 shows the cross-sectional view of the soil at the Atlanta District site. In borehole C soil samples, roots were present up to 13 ft.

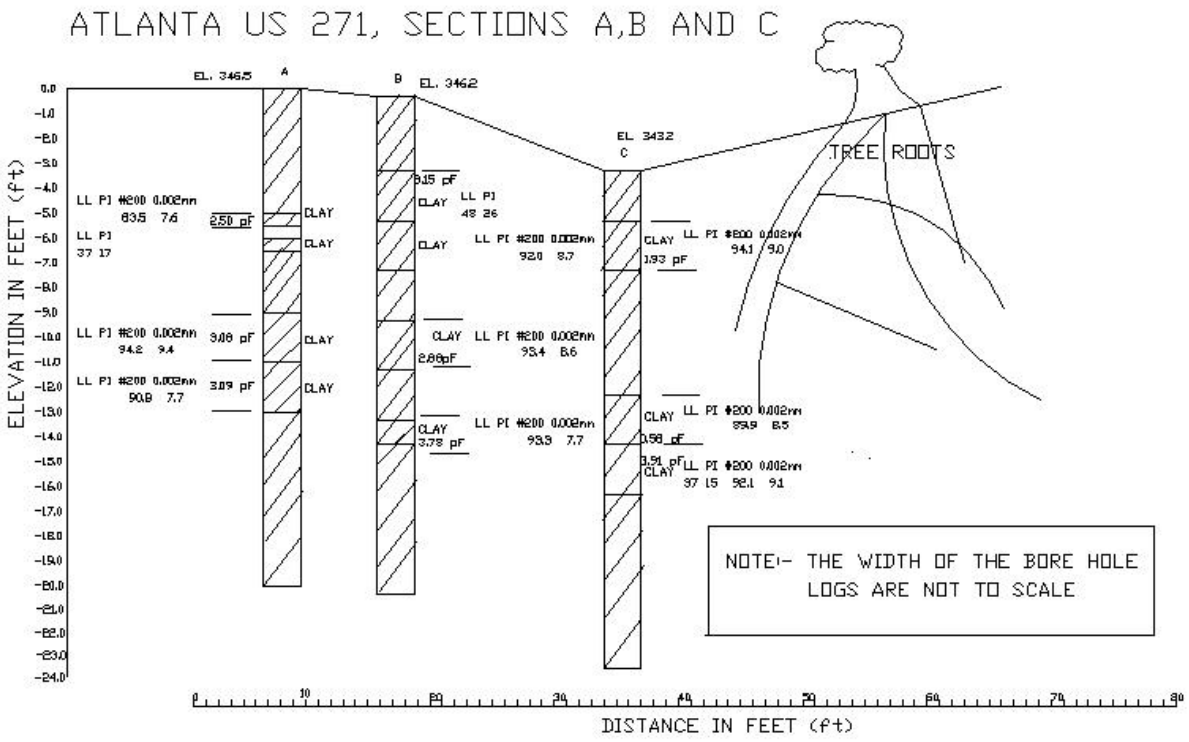

Figure 34. Cross-Sectional View at Boreholes A, B, and C.

AUSTIN LOOP 1

Location

This site is located on Loop 1 at SH 360 in Austin. An arrow indicates the area in Figure 35.

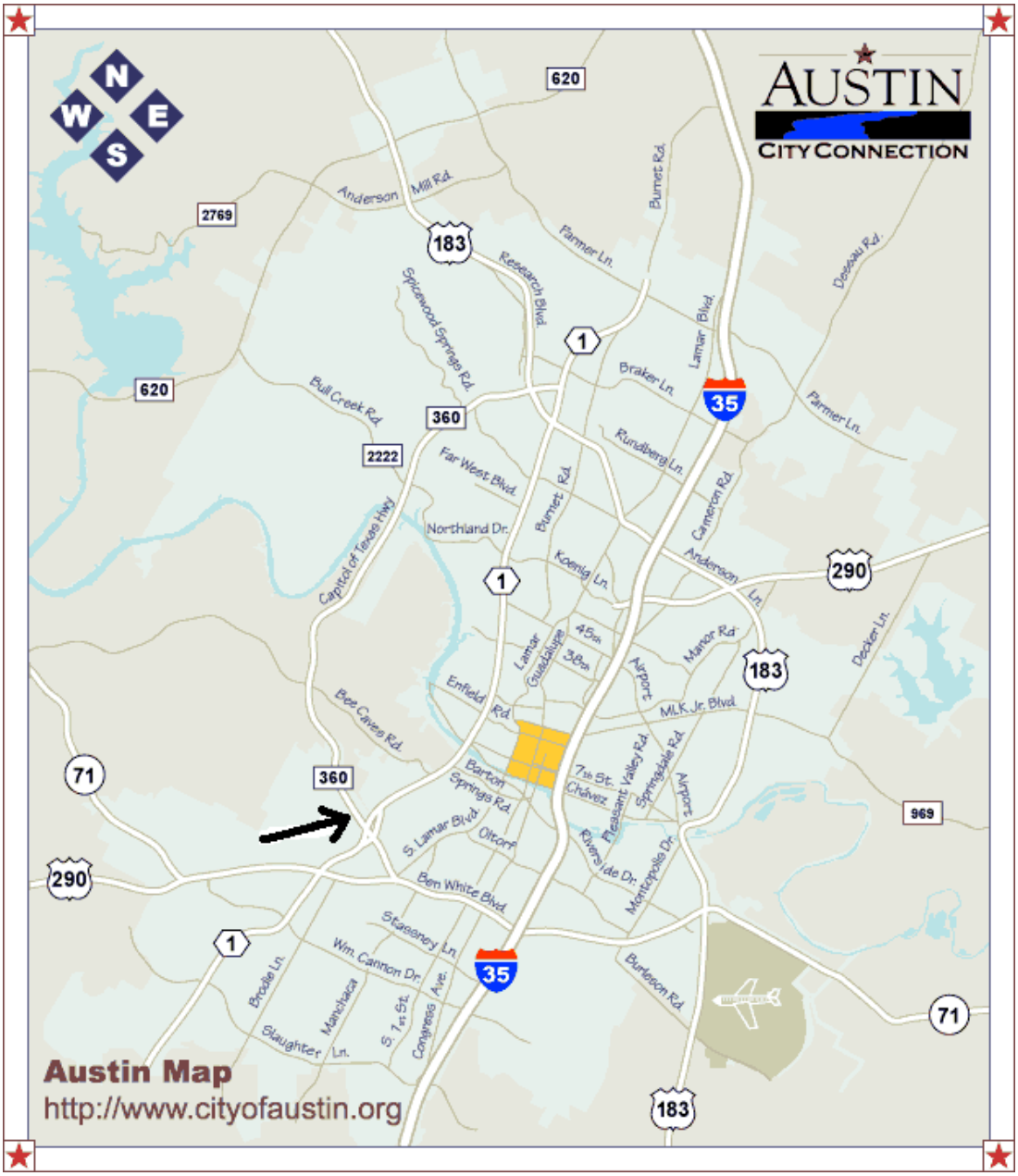

Figure 35. Map of Location of Site in Austin District. [25]

Site Description

This was a sloping site. It consisted of a shallow clay layer on a sloping limestone bed as shown in Figure 36. Borings B1, B2, and B3 were drilled about 2 ft from the frontage road curb as shown in Figure 37. The limestone bed was encountered at 7 ft at borehole B1, but there was not any indication of the limestone bed at borehole B3 until 20 ft. So, the dip and location of limestone bed in Figure 36 has been approximated.

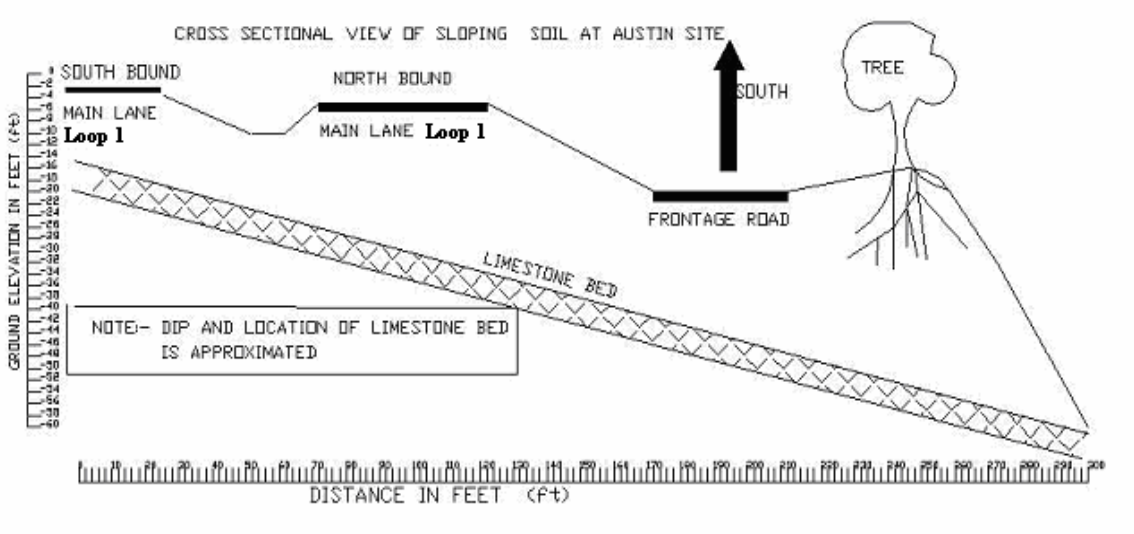

Figure 36. Cross-Sectional View of Sloping Soil at Austin District.

Researchers tested and analyzed soil samples from three boreholes B1, B2, and B3. The location and cross section along the boring can be seen in Figure 37.

Geologic Sections

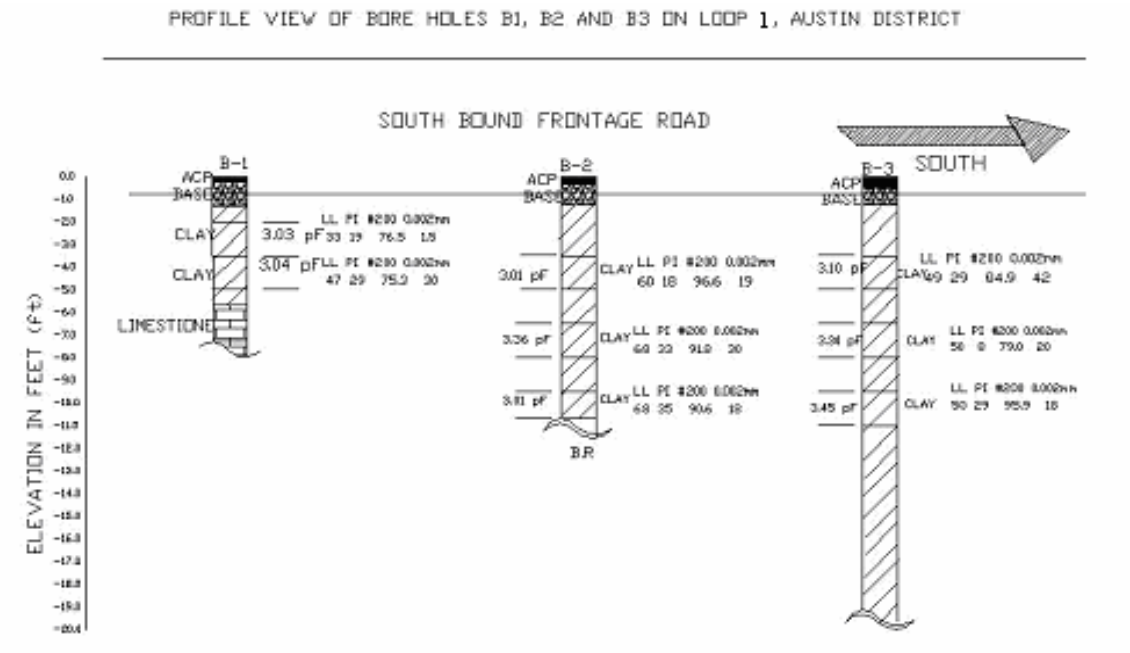

Figure 37. Cross-Sectional View at Bore Holes B1, B2, and B3.

At the time of survey the pavement was already repaved and the borehole locations were sealed. The soil profiles shown in Figure 37 are based on the borehole logs provided by TxDOT. The first two layers of each borehole suggested the presence of pavement as the top layer. The distance between boreholes B1, B2, and B3 are estimated, as surveys were not performed.

CHAPTER 3:
LABORATORY TESTS

DESCRIPTION

This chapter discusses the various laboratory tests conducted at TAMU. Atterberg's Limit, sieve analysis, and hydrometer analysis were conducted, along with the diffusion test, filter paper test, and pressure plates test.

The index properties can be used to determine diffusion coefficient and slope of moisture characteristic curve without actually conducting the diffusion and pressure plate test. Therefore, it is important to determine the index properties of the soil.

Atterberg Limits

The liquid limit and plastic limit are called the Atterberg Limits and represent the water content at which defined levels of consistencies are achieved. The limits may vary according to the clay minerals present and the percentage of clay in the mixture.

Sample Preparation. The soil sample, for liquid limit and plastic limit, was oven dried at 105 ºC. The sample was further broken into smaller pieces by using a hand rammer and then ground to finer particles using grinding machines. The ground sample was passed through a #40 sieve. The sample passing the sieve was collected and used for obtaining the Atterberg Limits.

Liquid Limit. For conducting the liquid limit test, the samples were mixed with distilled water and placed in a ceramic cup for moisture conditioning. Since the samples were high plasticity clays, they were kept covered for about 24 hrs. The container was covered with plastic wrap to avoid moisture loss. After moisture conditioning, researchers performed the liquid limit test as per ASTM D4318 [26].

Plastic Limit. Soil sample from the liquid limit test was used for the plastic limit. The test was performed as per ASTM D4318 [26].

Water Content

The soil samples provided by TxDOT were stored in moisture-controlled rooms to avoid the loss of moisture from the samples.

TxDOT provided in situ water content for the Atlanta District samples. For the Austin and Fort Worth Districts the water content for each sample was taken by TAMU technicians before and after conducting the diffusion test.

Sieve Analysis

Fine-grained plastic clay particles tend to adhere together when dried, even when subjected to grinding. Therefore, dry sieve analysis of such clays can mistake aggregates of fine particles for coarse-grained particles. To avoid this potential problem, a wet sieving procedure was used.

Sample Preparation. The soil sample was taken and oven dried for 24 hrs. The sample was ground to pass through #200 sieve, and 200 gm of sample was taken out for sieve analysis.

Procedure. The procedure for wet sieving was followed according to ASTM D1140-00[27], and 200 gm of soil sample was taken in a container. The sample was soaked in water for 2 hrs in order to prevent the finer materials from adhering to the larger particles. The sample solution was then passed through a #200 sieve. The water was passed through the sieve until clear water was passing the sieve. The sample retained on the sieve was obtained and oven dried. The loss in mass resulting from the wash treatment was calculated as mass percentage of material finer than 75 μm (#200) sieve by washing.

The percentage of soil passing a #200 sieve was calculated per ASTM D1140-00[27].

Hydrometer Analysis

A hydrometer analysis is the test used to determine the grain size distribution of the soils passing a #200 sieve. It is based on Stokes' law, which relates the terminal velocity of a free-falling sphere in a liquid to its diameter. A series of density measurements at known depth of suspension and at known times of settlement gives the percentages of particles finer than the diameters given by Stokes' law. Thus, the series of readings reflects the amount of different sizes of particles in the fine-grained soils.

Sample Preparation. A dispersing solution was prepared by mixing 40 gm of calgon in 1000 ml of distilled water. This solution was required for defloccution of particles, as the clay particles have a tendency to adhere to each other and form larger masses.

The researchers took 50 gm of soil sample passing the #200 sieve for the hydrometer analysis. The soil sample was mixed with 125 ml of dispersing solution. Finally, distilled water was added to a make total of 1000 ml volume of suspended solution.

Procedure. The hydrometer test was conducted as per ASTM D422-63 [28]. The suspension was kept undisturbed, and readings were taken at 2, 4, 15, 30, 60, 90, 120 sec and 5, 15, 30 and 60 minute interval. The combined sieve and hydrometer analyses permitted estimates of the clay fraction of the soil; i.e. the percentage of particles finer than 2 μm.

Matric and Total Suction

Soil suction is the quantity that can be used to characterize the effect of moisture on volume, and it is a measurement of the energy or stress that holds the soil water in the pores. Surface tension at the air-water interface in an unsaturated soil will lead to negative water pressure in the soil and therefore referred to as matric suction. Matric suction varies with the soil's moisture content.

The total suction is expressed as a positive quantity and is defined as the sum of matric and osmotic suction. Researchers used the filter paper test to determine the initial total suction and matric suction of the soil sample. Thermocouple psychrometers were used to determine the total suction of soil over a period of time.

Filter Paper Test

The suction range of filter paper is from 0.1 to more than 1000 tons/ft^2. The filter paper test provides the initial total and matric suction of the soil sample for the determination of the diffusion coefficient. The procedure to determine total and matric suction using filter paper is given in Appendix A in Volume 2 of this report.

Total Suction Measurement

The total suction of a soil specimen can be measured using thermocouple psychrometers with the HR 33T microvoltmeter and CR7 devices. The detailed procedures for HR 33T and CR7 are given in Appendices B and C respectively in Volume 2 of this report.

Diffusion Coefficient

The diffusion coefficient can be measured in the laboratory as well as calculated using the empirical relationships involving index properties of soil. The laboratory test is based on the test proposed by Mitchell [29] (1979).

The samples were provided by the Texas Department of Transportation. These samples were stored in a moisture and temperature-controlled environment prior to testing.

The TAMU tests employed the drying procedure, described in Appendix D Volume 2, by sealing the sides and one end of the sample. The other end of the sample was left open to permit the flow of moisture out of the sample. The first psychrometer gave the most reliable data for the α coefficient determination. For the samples where the first psychrometer gave insufficient data, the α coefficient was calculated from the second psychrometer data.

Sample Selection

For the Fort Worth District site, two samples were taken from each borehole. For the Atlanta and Austin District sites, three soil samples were taken for each borehole. The samples were taken from the top, middle, and bottom depths of each borehole.

Suction-Water Content Curve

The constitutive relationship between water content or degree of saturation and suction is called the soil-water content curve. It provides a conceptual framework in which the behavior of unsaturated soils can be understood. This relationship generally depends on the particle size distribution of the soil. Each soil has a unique characteristic curve.

The pressure plate test was used in the laboratory to determine the relationship between water content and matric suction of soils. It was used to determine the desorption or drying soil-water retention curve. A typical pressure plate apparatus is shown in Figure 38.

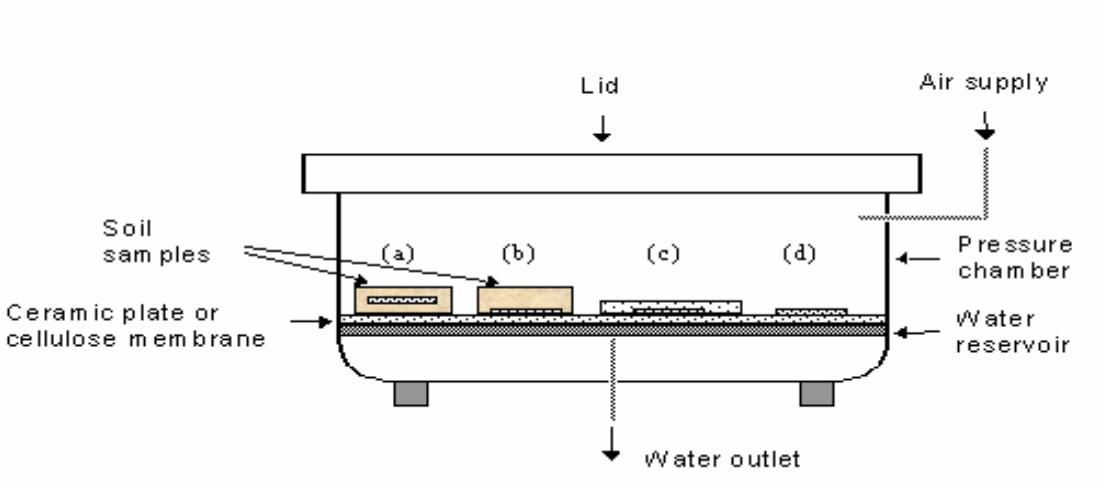

Figure 38. Pressure Plate Apparatus. (Source: Bulut, et al. [30])

The pressure plate apparatus consists of a high air entry porous ceramic plate to separate the water and air phases in a high air pressure chamber. The ceramic plate was saturated for 24 hrs prior to testing until no air bubbles were detected in the water outlet.

The soil samples were cut using a consolidometer ring and saturated completely with water. The chamber was filled with water to keep the sample and porous disk saturated. The chamber was closed and air pressure was applied. The setup was left for about 5 days until it reached equilibrium.

The water content of the sample was taken after the equilibrium period, and the air pressure was taken as the matric suction. Therefore, by estimating the water content of the sample at varying air pressure applied to the chamber with soil samples, the soil water content curve was developed.

SUMMARY OF LABORATORY TEST RESULTS

Fort Worth North Loop IH820

In the Fort Worth District there are three sections, each having five boreholes. The locations of the boreholes are given in Chapter 2.

The bore holes are designated as A1, A2, A3, A4, A5, B1, B2, B3, B4, B5, C1, C2, C3, C4 and C5 where A, B, and C depicts the section; and 1, 2, 3, 4, and 5 depicts the borehole number for each section.

The samples, up to a depth of 20 ft, were received from TxDOT. The samples were wrapped in one layer of aluminium foil and sealed in plastic bags. The average length of sample was 1 ft. The samples were kept in a moisture-controlled room before the testing. All the laboratory tests were conducted at TAMU.

For the diffusion test, two samples were taken from each borehole. One sample was taken from the top 6 ft and the second sample from 3 to 14 ft. The liquid limit varied from 36 to 63 percent and the plastic limit from 19 to 26 percent.

The summaries of the diffusion and filter paper tests are given in Table 7. The summaries of the Atterberg limit and hydrometer analysis are given in Table 8.

Table 7. Summary of Diffusion and Filter Paper Test for Fort Worth District.

No.	Sample No.	Depth (ft)	α coefficient (cm^2/sec)	Atomospheric Suction pF	Filter Paper Test (Initial Suction) pF	Filter Paper Test (Matric Suction) pF	Soil Description	Comments
1	A1	5-6	8.90x10-5	6.21	3.28	2.70	Tan color clay, small stones, roots, calcareous.	
2	A1	11-12	5.90x10-5	6.06	3.38	2.71	Light brown, silty, natural clay with gravels, shaley.	
3	A2	2-3	*3.06x10-5	6.21	4.59	4.58	Soft, dark brown clay.	α coefficient found from 2nd psychrometer. Results taken out by assuming intial suction.
4	A2	12-13	2.00x10-5	5.91	3.51	-	Soft, dark brown silty clay.	
5	A3	0-1	**8.66x10-5	6.22	4.92	4.76	Dark brown clay with roots and sandy.	Results taken out by assuming intial suction.
6	A3	9-10	5.05x10-5	6.21	3.25	3.02	Red brown color clay with limestone fragments, small cracks.	
7	A4	5-6	9.88x10-5	6.21	3.22	3.12	Tan color clay, with calcareous nodules, small roots.	
8	A4	10-11	0.33x10-5	6.22	4.26	3.93	Clay with limestones, sandy and cracks present, dry and hard.	
9	A5	3-4	7.86x10-5	6.21	3.02	2.58	Tan color clay, with calcareous nodules.	
10	A5	8-9	10.3x10-5	6.21	3.09	3.05	Tan color clay with gravels.	
11	B1	6-7	8.26x10-5	6.11	3.38	3.09	Light brown clay, calcareous, sandy on one side and clayey on the other.	
12	B1	9-10	8.6x10-5	5.93	3.20	3.18	Light brown clay, soft clay, silt present in small amount.	
13	B2	3-4	0.106x10-5	6.11	3.24	3.08	Dark brown color clay, calcareous, roots, large cracks.	Cracks on the cross section of open end.
14	B2	11-12	9.66x10-5	5.93	3.30	3.25	Tan color clay, shaley.	
15	B3	0-1	6.20x10-5	6.06	4.20	4.17	Light brown clay, with calcareous nodules, sandy.	α coefficient found from 2nd psychrometer.

* Diffusion coefficient for second psychrometer

** Initial suction assumed for calculation of diffusion coefficient

Table 7. (Continued)

No.	Sample No.	Depth (ft)	α coefficient (cm^2/sec)	Atomospheric Suction pF	Filter Paper Test (Initial Suction) pF	Filter Paper Test (Matric Suction) pF	Soil Description	Comments
16	B3	3-4	-	6.06	4.50	***4.53	Light brown clay, with limestone fragments and sandy.	Failed- First and second psychrometer did not work
17	B4	1-2	8.40x10-5	6.11	3.59	3.49	Dark brown clay, roots present, calcareous and cracks all around.	
18	B4	13-14	1.08x10-5	5.92	3.56	3.45	Tan color, shaley clay.	
19	B5	6-7	13.7x10-5	6.06	2.67	2.59	Tan color clay, silty, with calcareous nodules.	
20	B5	11-12	7.61x10-5	6.06	3.49	3.27	Light brown soft clay.	
21	C1	2-3	$3.73x10^{-5}$	6.22	3.28	2.89	Brown color clay, gravels present, small cracks.	
22	C1	6-7	$3.06x10^{-5}$	6.22	3.76	3.42	Dark brown soft clay.	
23	C2	4-5	$1.53x10^{-5}$	5.91	3.74	2.77	Tan color clay, silty.	
24	C2	5-6	$6.10x10^{-5}$	6.06	3.57	2.95	Tan color clay, silty.	
25	C3	6-7	$9.2x10^{-5}$	6.11	4.03	3.24	Light brown clay, calcareous and cracks present.	
26	C3	9-10	$0.93x10^{-5}$	6.75	3.38	3.11	Tan to light gray clay, shaley with calcareous nodules.	
27	C4	5-6	$1.93x10^{-5}$	5.93	3.38	3.11	Light brown clay, sandy with limestone, cracked and soft.	
28	C4	9-9.5	**$1.93x10^{-5}$	6.22	4.57	4.53	Light brown clay, soft, yellowish core & silty.	Results taken out by assuming initial suction.
29	C5	4-5	$2.93x10^{-5}$	6.22	3.61	3.13	Tan color clay, sandy with limestones.	
30	C5	7-8	$1.73x10^{-5}$	5.93	3.81	3.33	Light brown clay, shaley, hard.	

* Diffusion coefficient for second psychrometer

** Initial suction assumed for calculation of diffusion coefficient

*** One week equilibrium time not enough to obtain matric suction values

Table 8. Summary of Atterberg Limits and Hydrometer Test for Fort Worth District.

No.	Sample No.	Depth (ft)	LL	PL	PI	% clay (<0.002mm)	Fines Content (% passing #200)	Water Content (%)
1	A1	5-6	-	-	-	-	-	25.9
2	A1	11-12	45	23	22	21	84.15	18.0
3	A2	2-3	60	20*	40**	-	-	10.8
4	A2	12-13	-	-	-	-	-	24.8
5	A3	0-1	-	-	-	-	-	15.3
6	A3	9-10	63	20*	43**	30	93.57	23.8
7	A4	5-6	-	-	-	-	-	27.0
8	A4	10-11	49	21	28	-	-	8.8
9	A5	3-4	49	19	30	-	-	29.4
10	A5	8-9	-	-	-	-	-	19.3
11	B1	6-7	-	-	-	-	-	11.0
12	B1	9-10	58	20*	38**	-	-	19.1
13	B2	3-4	-	-	-	-	-	25.0
14	B2	11-12	53	21	32	-	-	18.4
15	B3	0-1	-	-	-	-	-	12.8

* Inferred PL values from the other soils with similar texture.

** PI values calculated from the inferred PL values.

Table 8. (Continued)

No.	Sample No.	Depth (ft)	LL	PL	PI	% clay (<0.002mm)	Fines Content (% passing #200)	Water Content (%)
16	B3	3-4	60	24	36	1	96.08	11.8
17	B4	1-2	-	-	-	-	-	11.4
18	B4	13-14	45	24	21	37	99.44	24.9
19	B5	6-7	36	21	15	-	-	11.3
20	B5	11-12	-	-	-	-	-	18.7
21	C1	2-3	62	26	36	25	99.68	22.8
22	C1	6-7	-	-	-	-	-	24.8
23	C2	4-5	49	19	30	-	-	25.0
24	C2	5-6	-	-	-	-	-	26.9
25	C3	6-7	-	-	-	-	-	18.0
26	C3	9-10	52	24	28	-	-	25.2
27	C4	5-6	50	19	31	-	-	15.5
28	C4	9-9.5	-	-	-	-	-	22.1
29	C5	4-5	-	-	-	-	-	17.8
30	C5	7-8	42	23	19	32	98.16	22.9

Atlanta US 271

There are three boreholes in the Atlanta District; one at the outside wheel path, the second in the middle of the shoulder, and the third in the ditch line. The location of the boreholes can be referred to in Chapter 2, Figure 32.

The samples are designated as A1, A2, A3, B1, B2, B3, C1, C2 and C3 where 'A', 'B', and 'C' depict the borehole number and '1', '2', and '3' depict the sample from the top, middle, and bottom depths of the borehole.

Samples up to a depth of 18 ft for each borehole were provided by TxDOT, along with the results of hydrometer analysis and in-situ water content. The average length of each sample was 2 ft. The diffusion test and Atterberg Limits were conducted at TAMU. The samples were well packed in one layer of aluminium foil and plastic bags to avoid the loss of moisture prior to testing. Further, the samples were kept in a moisture-controlled room to prevent the loss of water.

The diffusion test was conducted for three samples per borehole; one at a depth of 2 to 7 ft, the second at a depth of 9 to 11 ft, and the third at a depth of 11 to 14 ft. The Atterberg Limits were determined for samples at a depth of 6 to 6.5 ft (Borehole A), 3 to 5 ft (Borehole B) and 11 to 13 ft (Borehole C). The liquid limit was in the range of 37 to 48 percent and the plastic limit was in the range of 20 to 22 percent. The initial suction for all the depths at each borehole were determined to get the suction profile.

The summaries of the diffusion and filter paper tests are given in Table 9. The summaries of the Atterberg Limits and hydrometer analysis are given in Table 10.

Table 9. Summary of Diffusion and Filter Paper Test for Atlanta District.

No.	Sample No.	Depth (ft)	α coefficient (cm^2/sec)	Atomospheric Suction pF	Filter Paper Test (Initial Suction) pF	Filter Paper Test (Matric Suction) pF	Soil Description	Comments
1	A1	5-5.5	$4.83x10^{-5}$	6.06	2.84	2.50	Dark brown clay with stones.	
2	A2	9-11	$3.93x10^{-5}$	6.06	3.13	3.08	Tan color clay.	
3	A3	11-13	$1.23x10^{-5}$	6.06	3.21	3.09	Tan color clay.	Cracks found after the diffusion test.
4	B1	5-7	$5.66x10^{-5}$	5.79	3.38	3.15	Light brown, natural clay.	1-2 mm thick cracks on the open end. Cracks throughout the diameter after drilling. Cracks expanded on second day.
5	B2	9-11	$3.07x10^{-5}$	5.79	3.22	2.88	Light brown, natural clay.	
6	B3	13-14	$8.33x10^{-5}$	5.79	3.96	3.78	Tan color clay, sandy, dark brown tinge in some places, cracks on the surface.	Cracks increase after diffusion.
7	C1	2-4	$9.16x10^{-5}$	5.76	3.07	<2.50	Dark brown clay, sandy.	
8	C2	9-11	$13.1x10^{-5}$	5.76	3.43	<2.50	Light brown clay, sandy with roots.	
9	C3	11-13	$4.26x10^{-5}$	5.76	3.99	3.91	Light brown clay, sandy with roots.	

Table 10. Summary of Atterberg Limits and Hydrometer Test for Atlanta District.

No.	Sample No.	Depth (ft)	Depth of Sample for Atterberg Limit (ft)	LL	PL	PI	% Clay <0.002mm	Fines Content (% passing #200)	In-situ Water Content (%)
1	A1	5-5.5	6-6.5	37	20	17	7.6	83.5	20.5
2	A2	9-11					9.4	94.2	27.4
3	A3	11-13					7.7	90.8	23.3
4	B1	5-7	3-5	48	22	26	8.7	92.0	17.0
5	B2	9-11					8.6	93.4	26.8
6	B3	13-14					7.7	93.3	12.5
7	C1	2-4	11-13	37	22	15	9.0	94.1	16.1
8	C2	9-11					8.5	89.9	16.7
9	C3	11-13					9.1	92.1	15.8

Austin Loop 1

For the Loop 1 study, three boreholes were drilled on the frontage road on a sloping limestone bed. The location of the boreholes can be seen in Chapter 2, Figure 37.

The boreholes have been designated as B1, B2, and B3 followed by the depth from which the sample has been taken.

The average length of the sample was 1.5 ft. The diffusion, hydrometer test, and Atterberg Limits were conducted at TAMU. The samples were well packed in two plastic bags to avoid the loss of moisture. Further, the samples were kept in a moisture-controlled room to prevent the loss of water prior to testing.

The diffusion test was conducted for three samples per borehole; one at a depth of 2 to 5 ft, the second at a depth of 3.5 to 8 ft, and the third at a depth of 9.5 to 11 ft. For borehole B1 only two samples were found to be workable. The Atterberg Limits were determined for all the samples used for the diffusion test, and the liquid limit was in the range of 33 to 68 percent and plastic limit was in range of 14 to 21 percent.

The summaries of the diffusion and filter paper tests are given in Table 11. The summaries of the Atterberg Limits and hydrometer analysis are given in Table 12.

Table 11. Summary of Diffusion and Filter Paper Test for Austin District.

No.	Sample No.	Depth (ft)	α coefficient (cm^2/sec)	Atomospheric Suction pF	Filter Paper Test (Initial Suction) pF	Filter Paper Test (Matric Suction) pF	Soil Description	Comments
1	B1	2-3.5	$10.60x10^{-5}$	5.84	3.45	3.03	Tan color sandy clay, calcareous, soft, roots present and crack on face.	
2	B1	3.5-5	$5.65x10^{-5}$	5.84	3.53	3.04	Tan color sandy clay.	
3	B2	3.5-5	$7.66x10^{-5}$	5.76	3.21	3.01	Silty clay, gypsum, small stones present.	
4	B2	6.5-8	$6.30x10^{-5}$	5.76	3.39	3.03	Sandy clay, small stones, gypsum in small amount	
5	B2	9.5-10.7	$10.70x10^{-5}$	5.76	3.21	3.01	Soft silty clay, gravel, roots, no cracks	
6	B3	3.5-5	$3.20x10^{-5}$	5.9	3.46	3.10	Calcareous, gravelly clay, soft, stones present and tan color.	
7	B3	6.5-8	$1.82x10^{-5}$	5.9	3.64	3.30	Calcareous, gravelly clay, soft, stones present and tan color.	
8	B3	9.5-11	$4.66x10^{-5}$	5.76	3.77	3.45	Soft tan color clay, gravels present and no cracks.	

Table 12. Summary of Atterberg Limits and Hydrometer Test for Austin District.

No.	Sample No.	Depth (ft)	LL	PL	PI	% Clay <0.002mm	Fines Content (% passing #200)	Water Content (%)
1	B1	2-3.5	33	14	19	1.5	76.5	19.0
2	B1	3.5-5	47	18	29	30.0	75.3	19.4
3	B2	3.5-5	60	20*	40**	19.0	96.6	23.1
4	B2	6.5-8	68	20*	48**	30.0	91.8	23.0
5	B2	9.5-10.7	68	20*	48**	18.0	90.6	13.7
6	B3	3.5-5	49	20	29	42.0	84.9	21.2
7	B3	6.5-8	50	20*	30**	20.0	78.9	20.3
8	B3	9.5-11	50	21	29	18.0	95.9	24.1

* Inferred PL values from the other soils with similar texture.

** PI values calculated from the inferred PL values.

EMPIRICAL RELATIONS FOR SOILS

Slope of the Moisture-Suction Curve

The slope of the moisture-suction curve (S) can be obtained from the soil water characteristic curve, which is determined using the pressure plate apparatus. The parameter S can also be obtained from the empirical relationship given in TTI Project Report 197-28 [31]:

$$S = -20.29 + 0.155\,(LL) - 0.117\,(PI) + 0.0684\,(\text{percent Fines}) \qquad (57)$$

where:

LL = liquid limit

PI = plasticity index

percent Fines = percentage of particle sizes passing the #200 sieve on a dry weight basis

The slope of the moisture-suction curves for Fort Worth, Atlanta, and Austin are given in Tables 13, 14, and 15.

Table 13. Slope of the Moisture-Suction Curve for Fort Worth District.

District	No.	Sample No.	Depth (ft)	LL	PL	PI	% Clay <0.002mm	Fines Content (% passing #200)	S
FORT WORTH	1	A1	11-12	45	23	22	21	84.15	-10.13
	2	A2	2-3	60	20	40			-
	3	A3	9-10	63	20	43	30	93.57	-9.16
	4	A4	10-11	49	21	28	-	-	-
	5	A5	3-4	49	19	30	-	-	-
	6	B1	9-10	58	20	38	-	-	-
	7	B2	11-12	53	21	32	-	-	-
	8	B3	3-4	60	24	36	1	96.08	-8.63
	9	B4	13-14	45	24	21	37	99.44	-8.97
	10	B5	6-7	36	21	15	-	-	-
	11	C1	2-3	62	26	36	25	99.68	-8.07
	12	C2	4-5	49	19	30	-	-	-
	13	C3	9-10	52	24	28	-	-	-
	14	C4	5-6	50	19	31	-	-	-
	15	C5	7-8	42	23	19	32	98.16	-9.29

Table 14. Slope of the Moisture-Suction Curve for Atlanta District.

District	No.	Sample No.	Depth (ft)	LL	PL	PI	% Clay <0.002mm	Fines Content (% passing #200)	S
ATLANTA	1	A	6-6.5	37	20	17	7.6	83.5	-10.83
	2	B	3-5	48	22	26	8.7	92.0	-9.60
	3	C	11-13	37	22	15	9.1	92.1	-10.01

Table 15. Slope of the Moisture-Suction Curve for Austin District.

District	No.	Sample No.	Depth (ft)	LL	PL	PI	% Clay <0.002mm	Fines Content (% passing #200)	S
AUSTIN	1	B1	2-3.5	33	14	19	1.5	76.5	-12.17
	2	B1	3.5-5	47	18	29	30	75.3	-11.25
	3	B2	3.5-5	60	20	40	19	96.6	-9.06
	4	B2	6.5-8	68	20	48	30	91.8	-9.09
	5	B2	9.5-10.7	68	20	48	18	90.6	-9.17
	6	B3	3.5-5	49	20	29	42	84.9	-10.28
	7	B3	6.5-8	50	20	30	20	79.0	-10.65
	8	B3	9.5-11	50	21	29	18	95.9	-9.37

Volume Change Coefficient

The volume change coefficient is used to calculate the swell or shrink in soil by using Equation (58) given by Covar and Lytton[12]:

$$\frac{\Delta V}{V} = -\gamma_h \log_{10}\left(\frac{h_f}{h_i}\right) - \gamma_\sigma \log_{10}\left(\frac{\sigma_f}{\sigma_i}\right) \tag{58}$$

where:

ΔV = change in volume of soil

V = initial volume of soil

γ_h = volume change coefficient

h_f and h_i = initial and final water potential

γ_σ = mean principal stress compression index

σ_f and σ_i = normal stress terms

The volume change coefficient was determined using the Atterberg Limits, hydrometer analysis, and charts prepared by Covar and Lytton [12]. The volume change coefficient can be calculated using Equation (59):

$$\gamma_{h=(\%\text{fine clay})\ \text{x}\ \gamma_{100}} \tag{59}$$

where:

γ_{100} = volume change guide number

% fine clay = (% –2μ)/(% passing #200)

The volume change guide number was determined using the charts given by Covar and Lytton [12].

The volumetric change coefficients for the Fort Worth, Atlanta, and Austin sites are given in Tables 16, 17, and 18.

Table 16. Volumetric Change Coefficient for Fort Worth District.

District	No.	Sample No.	Depth (ft)	LL	PL	PI	% Clay <0.002mm	Fines Content (% passing #200)	Ac	LL/(%fc)	Zone	γ_{100}	γ_h
FORT WORTH	1	A1	11-12	45	23	22	21	84.15	0.88	1.80	III	0.142	0.0354
	2	A2	2-3	60	20	40	-	-	-	-	-	-	-
	3	A3	9-10	63	20	43	30	93.57	1.34	1.96	II	0.183	0.0588
	4	A4	10-11	49	21	28	-	-	-	-	-	-	-
	5	A5	3-4	49	19	30	-	-	-	-	-	-	-
	6	B1	9-10	58	20	38	-	-	-	-	-	-	-
	7	B2	11-12	53	21	32	-	-	-	-	-	-	-
	8	B3	3-4	60	24	36	1	96.08	34.59	57.65	III	0.05	0.0005
	9	B4	13-14	45	24	21	37	99.44	0.56	1.21	III	0.100	0.0372
	10	B5	6-7	36	21	15	-	-	-	-	-	-	-
	11	C1	2-3	62	26	36	25	99.68	1.44	2.47	III	0.236	0.0592
	12	C2	4-5	49	19	30	-	-	-	-	-	-	-
	13	C3	9-10	52	24	28	-	-	-	-	-	-	-
	14	C4	5-6	50	19	31	-	-	-	-	-	-	-
	15	C5	7-8	42	23	19	32	98.16	0.58	1.29	III	0.100	0.0326

Table 17. Volumetric Change Coefficient for Atlanta District.

District	No.	Sample No.	Depth (ft)	LL	PL	PI	% Clay <0.002mm	Fines Content (% passing #200)	Ac	LL/(%fc)	Zone	γ_{100}	γ_h
ATLANTA	1	A	6-6.5	37	20	17	7.6	83.5	1.87	4.07	III	0.083	0.0064
	2	B	3-5	48	22	26	8.7	92.0	2.75	5.08	III	0.050	0.0045
	3	C	11-13	37	22	15	9.1	92.1	1.52	3.74	III	0.238	0.0247

Table 18. Volumetric Change Coefficient for Austin District.

District	No.	Sample No.	Depth (ft)	LL	PL	PI	% Clay <0.002mm	Fines Content (% passing #200)	Ac	LL/(%fc)	Zone	γ_{100}	γ_h
AUSTIN	1	B1	2-3.5	33	14	19	1.5	76.5	9.69	16.83	I	0.380	0.007
	2	B1	3.5-5	47	18	29	30	75.3	0.73	1.18	I	0.108	0.043
	3	B2	3.5-5	60	20	40	19	96.6	2.03	3.05	I	0.350	0.069
	4	B2	6.5-8	68	20	48	30	91.8	1.47	2.08	II	0.209	0.068
	5	B2	9.5-10.7	68	20	48	18	90.6	2.42	3.42	II	0.350	0.070
	6	B3	3.5-5	49	20	29	42	84.9	0.59	0.99	II	0.933	0.462
	7	B3	6.5-8	50	20	30	20	79.0	1.18	1.97	II	0.163	0.041
	8	B3	9.5-11	50	21	29	18	95.9	1.55	2.66	III	0.240	0.045

Diffusion Coefficient

Diffusion coefficient (α) controls the rate of infiltration of surface moisture into the soil mass. It can be measured in the laboratory. The diffusion coefficient also can be estimated using empirical correlations to index properties.

The moisture diffusion coefficient can be evaluated by using Equations (60) and (61) given by Lytton [8]:

$$\alpha = |S| \, p\gamma_w / \gamma_d \tag{60}$$

where:

$|S|$ = slope of the pF versus gravimetric water content line

γ_d = dry unit weight of soil

γ_w = unit weight of water

The parameter p is determined from:

p = a measure of unsaturated permeability = $|h_0| \, k_0 / 0.434$ where

k_0 = the saturated permeability of the soil (calculated with γ_d =100 pcf, G_s=2.68, Lytton [8])

h_0 = the suction at which the soil saturates, approximately 200 cm

$$\alpha = 0.0029 - 0.000162(S) - 0.0122(\gamma_h) \tag{61}$$

where:

S = slope of the pF versus gravimetric water content line

γ_h = volume change coefficient

The comparison of diffusion coefficient using the two empirical correlations and laboratory tests is given in Tables 19 and 20. The comparison for the Atlanta District could not be provided due to insufficient data.

A variation in the diffusion coefficient evaluated by Equations (60) and (61) is produced because Equation (61) takes into account the cracks present in the soil mass in the field, and hence, the diffusion coefficient is higher.

Table 19. Comparison of Diffusion Coefficients for Fort Worth District.

District	No.	Sample No.	Depth (ft)	Saturated Permeability of soil (k_0, cm/sec)	Diffusion Coefficient (α, cm^2/sec) (60)	Diffusion Coefficient (α, cm^2/sec) (61)	Diffusion Coefficient (α, cm^2/sec) (laboratory)
FORT WORTH	1	A1	11-12	-	-	4.11E-03	8.90E-05
	2	A2	2-3	-	-	-	-
	3	A3	9-10	3.50E-09	9.21E-06	3.67E-03	3.06E-05
	4	A4	10-11	-	-	-	-
	5	A5	3-4	-	-	-	-
	6	B1	9-10	-	-	-	-
	7	B2	11-12	-	-	-	-
	8	B3	3-4	-	-	-	-
	9	B4	13-14	1.02E-08	2.63E-05	3.90E-03	7.86E-05
	10	B5	6-7		-	-	-
	11	C1	2-3	1.00E-08	2.32E-05	3.49E-03	8.26E-05
	12	C2	4-5	-	-	-	-
	13	C3	9-10	-	-	-	-
	14	C4	5-6	-	-	-	-
	15	C5	7-8	1.08E-08	2.88E-05	4.01E-03	6.20E-05

Table 20. Comparison of Diffusion Coefficients for Austin District.

District	No.	Sample No.	Depth (ft)	Saturated Permeability of soil (k_0, cm/sec)	Diffusion Coefficient (α, cm^2/sec) (60)	Diffusion Coefficient (α, cm^2/sec) (61)	Diffusion Coefficient (α, cm^2/sec) (laboratory)
AUSTIN	1	B1	2-3.5	-	-	4.78E-03	-
	2	B1	3.5-5	1.02E-08	3.30E-05	4.11E-03	5.65E-05
	3	B2	3.5-5	-	-	3.59E-03	7.66E-05
	4	B2	6.5-8	2.50E-09	1.69E-05	3.69E-03	6.30E-05
	5	B2	9.5-10.7	6.00E-09	2.31E-05	3.82E-03	1.07E-04
	6	B3	3.5-5	4.50E-09	8.87E-06	4.05E-03	3.21E-05
	7	B3	6.5-8	-	-	3.90E-03	1.82E-05
	8	B3	9.5-11	-	-	3.89E-03	4.66E-05

CHAPTER 4:
COMPUTATIONAL MODEL DEVELOPMENT

INTRODUCTION

In this chapter, the sequentially coupled unsaturated transient flow and deformation model employed in the finite element method (FEM) computer program FLODEF is described. The theoretical background of the program WinPRES to estimate the development of pavement roughness on expansive soil subgrades is presented. FLODEF and WinPRES have a friendly graphic user interface (GUI) for inputting data and viewing output results.

Finite Element Analysis of Transient Flow and Deformation

The computer program FLODEF computes the unsaturated moisture flow and movement in an expansive clay domain using a sequential analysis of flow and deformation. Moisture flow is analyzed through Mitchell's model by converting the nonlinear partial differential equation given in the modified Darcy's law into an ordinary partial differential equation. Two-dimensional soil deformations are calculated with a nonlinear elastic model for each incremental time step.

Transient Flow Model

The transient flow model for unsaturated moisture flow through porous media is based on Darcy's law and modified by Richards given as:

$$C(\phi)\ \frac{\partial \phi}{\partial t} = \frac{\partial}{\partial x_i}[K_{ij}(\phi)\{\frac{\partial \phi}{\partial x_j} + \frac{\partial Z}{\partial x_j}\}] - Q(\phi, x_i, t) \qquad i, j = 1,3 \qquad (62)$$

where:

$C(\phi)$ = the slope of the desorption curve ($\frac{d\theta}{d\phi}$)

$K_{ij}(\phi)$ = the permeability tensor

$Q(\phi, x_i, t)$ = A source or sink term (heat flux) that may be described as a variable function of matric potential ϕ, spatial coordinates, and time

By employing Mitchell's two assumptions [32]: (a) the unsaturated permeability is linearly related to the reciprocal of total suction; (b) the desorption relationship is linear when the matric potential is expressed in terms of pF, then moisture flow through unsaturated soil domain is defined by:

$$v = -k_0 \frac{h_0}{h} \frac{dh}{dx} \tag{63}$$

where:

v =velocity of flow (cm/sec)

k_0=saturated permeability (cm/sec)

h_0=total suction

h= suction in cm of water

Soil suction is conveniently measured in logarithmic units of pF, where $u(pF)=\log_{10}h=0.4343\log_e h$, so:

$$\frac{d}{dx}(u) = \frac{0.4343}{h} \frac{dh}{dx}$$

$$v = \frac{k_0 h_0}{0.4343} \frac{d}{dx}(u) \tag{64}$$

Through the application of Darcy's law and moisture flow continuity equation, the unsaturated moisture flow for a two- dimensional soil domain can be modeled with log-linear solution of Mitchell's equation:

$$\frac{\partial^2 u}{\partial x^2} + \frac{\partial^2 u}{\partial y^2} + \frac{f(x,y,t)}{p} = \frac{1}{\alpha} \frac{\partial u}{\partial t}$$
$$\alpha = \frac{\gamma_w}{\gamma_d} \frac{p}{c}, \; c = \frac{\partial w}{\partial u}, \quad p = \frac{k_0 h_0}{0.4343} \tag{65}$$

where:

α = diffusion coefficient

γ_w = water density

γ_d =soil dry density

c = inverse slope of log suction (pF) vs. gravimetric water content curve (pF^{-1})

f(x,y,t) = a flow quantity which may be used to model a moisture source or sink with respect to space and time

Mitchell modeled the effects of climate (rainfall and evapotranspiration) by a sinusoidal change in suction over time at the soil surface. For a sinusoidal suction change at the soil surface of frequency n, where $u(0,t)=u_e+u_0\cos(2\pi nt+\varphi\ \pi)$, given that u_e is the equilibrium matric potential, u_0 is the amplitude of matric potential sinusoidal curve change, n is the frequency of weather change (cycles/year),and φ is the phase angle of sinusoidal curve, the one-dimensional analytical solution for suction u(y,t) at any depth y may be obtained from:

$$u(y,t)=u_e+u_0 e^{-(\sqrt{\frac{n\pi}{\alpha}})y}\cos(2\pi nt-\sqrt{\frac{n\pi}{\alpha}}y+\varphi\pi) \qquad (66)$$

The parameters u_e, u_0, α ,n , and φ have been expressed above.

Mitchell suggests the use of step functions (constant suction values in climatic cycles) for the modeling of arid and wet climates as these comprise relatively longer continuous periods of wet or dry followed by shorter ones.

In FLODEF, nine different regions (**El Paso/ Snyder/Wichita Falls/ Converse/ Seguin /Dallas/Ennis//Houston/Port Arthur**) are studied for soil suction variation and deformation calculation. The initial moisture conditions at the start of analysis fall into three categories: wet condition (winter season); equilibrium condition (spring/ fall season); and dry condition (summer season). Table 21 summarizes the values of equilibrium matric suction u_e, amplitude of matric potential u_0, and climate variation frequency for these regions.

Table 21. Initial Conditions for the Analysis.

City	TMI	Equilibrium Suction (pF)	Initial Condition					
			Wet		Equilibrium		Dry	
			Amplitude (pF)	Phase	Amplitude (pF)	Phase	Amplitude (pF)	Phase
El Paso	-46.8	4.5	0.75	-1.0	0.75	-0.5	0.75	0.0
Snyder	--	3.9	0.60	-1.0	0.60	-0.5	0.60	0.0
Wichita Falls	--	3.9	0.60	-1.0	0.60	-0.5	0.60	0.0
Converse	-21.3	3.85	0.65	-1.0	0.65	-0.5	0.65	0.0
Seguin	-21.3	3.85	0.65	-1.0	0.65	-0.5	0.65	0.0
Dallas	-11.3	3.6	1.00	-1.0	1.00	-0.5	1.00	0.0
Ennis	-11.3	3.8	0.70	-1.0	0.70	-0.5	0.70	0.0
Houston	14.8	3.1	1.00	-1.0	1.00	-0.5	1.00	0.0
Port Arthur	26.8	2.9	0.75	-1.0	0.75	-0.5	0.75	0.0

The dynamic boundary condition (surface suction variation) has combined sinusoidal function $u(0,t) = u_m + \cos(2\pi nt + \varphi'\pi)$ with step function, where u_m is the mean moisture potential value at the surface, n is the climate pattern change frequency (cycles/year), and φ' is the phase angle with respect to initial condition (dry/equilibrium/wet). Figure 39 demonstrates the surface suction variation with time at El Paso.

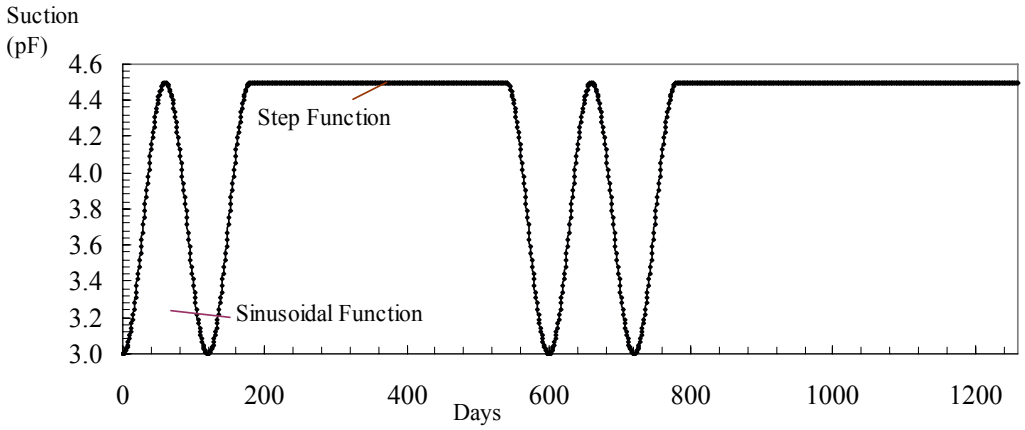

Figure 39. Surface Suction Variation with Time at El Paso, Initial Wet.

Deformation Model

A nonlinear elastic model is applied to compute the incremental deformation value for each element node in the expansive soil domain. The Young's Modulus E at each element's integration point is a function of its current mean principal normal stress, σ_m; matric potential, h_m; Poisson's ratio, ν; and suction volumetric change index, γ_h, as shown below:

$$E = \frac{(\sigma_m - \theta h_m)(1 + \frac{0.4343}{sw})}{\gamma_h(0.435)} \frac{(1+\nu)(1-2\nu)}{(1-\nu)} \qquad (67)$$

Given:

σ_m = current mean principal normal stress at this integration point

v = Poisson's Ratio

γ_h = suction volumetric change index

s = soil desorptive curve slope (suction vs gravimetric water content w)

w = gravimetric water content (decimal)

h_m = total matric potential at current incremental time step

θ = current volumetric water content at this point

The volumetric strain, ε_v, created in each incremental time step is calculated in the form of Dr. Lytton's equation ("-" sign for shrinkage case and "+" sign for swelling case) [31] :

$$\varepsilon_v = -\gamma_h \log \frac{h_f}{h_i} \pm \gamma_\sigma \log \frac{\sigma_f}{\sigma_i} \qquad (68)$$

where:

γ_h = suction volumetric change index

γ_σ = mechanical stress volumetric change index

h_f = current suction value (pF) at the integration point

h_i = suction value for previous time step (pF) at the integration point

σ_f = current mean principal normal stress at the integration point

σ_i = minimal mechanical stress level for overburden effect, usually expressed as the vertical mechanical stress, caused by 80 cm soil layer depth

FLODEF Validation

To validate the computer program, the analysis results from FLODEF have been compared with those of the ABAQUS program. The two are matched very closely as shown in Figures 40 and 41.

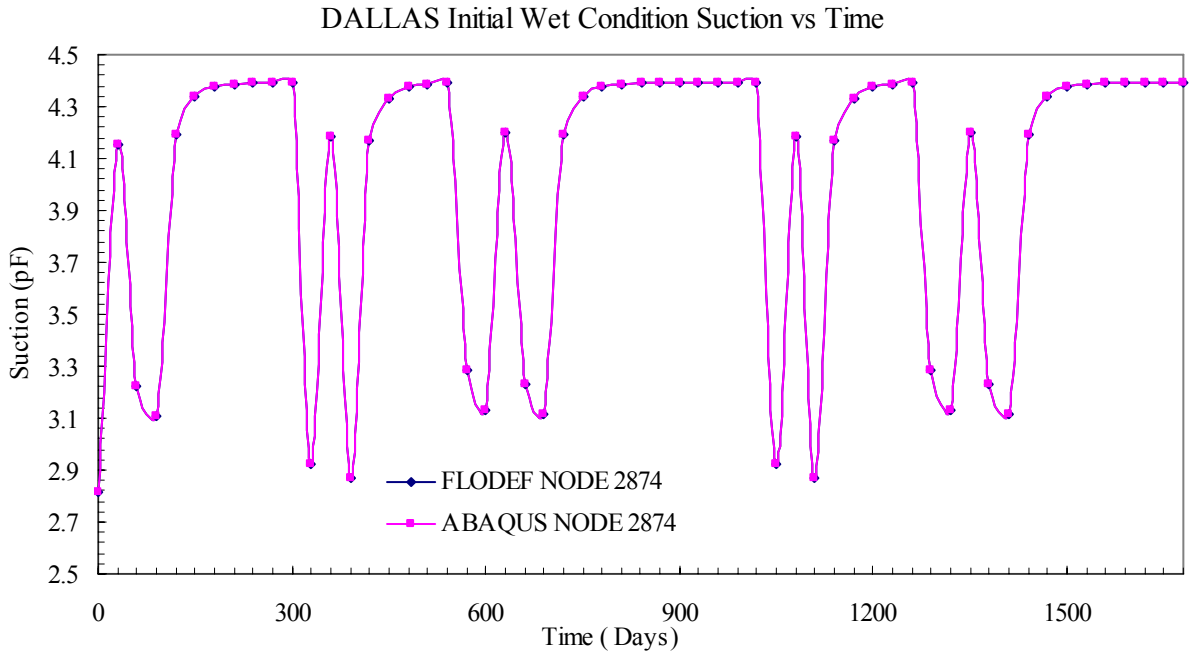

Figure 40. FLODEF and ABAQUS Results Comparison (Suction).

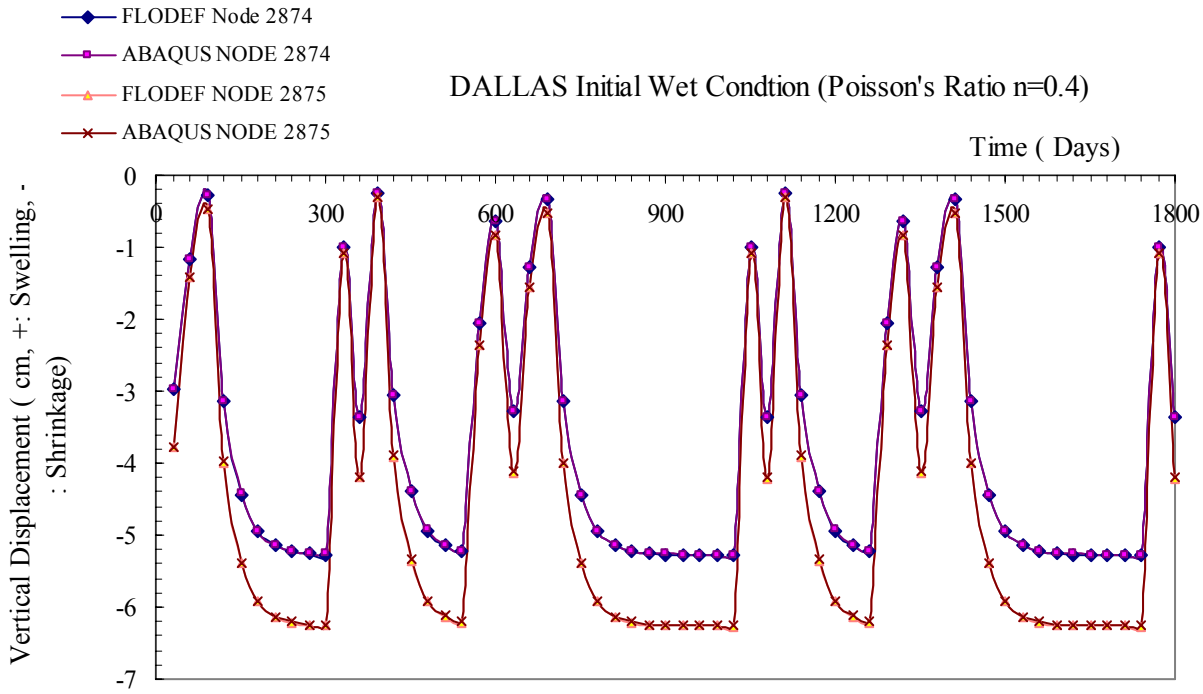

Figure 41. FLODEF and ABAQUS Results Comparison (Vertical Displacement).

THEORETICAL BACKGROUND OF PAVEMENT DESIGN PROGRAM

The program WinPRES is a model to estimate the development of pavement roughness on expansive soil subgrades, including the effects of the depth of a vertical barrier and thickness of inert and stabilized soil. The program generates graphically a suction envelope at the edge of the pavement, calculates vertical movement at the edge of the pavement and at any wheel path of interest, and then estimates the serviceability index and the international roughness index with time.

This program has been refined and advanced from the previous one, PRES.exe, developed by Jayatilaka (1999) [7]. A more realistic suction profile with depth is added. The crack fabric factor, f; initial mean principal stress, σ_i; and the lateral earth coefficient K_0, are refined as noted in Chapter 1. The method to determine suction compression index (SCI), γ_h, is modified using low cost and easily available testing methods such as Atterberg Limits and soil particle size distributions instead of using cation exchange activity (CEAc). The suction-versus-volumetric water content curves as simplified for natural, inert, and stabilized soil are used to estimate the depth of available moisture (d_{am}) and the mean principal stress compression index, γ_σ. The effects of the thickness of inert and stabilized soil are added and the program is extended to be used in both rigid and flexible pavement system.

A volume change model was developed to estimate the vertical movement at any point on a pavement surface in order to correlate the vertical movement to the rate of increase of roughness measurements made in different wheel paths of the pavement sections. This model estimates the total vertical movement including the swelling and shrinkage in a single column soil at the edge of the pavement using the subgrade soil properties and extreme suction envelope for the given locality based on the Thornthwaite moisture index and drainage conditions. The probable vertical movement (PVM) in any given wheel path is then calculated using a set of regression equations.

The model which predicts the rate of increase of pavement roughness in terms of serviceability index and international roughness index with time, is based upon the predicted movement of the subgrade soil and the roughness measurements that were observed in the monitoring program conducted by TTI for over 15 years on Texas pavements.

The vertical movement model and the roughness model developed were then assembled in the program PRES written in the Fortran language. The input data are entered to the new program through a WINDOWS graphical user interface developed using a Visual Basic tool.

Two-Dimensional Vertical Movement

Jayatilaka (1999) [7] suggested a regression model to estimate the relationship between one-dimensional and two-dimensional vertical movement, using the two programs MOPREC and FLODEF developed by Gay (1994) [6]:

$$\frac{VM_{2D}}{VM_{1D}} = \xi_1 \exp\left[\left(\xi_2 \frac{d}{D}\right)^{\xi_3}\right] \tag{69}$$

where:

VM_{2D}	=	two dimensional vertical movement
VM_{1D}	=	one dimensional vertical movement
d	=	distance from the center of the pavement to the point where the vertical movement needs to be calculated
D	=	half width of the pavement
ξ_1, ξ_2, ξ_3	=	regression coefficients

The FLODEF program calculates the transient unsaturated moisture flow and deformation in an expansive clay using a sequential analysis of flow and deformation. The one-dimensional vertical movement program MOPREC was used in the development of regression equations for the estimation of vertical movement in a two-dimensional domain.

The regression equations for the parameters ξ_1, ξ_2, and ξ_3 were developed using a multiple linear regression analysis with the statistical analysis software package developed by SAS Institute, Inc. :

For pavement width less than 18.0 m:

$$\xi_1 = 0.0561 + 1.5872(0.67 d_{am}) + 0.1244(S_m) - 0.1936(\log_e D) - 0.0007139(VM_{1D} * S_m) - 0.1443(DB * 0.67 d_{am}) \tag{70 a}$$

$$\xi_2 = -0.068 + 0.09134(S_m) - 0.101(DB) - 0.000188(TMI^2) \quad \text{(70 b)}$$
$$+0.321(\log_e D) + 0.000153(VM_{1D} * S_m) + 0.000706(VM_{1D} * DB)$$

$$\xi_3 = \exp(1.8061 - 0.4397(S_m) + 0.4711(\log_e D) + 0.08855(DB^2) \quad \text{(70 c)}$$
$$-0.000143(VM_{1D} * TMI) + 0.003022(VM_{1D} * DB)$$
$$-1.2592(DB * 0.67d_{am}))$$

For pavement width less than 22.0 m:

$$\xi_1 = 0.3736 + 0.4141(0.67d_{am}) + 0.04078(S_m) - 0.0924(\log_e D) \quad \text{(71 a)}$$
$$-0.000426(VM_{1D} * S_m) - 0.02584(DB * 0.67d_{am})$$

$$\xi_2 = +0.0298 + 0.09345(S_m) - 0.08724(DB) - 0.00001643(TMI^2) \quad \text{(71 b)}$$
$$+0.1701(\log_e D) + 0.00049(VM_{1D} * S_m) + 0.000256(VM_{1D} * DB)$$

$$\xi_3 = \exp(3.5562 - 0.8125(S_m) + 0.3707(\log_e D) + 0.05649(DB^2) \quad \text{(71 c)}$$
$$-0.000306(VM_{1D} * TMI) - 1.6175(0.67d_{am})$$
$$-0.4207(DB * 0.67d_{am})$$

where:

VM_{1D} = vertical movement from 1-D program (mm)

DB = depth of barrier (m)

d_{am} = depth of available moisture (m)

D = half width of pavement (m)

S_m = mean suction at site (pF)

TMI = Thornthwaite moisture index

The depth of available moisture refers to the quantity of water that the soil is capable of storing for use by plants. It depends on soil properties that affect the retention of water and the depth of the root zone. The depth of available moisture is estimated from the following relationship:

$$d_{am} = \sum_{i=1}^{N} (\theta_{wi} - \theta_{di}) \Delta z_i \quad (72)$$

where:

Δz_i = thickness of element in the ith layer

N = number of layers

θ_{wi} = volumetric moisture content in the wetting suction envelope of the ith layer

θ_{di} = volumetric moisture content in the drying suction envelope of the ith layer

Roughness Model

The sigmoidal models with respect to PSI and IRI to estimate the loss of serviceability and increase of roughness with time are given by:

With respect to PSI:

$$PSI = PSI_0 - (PSI_0 - 1.5) \exp\left[-\left(\frac{\rho_s}{t} \right)^{\beta_s} \right] \quad (73)$$

With respect to IRI:

$$IRI = IRI_0 + (4.2 - IRI_0) \exp\left[-\left(\frac{\rho_i}{t} \right)^{\beta_i} \right] \quad (74)$$

where:

PSI_0 = initial serviceability index of the pavement (usually 4.2)

t = time in months

IRI_0 = initial IRI in m/km or in/mile (usually 1.19m/km)

$\rho_s, \beta_s, \rho_i, \beta_i$ = roughness parameters

A terminal PSI of 1.5 corresponds to an IRI of 4.2 m/km. In the roughness parameters, the best values for β_s and β_i were found to be 0.66 and 0.56, respectively, using nonlinear regression. Considering the development of roughness caused by both traffic and expansive soil, the parameters ρ_s and ρ_i were suggested by the following forms:

$$\rho_s = A_s - B_s \Delta H \quad (75\ a)$$

$$\rho_i = A_i - B_i \Delta H \quad (75\ b)$$

where:

ΔH = total vertical movement in mm, including both shrinkage and swelling

A_s, A_i = parameters that are functions of traffic, structural number (SN) of the flexible pavement, pavement section, and resilient modulus of subgrade soil (M_r)

B_s, B_i = constants

The values of B_s and B_i were estimated for a site by assigning a reliability and using the following relationships:

$$B_s = 17.960 + 4.195Z \quad (76\text{ a})$$

$$B_i = 35.817 + 8.158Z \quad (76\text{ b})$$

where:

Z = standard normal variable corresponding to the assigned reliability

Z can be determined from Table 22.

Table 22. Standard Normal Deviates for Various Levels of Reliability.

Reliability (%)	Standard Normal Deviate (Z)	Reliability (%)	Standard Normal Deviate (Z)
50	0.000	93	-1.476
60	-0.253	94	-1.555
70	-0.524	95	-1.645
75	-0.674	96	-1.751
80	-0.841	97	-1.881
85	-1.037	98	-2.054
90	-1.282	99	-2.327
91	-1.340	99.9	-3.090
92	-1.405	99.99	-3.750

The parameters A_s and A_i were estimated using the American Association of State Highway and Transportation Officials (AASHTO) design equation (AASHTO 1993) [33] for flexible pavements.

Roughness Parameter, A_s in the Flexible Pavement

The AASHTO design based on the results of the AASHTO road test for flexible pavements is as follows:

$$\log_{10} W_{18} = -ZS_0 + 9.36\log_{10}(SN+1) - 0.20 + \frac{\log_{10}\left[\frac{\Delta PSI_w}{PSI_0 - 1.5}\right]}{0.4 + \frac{1094}{(SN+1)^{5.19}}} + 2.32\log_{10} M_r - 8.07 \quad (77)$$

where:

W_{18} = 80KN (18 kip) single-axle load applications

Z = standard normal deviate

S_0 = combined standard error, 0.44 in flexible pavements (AASHTO) [33]

SN = structural number of pavement, in inches

ΔPSI_w = loss of serviceability due to traffic

PSI_0 = initial serviceability (usually 4.2)

M_r = resilient modulus of subgrade soil, in lbf/in^2

The 80 kN single-axle load applications for a specific time interval in the analysis period can be calculated from the following traffic equation used by the Texas Department of Transportation:

$$W_{18} = \frac{N_c}{C(r_0 + r_c)}\left[2r_0 t_k + \left[\frac{r_c - r_0}{C}\right] t_k^2\right] \quad (78)$$

where:

W_{18} = the total accumulated number of 80 kN (18 kip) ESALs up to the time, t_k

C = analysis period

t_k = time in years

r_0 = average daily traffic (ADT) in one direction when t_k =0.0

r_c = average daily traffic (ADT) in one direction when $t_k = C$

N_c = total 80 kN (18 kip) ESALs over the analysis period, C (provided by TxDOT's TPP Division)

Equation (77) is modified to:

$$\log_{10}\left[\frac{\Delta PSI_w}{(PSI_0 - 1.5)}\right] = \lambda \tag{79}$$

where λ is given by:

$$\lambda = \left[0.4 + \frac{1094}{(SN+1)^{5.19}}\right] x \left[\log_{10} W_{18} - 9.36\log_{10}(SN+1) + 8.07 - 2.32\log_{10} M_r + ZS_0\right] \tag{80}$$

Equation (79) can be expressed as:

$$\Delta PSI_w = (PSI_0 - 1.5)10^{\lambda} \tag{81}$$

From Equation (73), the total serviceability loss (ΔPSI_t) is given by:

$$\Delta PSI_t = (PSI_0 - 1.5)\exp\left[-\left(\frac{\rho_s}{t}\right)^{0.66}\right] \tag{82}$$

When the vertical movement (ΔH) is equal to zero, from Equation (73), $\rho_s = A_s$. Then, the total loss of serviceability calculated from Equation (82) is equal to the serviceability loss due to traffic (ΔPSI_w) as follows:

$$\Delta PSI_w = (PSI_0 - 1.5)\exp\left[-\left(\frac{A_s}{t}\right)^{0.66}\right] \tag{83}$$

Solving Equations (81) and (83), A_s is given by:

$$A_s = t\left[\log_e(10^{-\lambda})\right]^{\left(\frac{1}{0.66}\right)} \tag{84}$$

A value of t of 480 months (=40 years) is assumed to be the time required for the roughness due to expansive clays to be complete, and λ is estimated for 40 years. This value of A_s is used in Equations (73) and (75 a) to predict the PSI history of a flexible pavement on expansive clay.

Roughness Parameter, A_i in the Flexible Pavement

Since the AASHTO design equation is not available in terms of IRI, the parameter A_i cannot be estimated directly as in the case of A_s. A regression relationship between PSI and IRI was developed using PSI and IRI values calculated in the previous study by Jayatilaka (1999) [7] :

$$IRI = 8.4193 \exp(-0.4664 PSI) \tag{85}$$

where IRI is in m/km.

Using Equation (85) and assuming an initial serviceability index of 4.2, the PSI at any time is given by:

$$PSI = PSI_0 - (PSI_0 - 1.5)10^{\lambda} \tag{86}$$

When $PSI_0 = 4.2$, this equation is simplified to:

$$PSI = 4.2 - 2.7(10^{\lambda}) \tag{87}$$

From Equation (85), the corresponding IRI is given by:

$$IRI = 8.4193 \exp\left[-0.4664(4.2 - 2.7(10^{\lambda}))\right] \tag{88}$$

From Equation (85), the initial IRI, which corresponds to PSI of 4.2, is estimated to be 1.19(m/km). Then the change in IRI due to traffic (ΔIRI_w) is given by:

$$\Delta IRI_w = 8.4193 \exp\left[-0.4664(4.2 - 2.7(10^{\lambda}))\right] - 1.19 \tag{89}$$

From Equation (74), the total change in IRI (ΔIRI_t) is given by:

$$IRI_t = (4.2 - 1.19) \exp\left[-\left(\frac{\rho_i}{t}\right)^{0.56}\right] \tag{90}$$

When the vertical movement (ΔH) is equal to zero, from Equation (75 b), $\rho_i = A_i$.

Then, the total change in IRI calculated from Equation (90) is equal to the change in IRI due to traffic (ΔPSI_w) as follows:

$$\Delta IRI_w = 3.01 \exp\left[-\left(\frac{A_i}{t}\right)^{0.56}\right] \tag{91}$$

Solving Equations (89) and (91), A_i is given by:

$$A_i = t\left[\log_e\left(\frac{3.01}{8.4193\exp\left(-0.4664(4.2-2.7(10^{\lambda}))-1.19\right)}\right)\right]^{\left(\frac{1}{0.56}\right)} \tag{92}$$

As in the case of PSI, t is taken as 480 months and λ is estimated for 40 years.
This equation for A_i is used in Equations (74) and (75 b) to predict the IRI history of a flexible pavement on expansive soil.

Roughness Parameter, A_s in the Concrete Pavement

A similar process is used to find the A and B coefficients to predict the roughness and riding quality development due to both traffic and expansive clays. The process starts with the AASHTO 1993[33] concrete pavement design program for rigid pavements as follows:

$$\log_{10} W_{18} = -Z_R S_0 + 7.35\log_{10}(D+1) - 0.06 + \frac{\log_{10}\left[\frac{\Delta PSI}{4.5-1.5}\right]}{1+\frac{1.624\times10^7}{(D+1)^{8.46}}} \tag{93}$$

$$+(4.22-0.32p_t)\log_{10}\left[\frac{S_c' C_d\left(D^{0.75}-1.132\right)}{215.63J\left(D^{0.75}-18.42/\left(E_c/k\right)^{0.25}\right)}\right]$$

where:

D = thickness of concrete layer (inches)

S_c' = modulus of rupture of concrete (psi)

J = load transfer coefficient

C_d = drainage coefficient

E_c = modulus of elasticity of Portland cement concrete (psi)

k = modulus of subgrade reaction (lb/in^3)

S_0 = combined standard error, 0.34 in rigid pavements (AASHTO) [33]

Z_R = standard normal deviate

p_t = terminal present serviceability index

ΔPSI = Loss of serviceability due to traffic

Equation (93) is modified to

$$\log_{10}\left[\frac{\Delta PSI_w}{(PSI_0 - 1.5)}\right] = \lambda \tag{94}$$

where λ is given by:

$$\lambda = \left[1 + 1.624\times10^7/(D+1)^{8.46}\right]\times\lambda' \tag{95}$$

where:

$$\lambda' = \log_{10} W_{18} - 7.35\log_{10}(D+1) + 0.06 - (4.22 - 0.32\,p_t)\log_{10}\left[\frac{S_c' C_d\left(D^{0.75} - 1.132\right)}{215.63J\left(D^{0.75} - 18.42/\left(E_c/k\right)^{0.25}\right)}\right] + Z_R S_0 \tag{96}$$

Equation (95) can be expressed as:

$$\Delta PSI_w = (PSI_0 - 1.5)10^{\lambda} \tag{97}$$

From Equation (73), the total serviceability loss (ΔPSI_t) is given by:

$$\Delta PSI_t = \left(PSI_0 - 1.5\right)\exp\left[-\left(\frac{\rho_s}{t}\right)^{0.66}\right] \tag{98}$$

When the vertical movement (ΔH) is equal to zero, from Equation (73), $\rho_s = A_s$. Then, the total loss of serviceability calculated from Equation (98) is equal to the serviceability loss due to traffic (ΔPSI_w) as follows:

$$\Delta PSI_w = (PSI_0 - 1.5)\exp\left[-\left(\frac{A_s}{t}\right)^{0.66}\right] \tag{99}$$

Solving Equations (97) and (99), A_s is given by:

$$A_s = t\left[\log_e(10^{-\lambda})\right]^{\left(\frac{1}{0.66}\right)} \tag{100}$$

where t = 40 yrs = 480 months is the time at which all of the roughness developed by expansive soils is estimated to be complete.

Roughness Parameter, A_i in the Concrete Rigid Pavement

Using Equation 83 and assuming an initial serviceability index of 4.5, the PSI at any time is given by:

$$PSI_0 - PSI = (PSI_0 - 1.5)10^{\lambda} \tag{101}$$

Since $PSI_0 = 4.5$ from the AASHTO Road Test, this is simplified by:

$$PSI = 4.5 - (3.0)10^{\lambda} \tag{102}$$

From Equation (85), the corresponding IRI is given by:

$$IRI = 8.4193\exp\left[-0.4664(PSI)\right] \tag{103}$$

From rearranging Equation (103)

$$IRI = 8.4193\exp\left[-0.4664(4.5 - (3.0)10^{\lambda})\right] \tag{104}$$

The initial IRI corresponding to an initial $PSI_0 = 4.5$ is estimated to be 1.032 (m/km). Then the change in IRI due to traffic (ΔIRI_w) is given by:

$$\Delta IRI_w = 8.4193\exp\left[-0.4664(4.5 - 3.0(10)^{\lambda})\right] - 1.032 \tag{105}$$

Then, the total change of IRI is:

$$\Delta IRI_t = (4.2 - 1.032)\exp\left[-\frac{\rho_i}{t}\right]^{0.56} \tag{106}$$

If $\Delta H = 0.0$ and $\rho_i = A_i$, then the total change in IRI obtained from Equation (106) is equal to the change in IRI due to traffic alone as follows:

$$\Delta IRI_w = (3.168)\exp\left(-\frac{A_i}{t}\right)^{0.56} \tag{107}$$

Solving Equations (105) and (107), A_i is given by:

$$A_i = t\left[-\log_e\left(\frac{3.168}{8.4193\exp\left[-0.4664(4.2-3.0(10))^{\lambda}\right]}\right)\right]^{-\left(\frac{1}{0.56}\right)} \tag{108}$$

where as before t = 40 years, or 480 months, and λ_r is determined for the 40-year period.

These equations for both flexible and rigid pavements are used to estimate the rate of increase roughness (IRI) and decrease of riding quality (PSI) due to both traffic and expansive clay movements.

CHAPTER 5:
TRANSIENT FLOW–DEFORMATION ANALYSIS OF PROJECT SITES

INTRODUCTION

In this chapter, the case studies of transient flow–deformation analysis of four different field sites (Fort Worth North Loop 820 study sections A and B, Atlanta US 271, Austin Loop 1) with FLODEF are presented. The effects of paving the median, various depths of vertical moisture barriers, various depths of lime stabilization, various depths of "inert" material, and various paving widths of shoulder are studied and summarized.

FORT WORTH NORTH LOOP IH 820 STUDY SECTION A

Two-Dimensional Model

In order to broaden the existing pavement structure, an additional embankment is proposed to add to the original pavement in the Fort Worth North Loop IH 820 study section A site. The proposed pavement structure will be composed of 12 inches of continuously reinforced concrete pavement (CRCP) and 4 inches asphaltic concrete pavement (ACP).The pavement cross section for this two-dimensional finite element method analysis is shown in Figure 42.

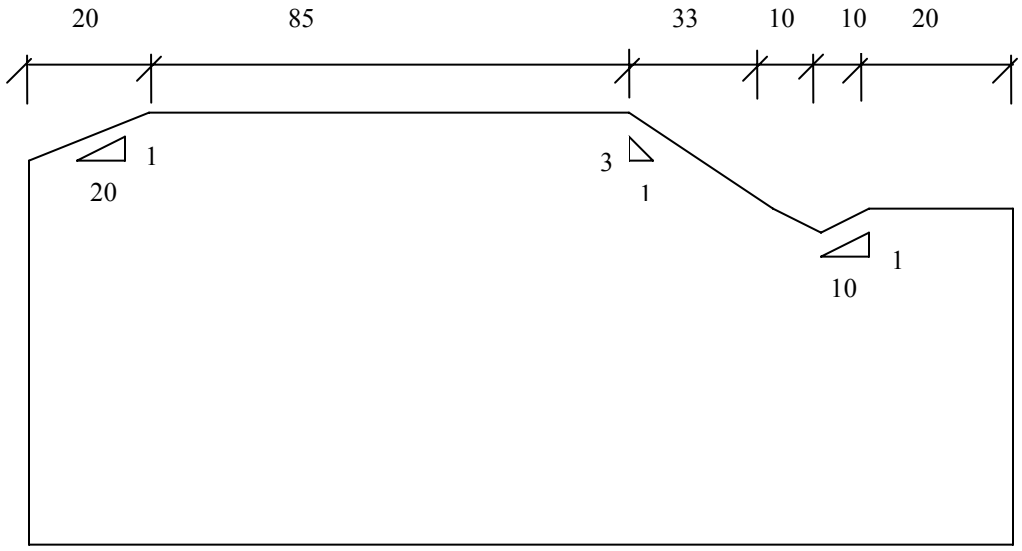

Figure 42. Fort Worth North Loop 820 Study Section A Pavement Cross Section Sketch.

No Moisture Control Measures

From the FEM analysis, for a 20- year period, the vertical displacement at the outer wheel path will be around 0.7 inch swelling (initial dry condition), 1.2 inch shrinkage (initial wet condition) , as shown in Figure 43.

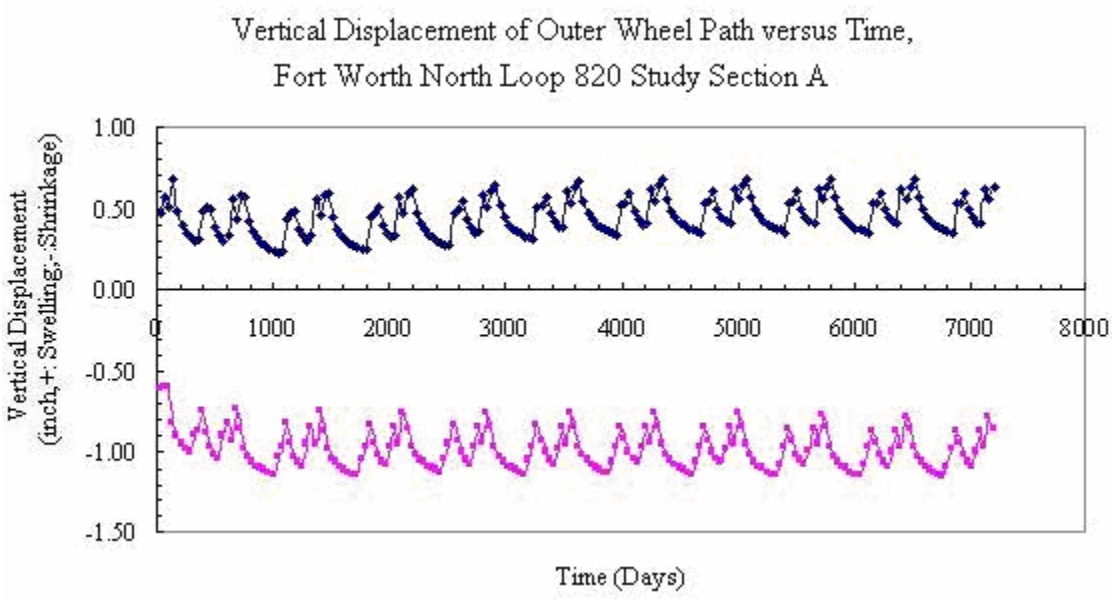

Figure 43. No Moisture Control Measures (Fort Worth North Loop 820 Study Section A).

Effects of Various Depths of Vertical Moisture Barriers

A vertical moisture barrier can be used in highway pavements to minimize the surface deformation by reducing the subgrade moisture changes beneath the pavement structure. The parameter studies of the effects of various depths of vertical moisture barriers on volumetric movement have been obtained in this FEM analysis.

Two different depths of vertical moisture barrier, i.e., 4 ft and 8 ft have been employed for the comparison. The vertical barrier is internally built with a 2 ft width outside the pavement surface course edge. The analysis results are plotted in Figures 44 and 45 below.

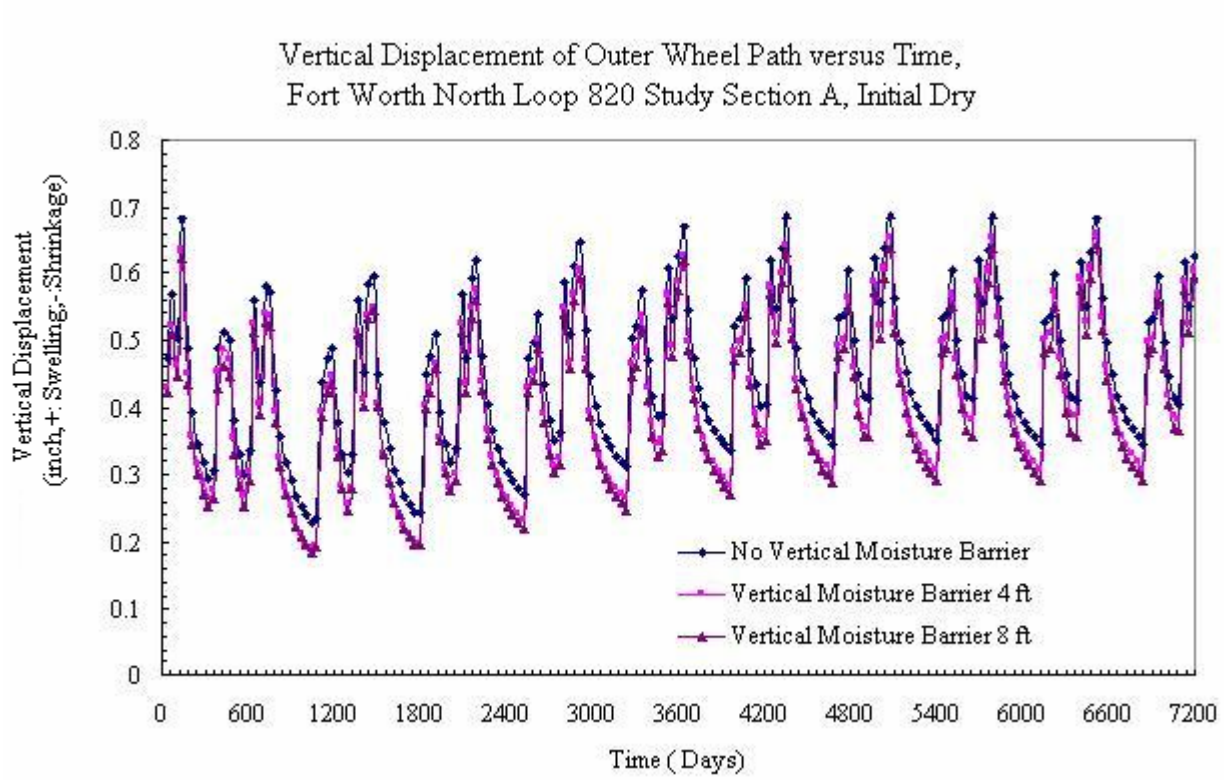

Figure 44. Vertical Displacement Measures with Various Depths of Vertical Moisture Barriers, Initial Dry (Fort Worth North Loop 820, Study Section A).

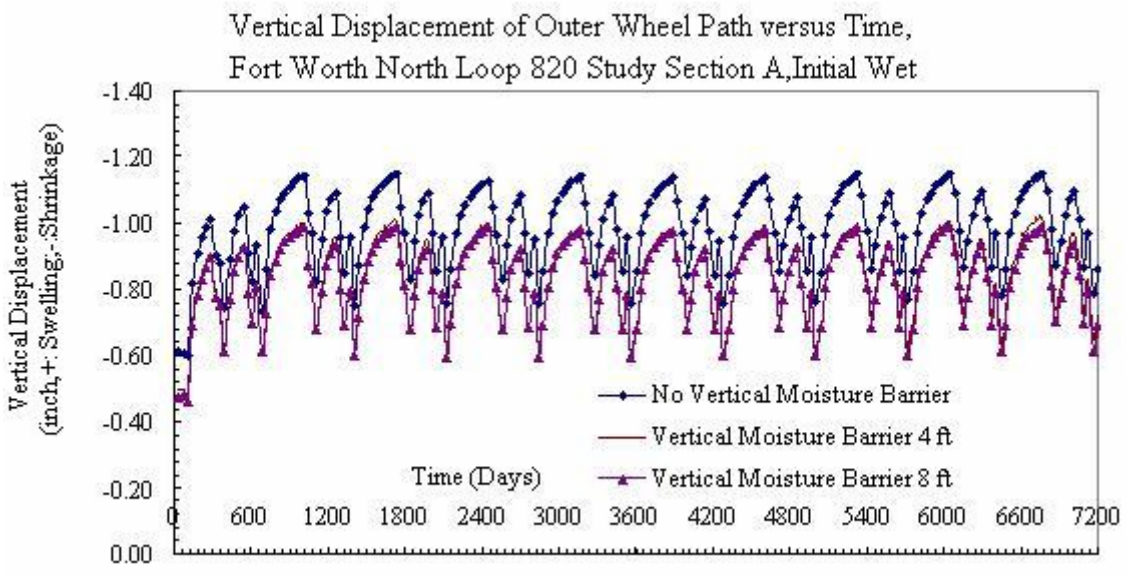

Figure 45. Vertical Displacement Measures with Various Depths of Vertical Moisture Barriers, Initial Wet (Fort Worth North Loop 820, Study Section A).

From Figure 44 and Figure 45, it seems that for "no vertical moisture barrier" case, the total shrinkage and swelling value is around 2 inches. The installation of a vertical moisture barrier can reduce the shrinkage and swelling value to be around 1.4 inches for 4 ft vertical moisture barrier case. The vertical displacement difference for 4 ft and 8 ft vertical moisture barrier is not significant in this analysis.

Effects of Various Depths of Lime Stabilization

The effect of various depths of lime stabilization on controlling pavement surface deformation has also been studied in this analysis. 18 inch depth lime stabilization, as usually used in engineering practice, has been proposed for the comparison (see Figures 46 and 47).

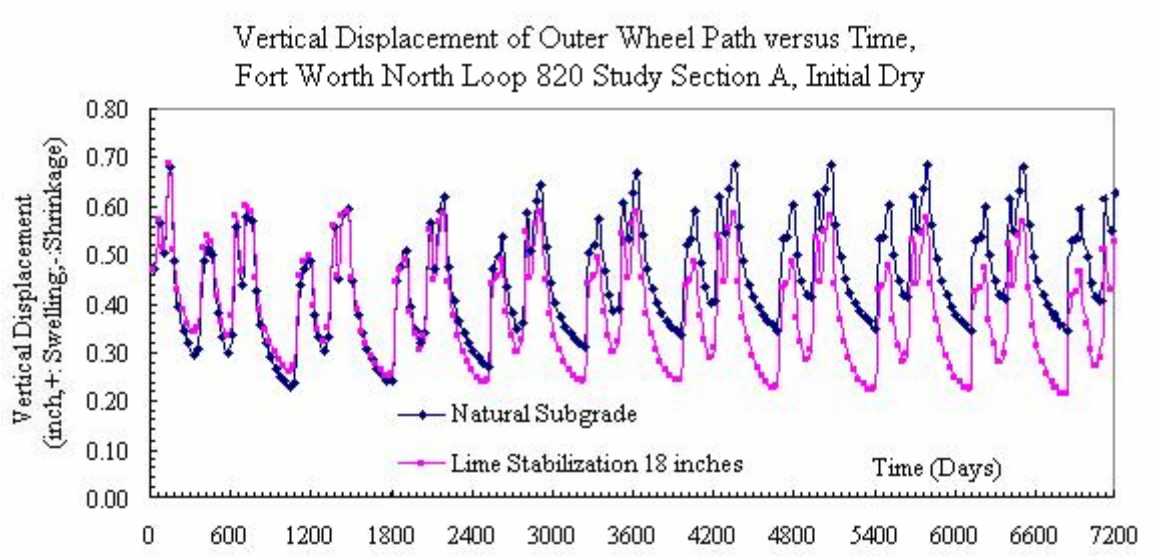

Figure 46. Vertical Displacement Measures with Different Depths of Lime Stabilization (Fort Worth North Loop 820 Study Section A, Initial Dry).

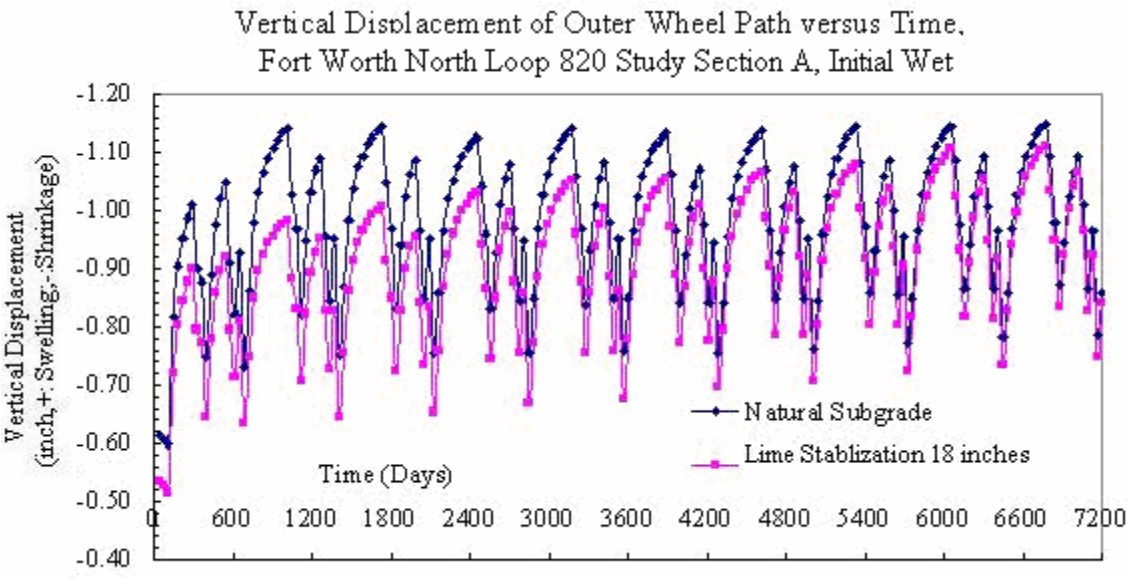

Figure 47. Vertical Displacement Measures with Different Depths of Lime Stabilization (Fort Worth North Loop 820 Study Section A, Initial Wet).

From Figure 46 and Figure 47, it can be seen that for the " natural subgrade" case, the vertical shrinkage and swelling value is around 1.9 inches. With the 18 inches lime stabilization, the value can be controlled in 1.4 inches at 20 years' time range.

Effects of Various Depths of "Inert" Material

Two different depths of "inert" material, 2 ft and 6 ft, are currently used for this study. The results are shown in Figures 48 and 49 below.

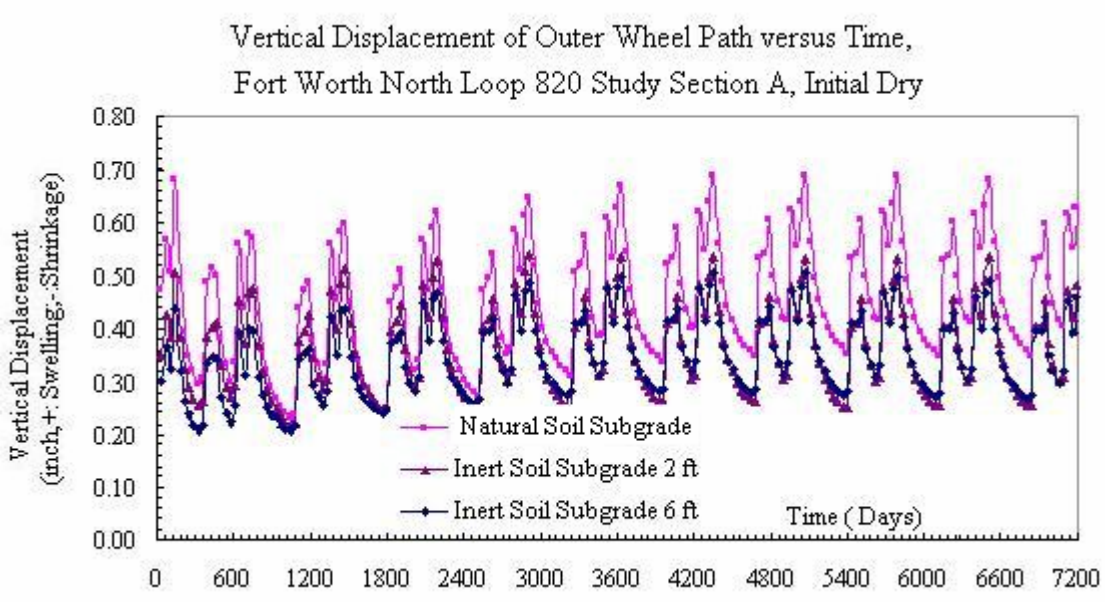

Figure 48. Vertical Displacement Measures of Various Depths of "Inert" Material (Fort Worth North Loop 820 Study Section A, Initial Dry).

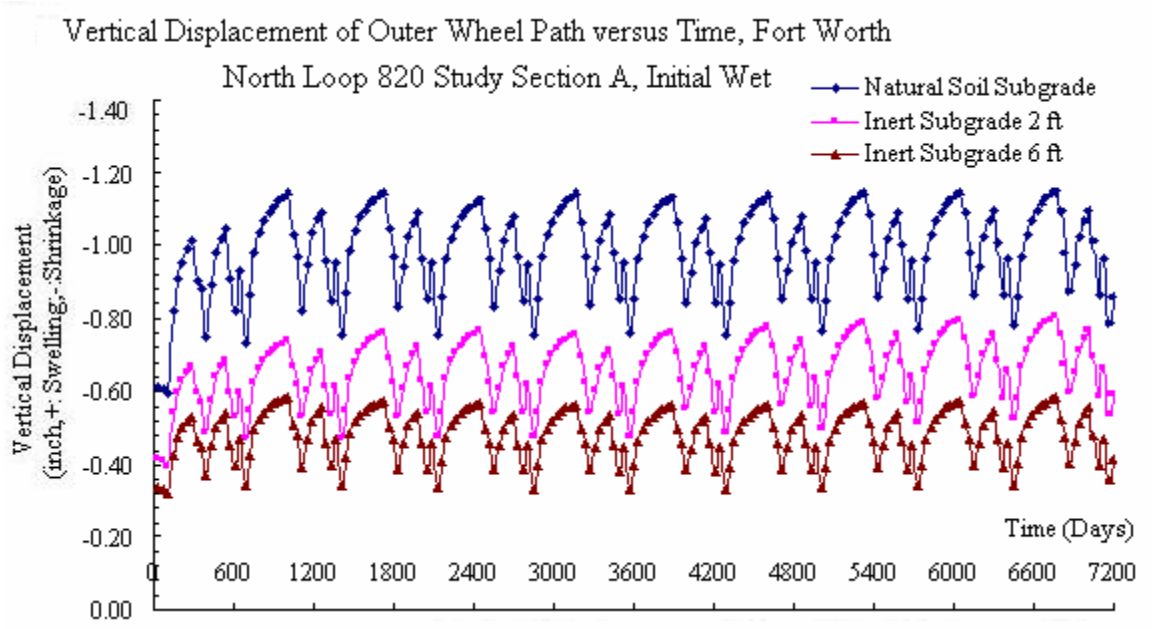

Figure 49. Vertical Displacement Measures of Various Depths of "Inert" Material (Fort Worth North Loop 820 Study Section A, Initial Wet).

From Figure 48 and Figure 49, it can be inferred that for “natural subgrade” case, the total vertical movement (shrinkage and swelling) is around 1.9 inches, while for “inert subgrade” case, the total vertical movement is controlled below 1.2 inches. The replacement of natural subgrade with inert soil can reduce the vertical soil movement to a considerable degree.

Effects of the Paved Median

In engineering practice, paving the median is also an effective method to reduce surface vertical movement. The effect of paving the median on the outer wheel path vertical displacement measures at two different initial conditions (initial dry, initial wet) are studied in Figures 50 and 51.

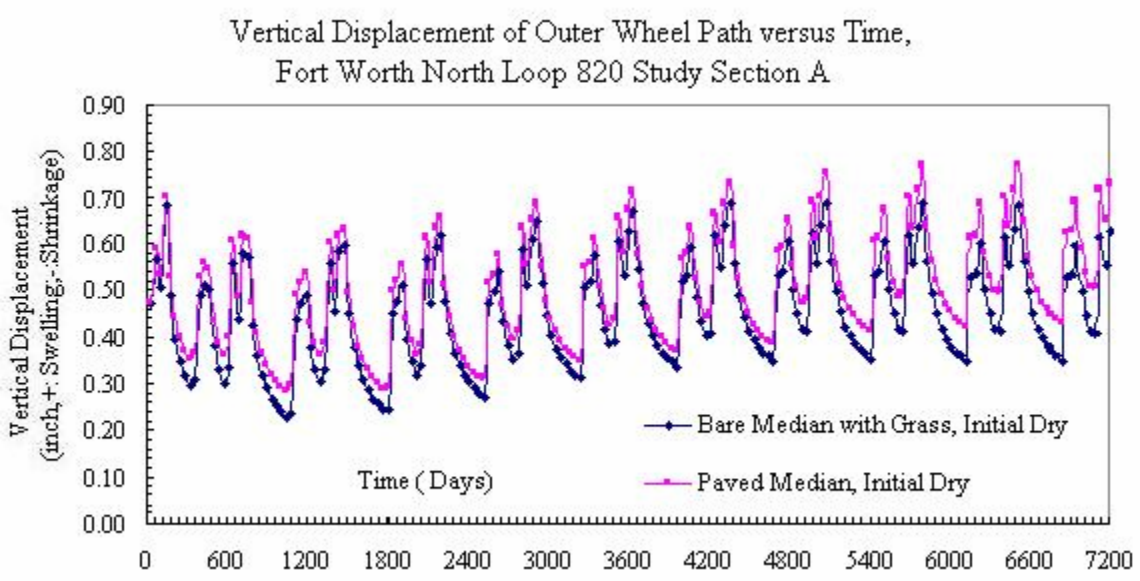

Figure 50. Vertical Displacement Measures of Median Condition (Fort Worth North Loop IH 820 Study Section A, Initial Dry)

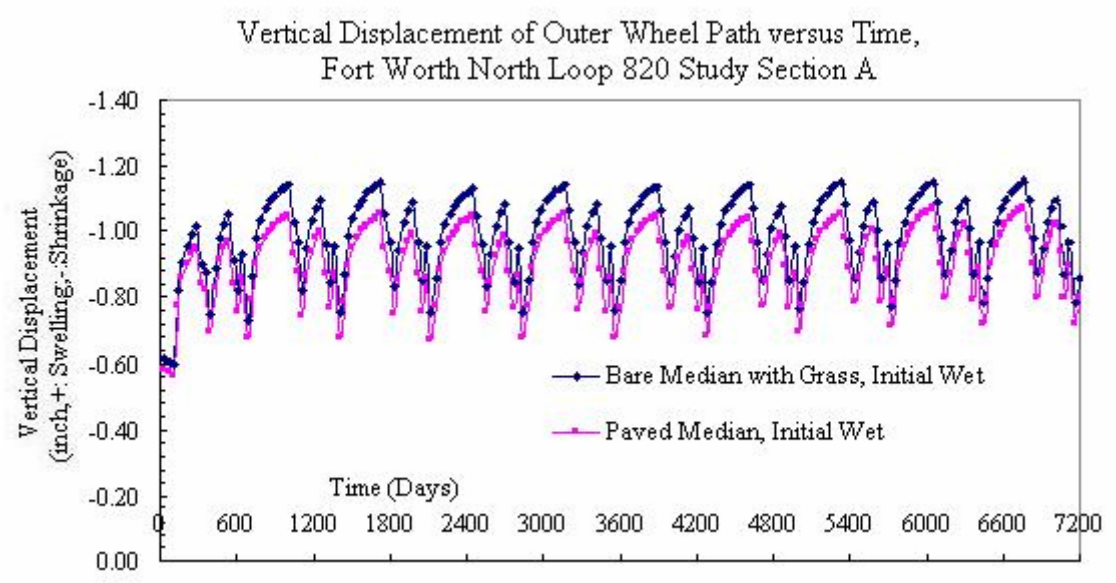

Figure 51. Vertical Displacement Measures of Median Condition (Fort Worth North Loop IH 820 Study Section A, Initial Wet).

From Figure 50 and Figure 51, it can be shown that the effect of paved median condition at initial dry condition on soil swelling is not obvious. Meanwhile, the paved median condition has a significant effect on controlling soil shrinkage movement at initial wet condition.

FORT WORTH NORTH LOOP IH 820 STUDY SECTION B

Two-Dimensional Model

The proposed pavement cross section used for FEM (finite element method) analysis in Fort Worth Loop IH 820 study section B is illustrated in Figure 52. The proposed pavement structure will be composed of 12 inches of continuously reinforced concrete pavement (CRCP) and 4 inches asphaltic concrete pavement (ACP).

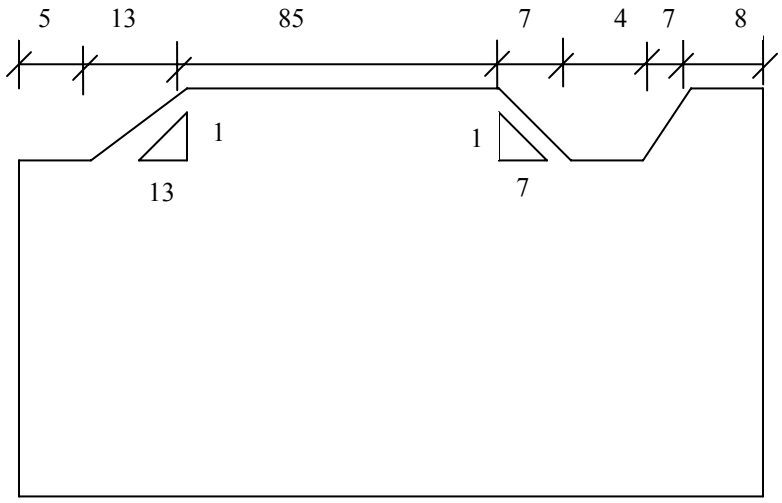

Figure 52. Fort Worth North Loop 820 Study Section B Pavement Cross Section Sketch.

No Moisture Control Measures

The computation results for no moisture control measures at two different initial conditions (initial dry, initial wet) are demonstrated in Figure 53 below.

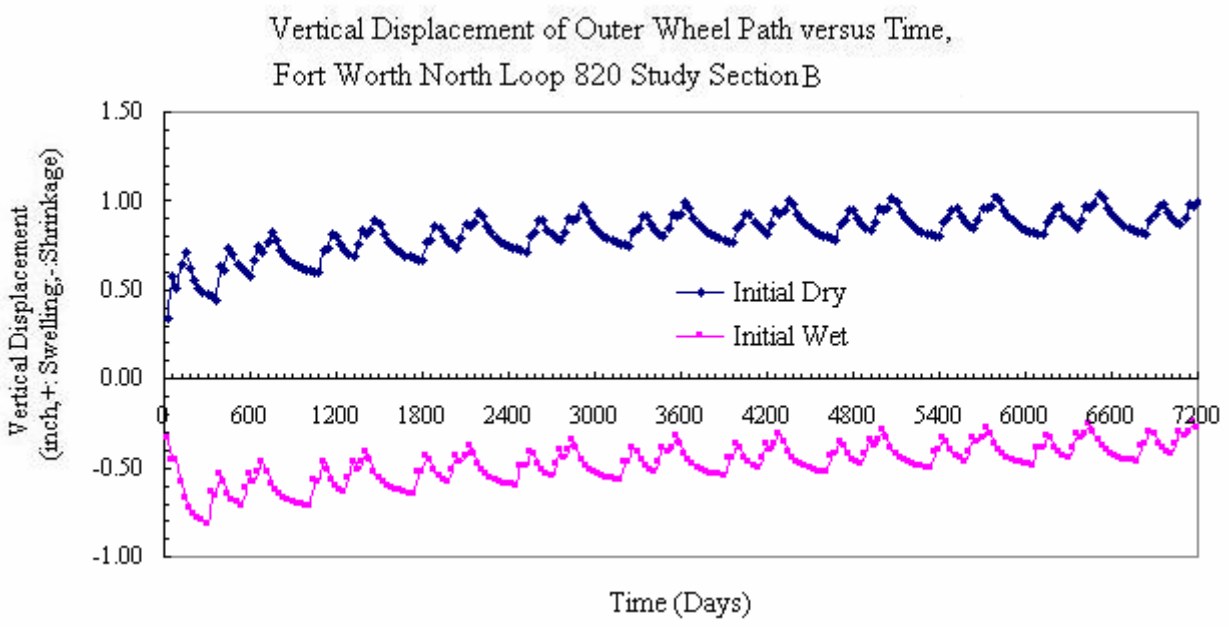

Figure 53. No Moisture Control Measures at Fort Worth North Loop 820 Study Section B.

From Figure 52, it can be inferred that the total vertical soil movement at no moisture control condition at Fort Worth North loop 820 study section A is around 2 inches.

Effects of Various Depths of Vertical Moisture Barriers

The parameter studies of various depths of vertical moisture barriers (4 ft and 8 ft) on the effect of vertical displacement controls are shown in Figure 54 below.

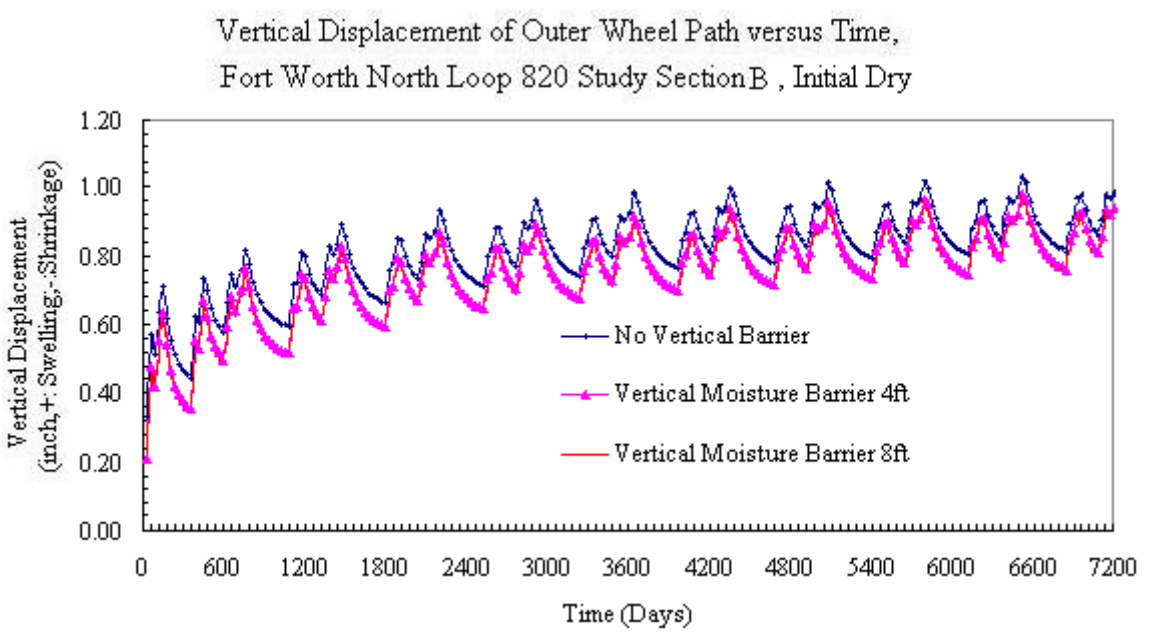

Figure 54. Vertical Displacement Measures of Various Depths of Vertical Moisture Barriers at Fort Worth North Loop 820 Study Section A.

From Figure 54, it can be seen that the installation of vertical moisture barrier can reduce the vertical soil movement to some degree in the analysis study of Fort Worth Loop 820 Study Section A.

Effects of Various Depths of Lime Stabilization

For this site, 18 inch of lime stabilization has been used for the comparison. The corresponding vertical displacements at the outer wheel path for a 20- year period have been shown in Figure 55.

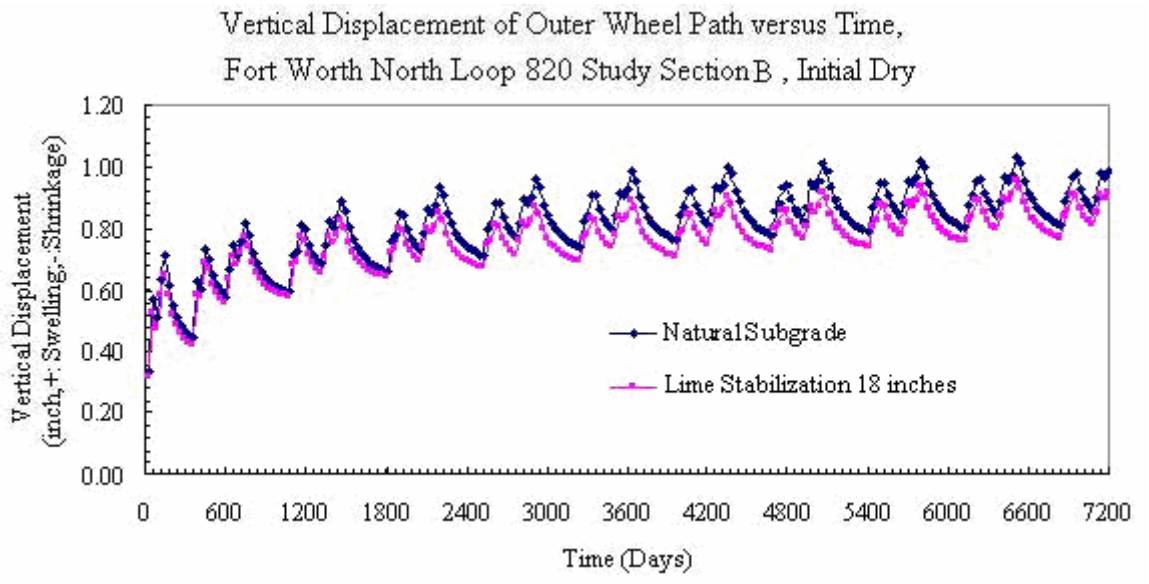

Figure 55. Vertical Displacement Measures of Various Depths of Lime Stabilization at Fort Worth North Loop 820 Study Section B.

Figure 55 indicates that the use of lime stabilization can reduce the soil vertical displacement to a great degree.

Effects of Various Depths of "Inert" Material

Figure 56 shows the effect of various depths of "inert" material (2 ft and 6 ft) on the vertical displacement measures of the outer wheel path. It can be inferred that employment of inert soil can control the vertical movement (Figure 56 shows the case of initial dry condition).

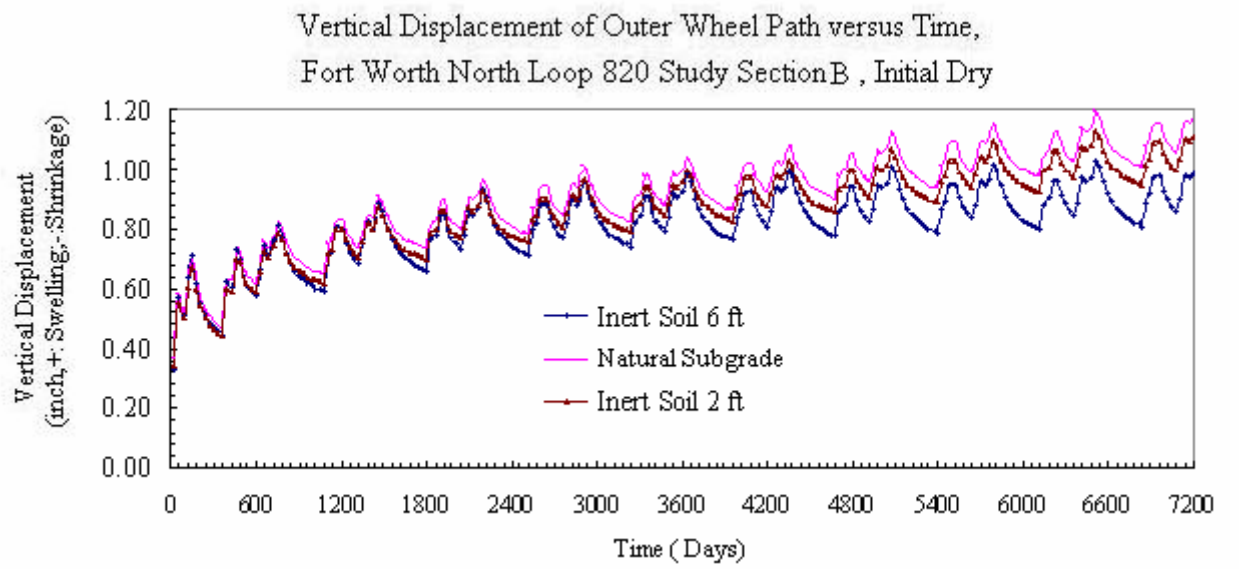

Figure 56. Vertical Displacement Measures of Various Depths of "Inert" Material at Fort Worth North Loop 820 Study Section B.

Effects of the Paved Median

The effect of paving median condition on vertical displacement control at two initial conditions (initial dry and initial wet) has been shown in Figures 57 and 58. It can also be concluded that the effect of paved median condition on controlling soil shrinkage movement is more significant than controlling soil swelling movement.

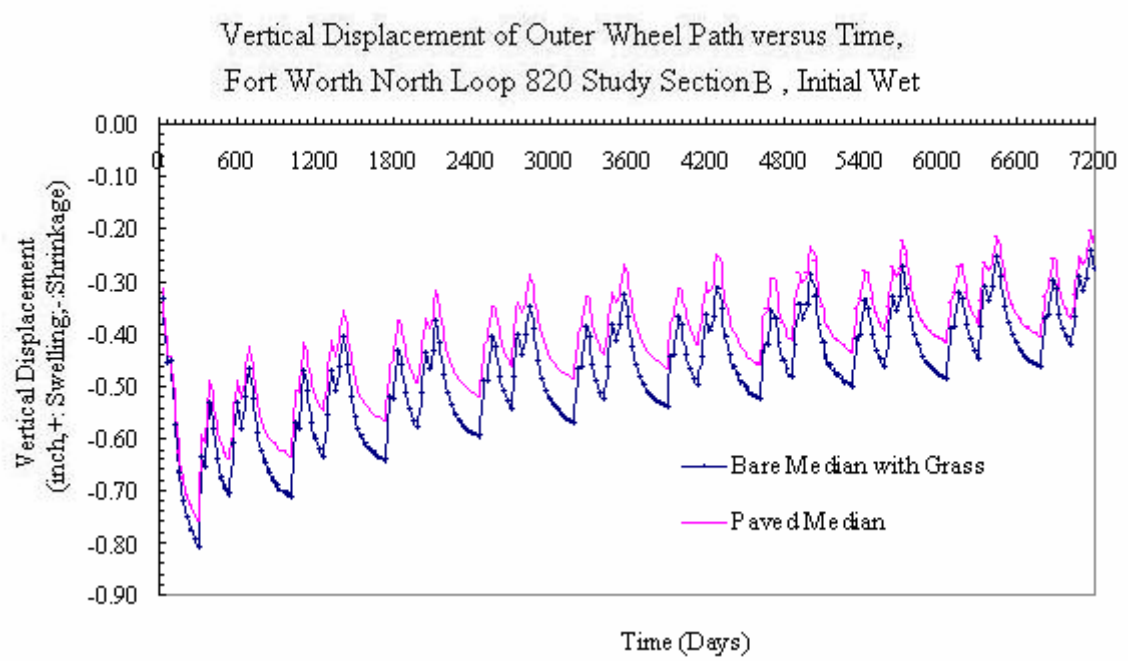

Figure 57. Vertical Displacement Measures of Paving Conditions (Fort Worth North Loop 820 Study Section B, Initial Wet).

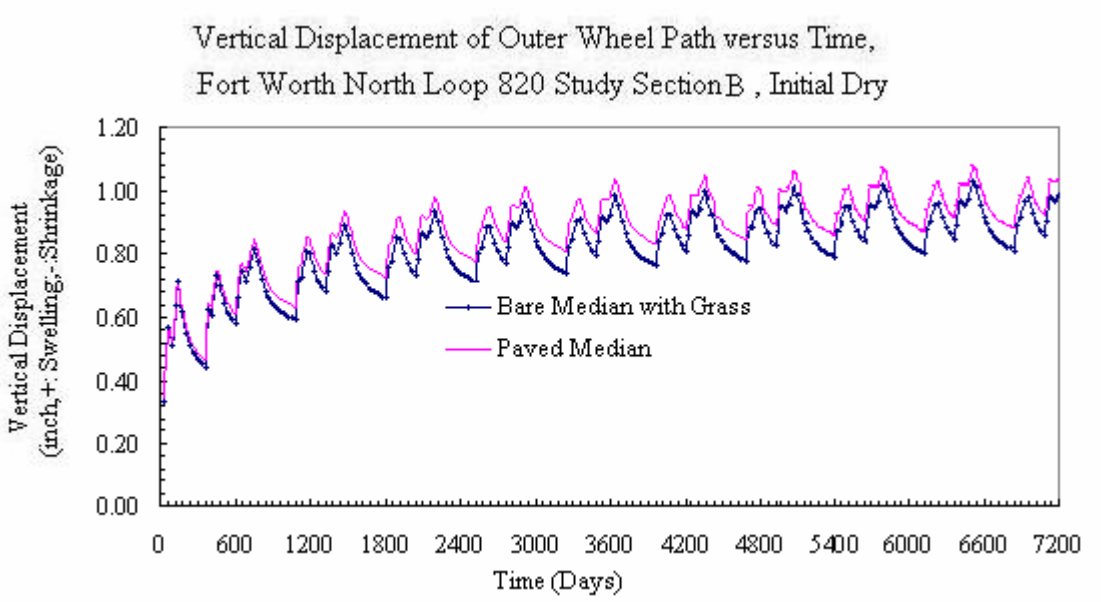

Figure 58. Vertical Displacement Measures of Paving Conditions (Fort Worth North Loop 820 Study Section B, Initial Dry).

ATLANTA US 271

Two-Dimensional Model

In the Atlanta US 271 site, there are trees existing in region AB (from the ditch line through the median). In the two-dimensional finite element analysis, the tree root zone depth is assumed to be 14 ft according to the borehole data. The analyzed cross section is shown in Figure 59.

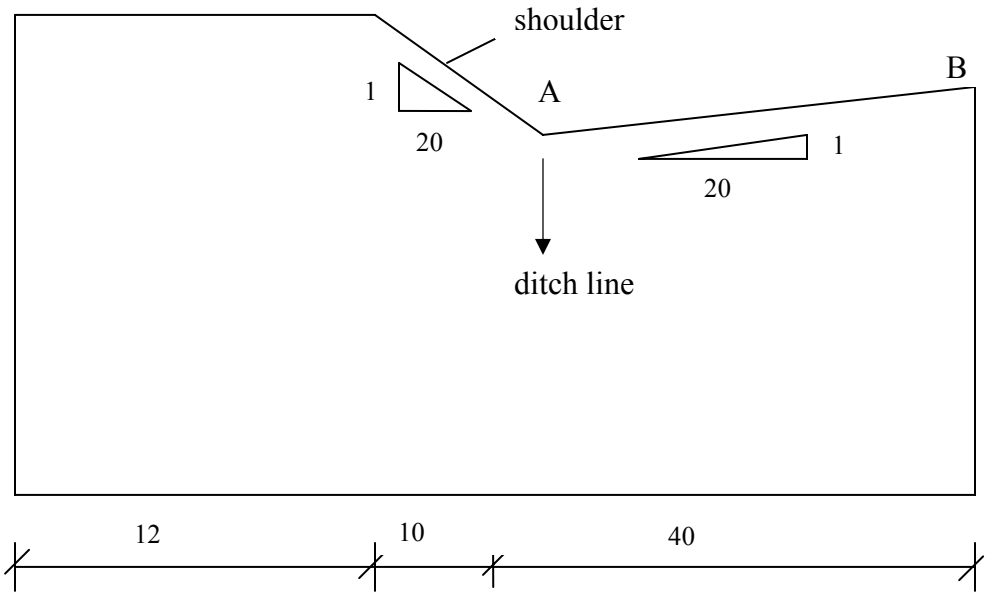

Figure 59. Atlanta US 271 Pavement Cross Section Sketch.

No Moisture Control Measures

The computation results for no moisture control measures in this site at two different initial conditions (initial dry and initial wet) is shown in Figure 60. At this site, the total soil vertical movement is around 1 inch.

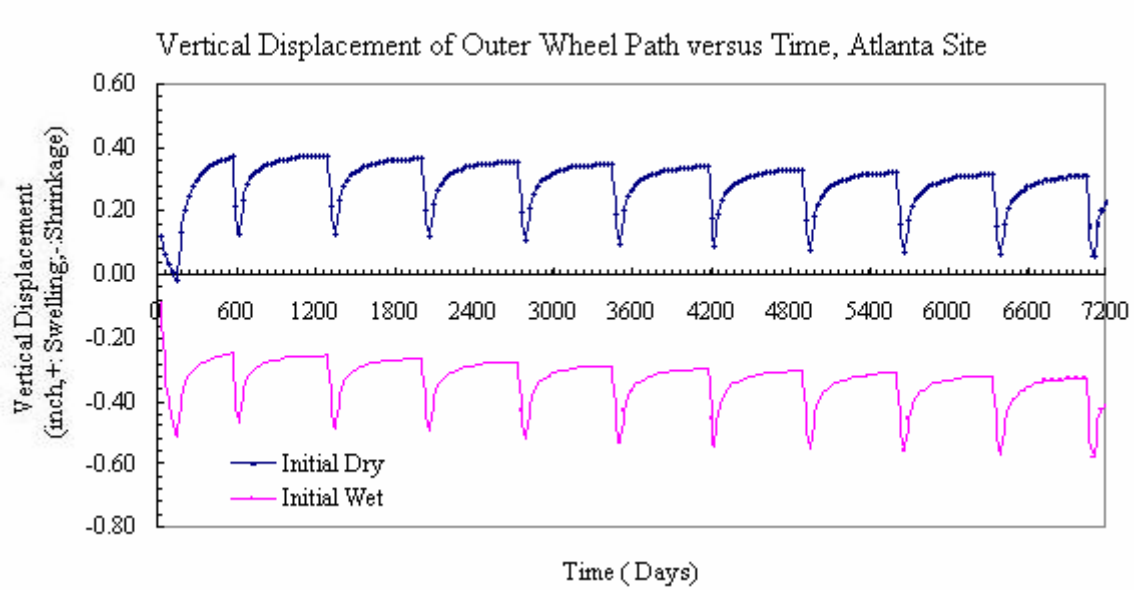

Figure 60. Vertical Displacement Measures at Atlanta US 271.

Effects of Various Depths of Vertical Moisture Barriers

As in Fort Worth Loop 820 study sections A and B, two different depths of various moisture barriers (4 ft and 8 ft) are compared in Figure 61.

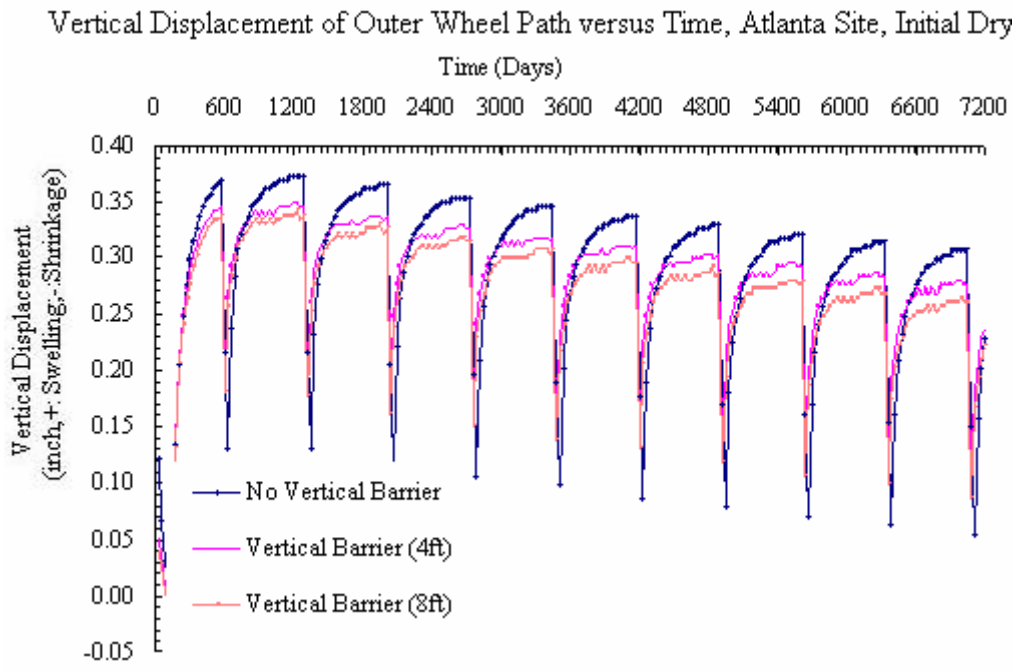

Figure 61. Vertical Displacement Measures of Various Depths of Vertical Moisture Barriers at Atlanta US 271.

As shown in Figure 61, the installation of a vertical moisture barrier can reduce the soil vertical movement.

Effects of Various Depths of Lime Stabilization

Figure 62 shows the effect of various depths of lime stabilization (8 inch and 18 inch) on controlling the vertical movement in the Atlanta US 271 site.

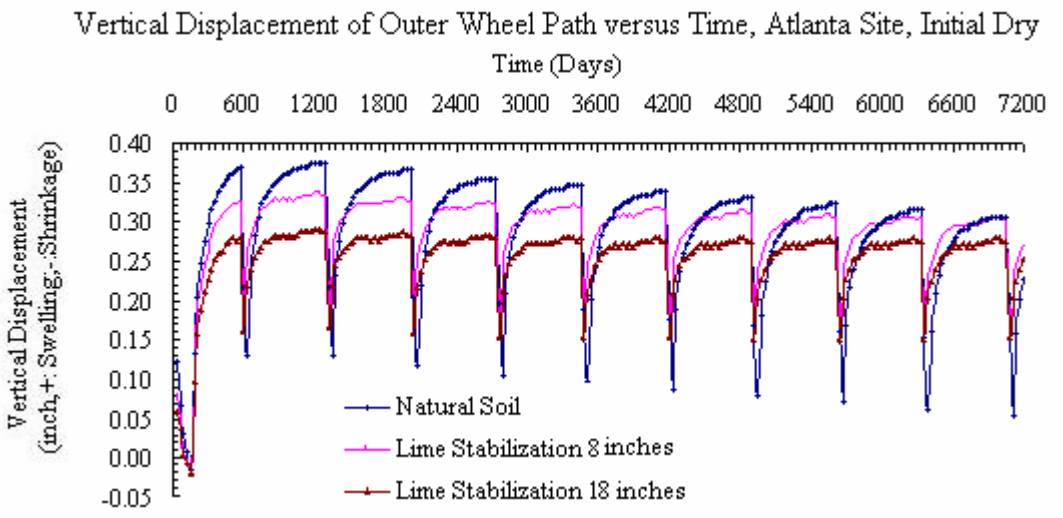

Figure 62. Vertical Displacement Measures of Various Depths of Lime Stabilization at Atlanta US 271.

As indicated in Figure 62, the use of lime stabilization can decrease the vertical soil movement to a significant degree.

Effects of Various Depths of "Inert" Material

Figure 63 gives the vertical movement measures for different depths of "inert" material (2 ft, 4 ft and 6 ft) for the subgrade materials. The effect of the replacement of natural soil with inert soil on controlling vertical soil movement is also shown in Figure 63. The soil vertical movement can be reduced as seen in the Figure 63.

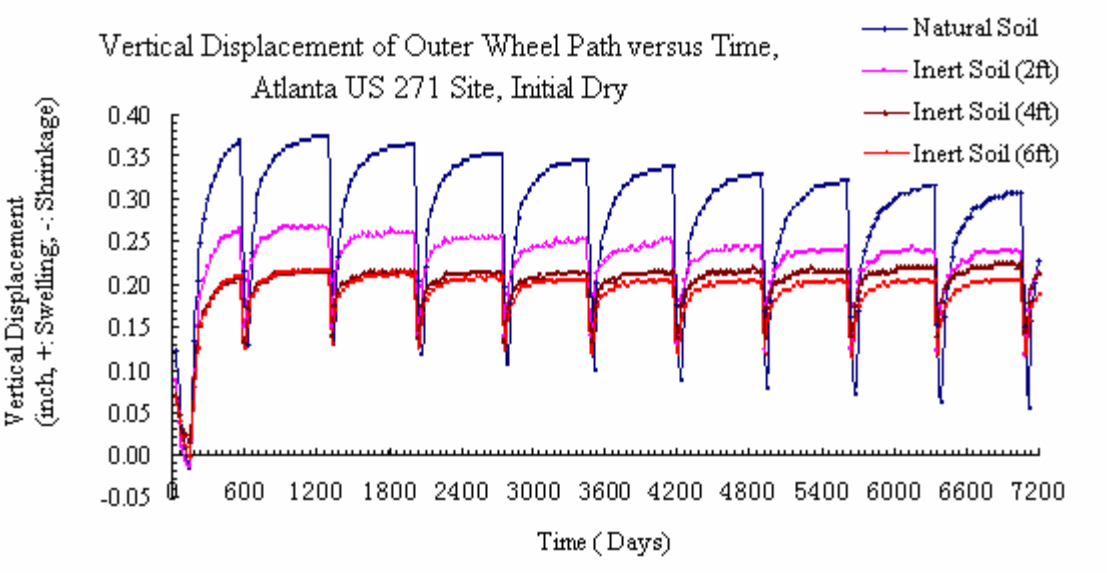

Figure 63. Vertical Displacement Measures of Various Depths of "Inert" Material at Atlanta US 271.

Effects of Paving Widths of Shoulder

Two types of paving shoulder widths (4 ft and 8 ft) have been used for the parameter study. The effect of the paving widths of shoulder on vertical displacement measures is shown in Figures 64 and 65. It can be seen that the employment of paved shoulder can significantly reduce the total soil vertical movement and the displacement change magnitude due to cyclic climate condition.

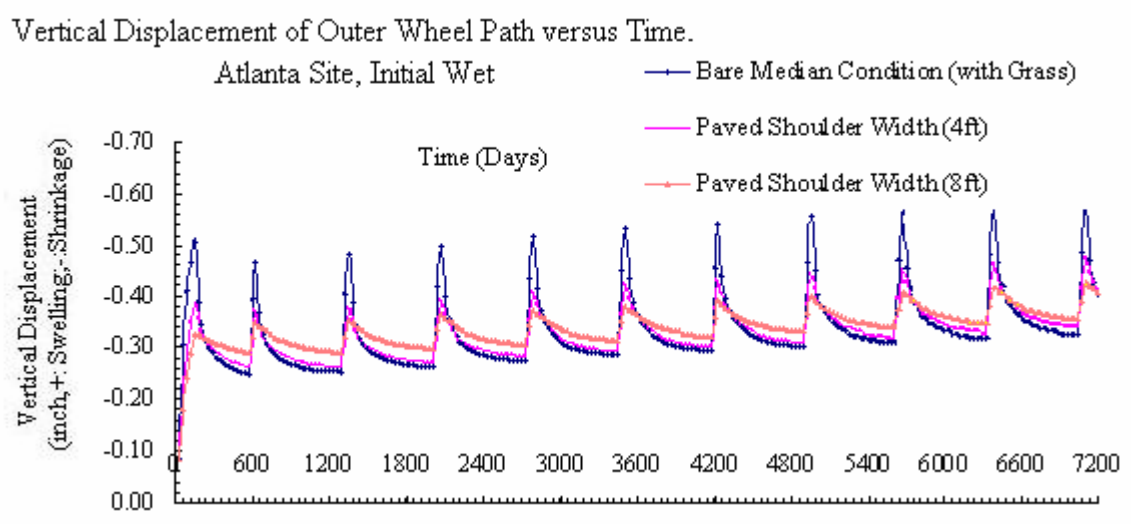

Figure 64. Vertical Displacement Measures of Various Width of Paving Shoulder at Atlanta US 271 (Initial Wet).

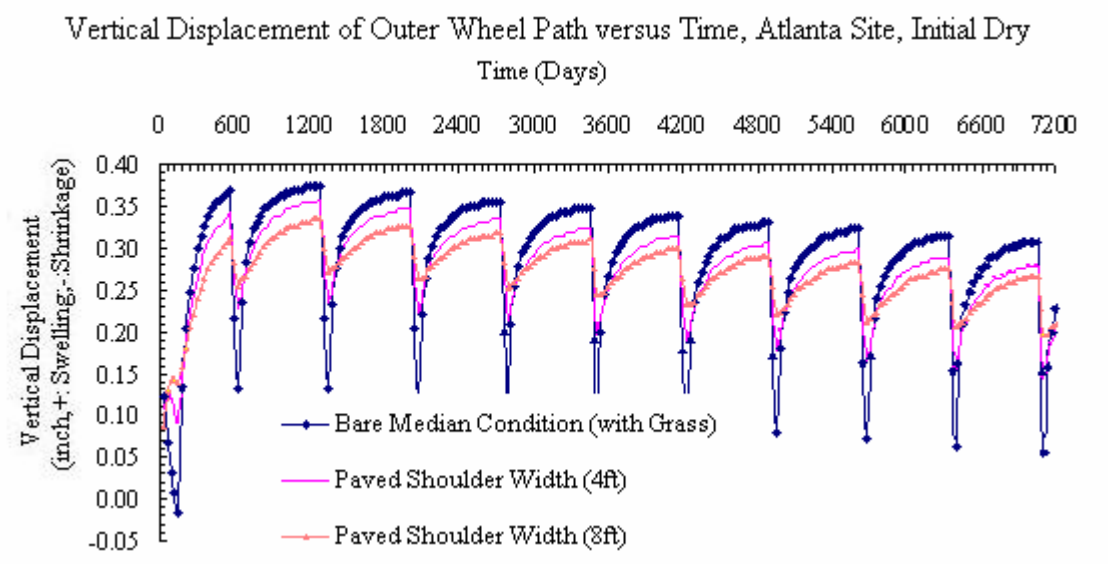

Figure 65. Vertical Displacement Measures of Various Width of Paving Shoulder at Atlanta US 271 (Initial Dry).

AUSTIN LOOP 1 UPHILL OF FRONTAGE ROAD AND MAIN LANE

Two-Dimensional Model

Figure 66 shows the analyzed two-dimensional pavement cross section for the analysis of vertical displacement measures at uphill of the frontage road and the main lane. In the field, there exists a long sliding intact limestone layer some depth beneath surface.

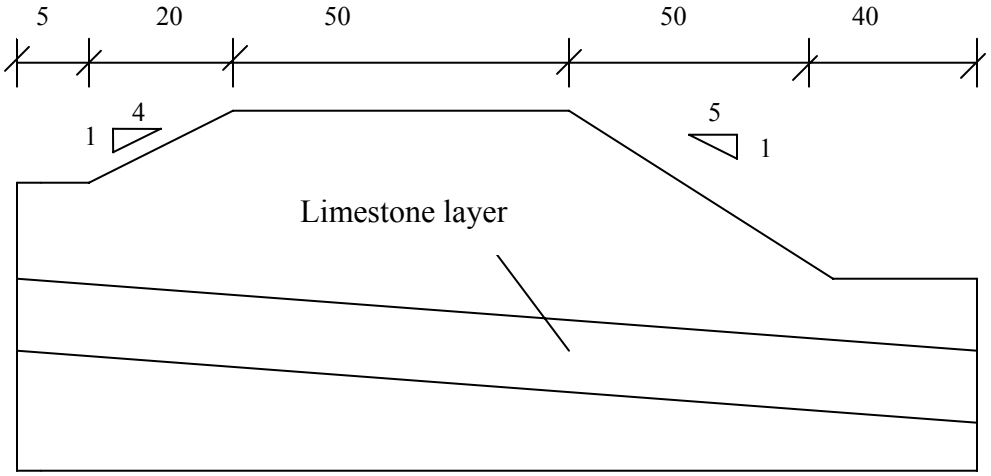

Figure 66. Austin Loop 1 Pavement Cross Section Sketch.

No Moisture Control Measures

The computation results for no moisture control measures for Austin Loop 1 at uphill outer wheel path of the frontage road and at uphill outer wheel path of the main lane are shown in Figures 67 and 68. The total vertical soil movement for no moisture control at the outer wheel path of uphill of Frontage road is around 1.4inches. The vertical soil movement value at the outer wheel path of uphill of main lane for no moisture control is around 1.6 inches.

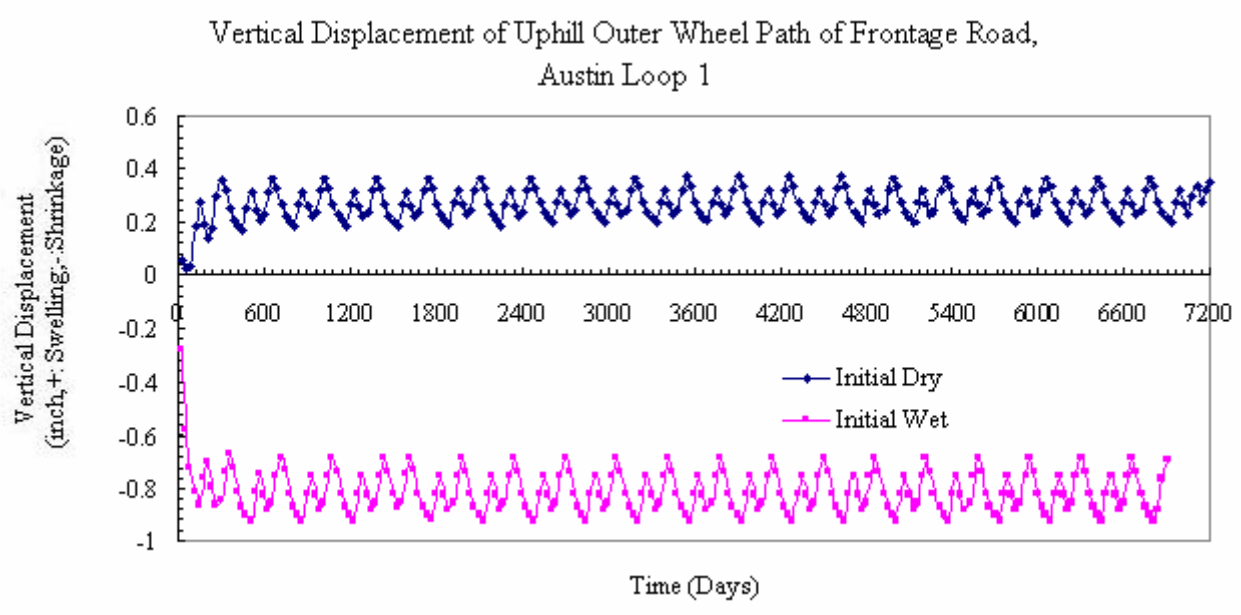

Figure 67. No Moisture Control Measures at Austin Loop 1 Uphill of Frontage Road.

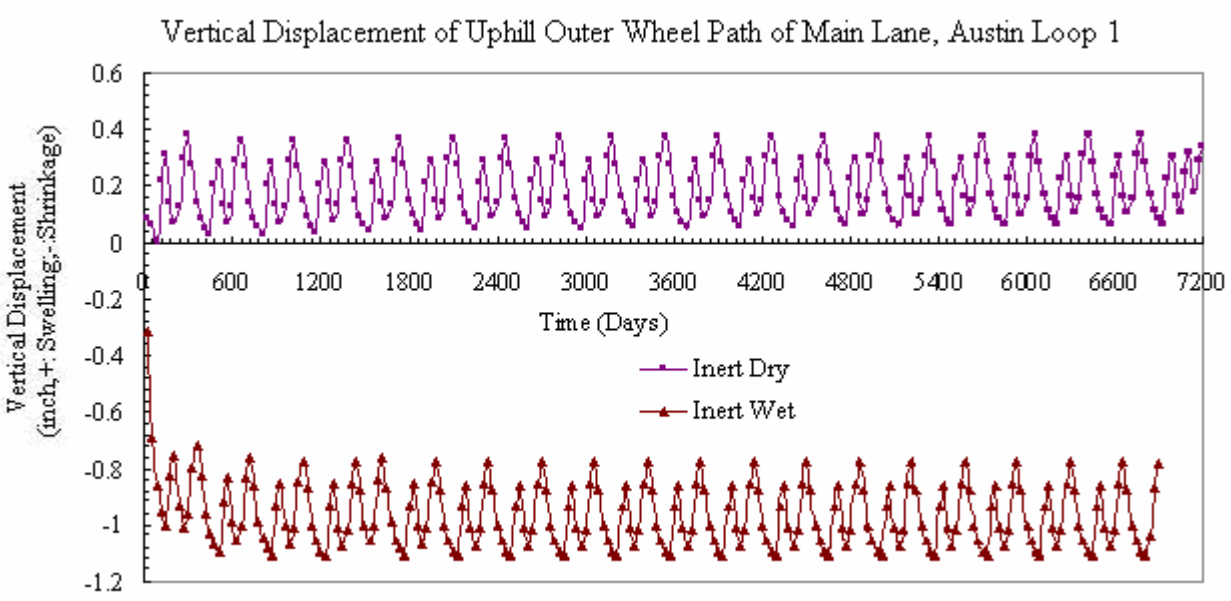

Figure 68. No Moisture Control Measures at Austin Loop 1 Uphill of Main Lane.

Effects of Various Depths of Vertical Moisture Barriers

Figures 69 to 72 demonstrate the effect of various depths of vertical moisture barriers, i.e., 4 ft and 8 ft, on the vertical movement of uphill outer wheel path of frontage road and main lane at Austin Loop 1 site. In this analysis, the installation of vertical moisture barrier has no help on reducing the vertical soil movement.

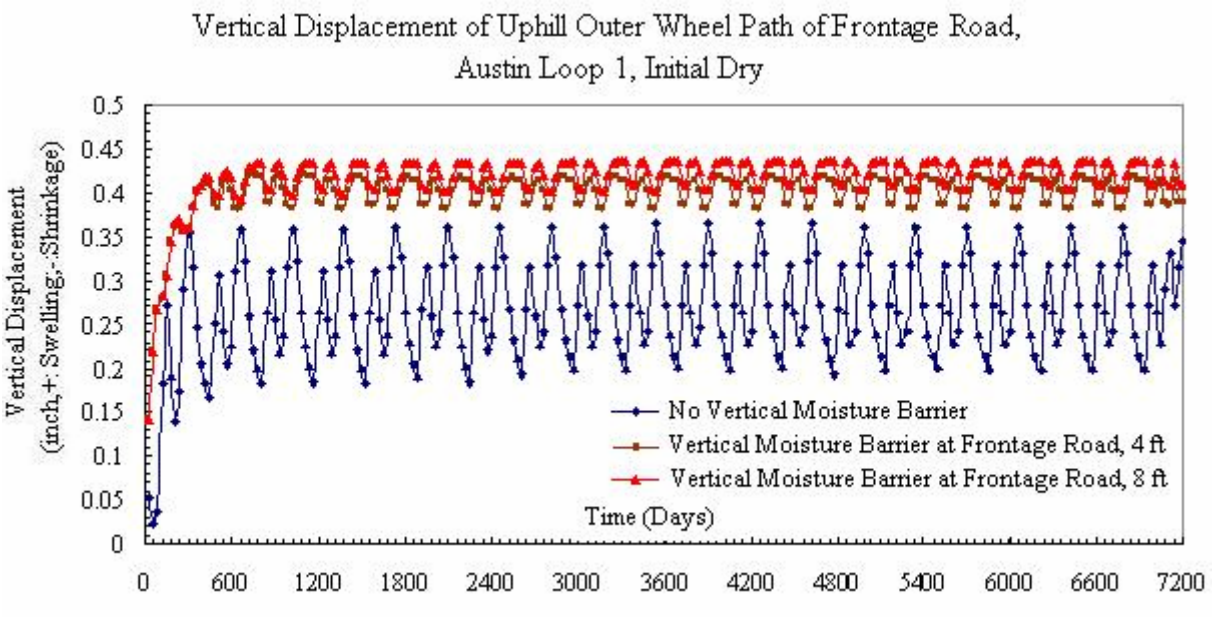

Figure 69. Vertical Displacement Measures at Uphill Outer Wheel Path of Frontage Road with Various Depths of Vertical Moisture Barrier Built at Frontage Road, Austin Loop 1 (Initial Dry).

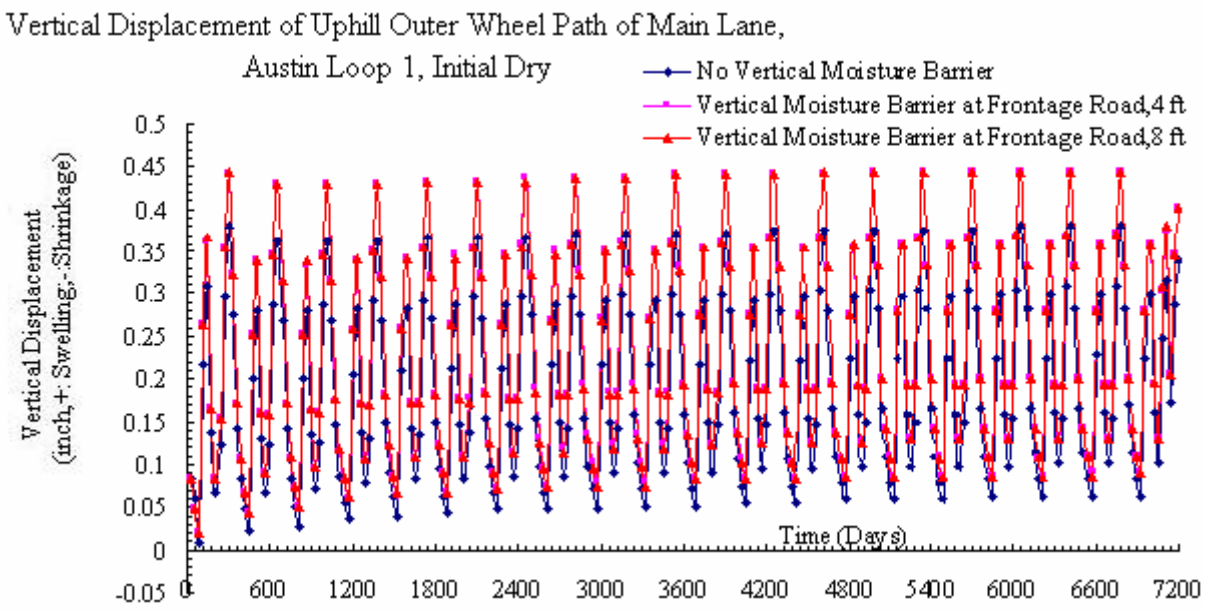

Figure 70. Vertical Displacement Measures at Uphill Outer Wheel Path of Main Lane with Various Depths of Vertical Moisture Barrier Built at Frontage Road, Austin Loop 1 (Initial Dry).

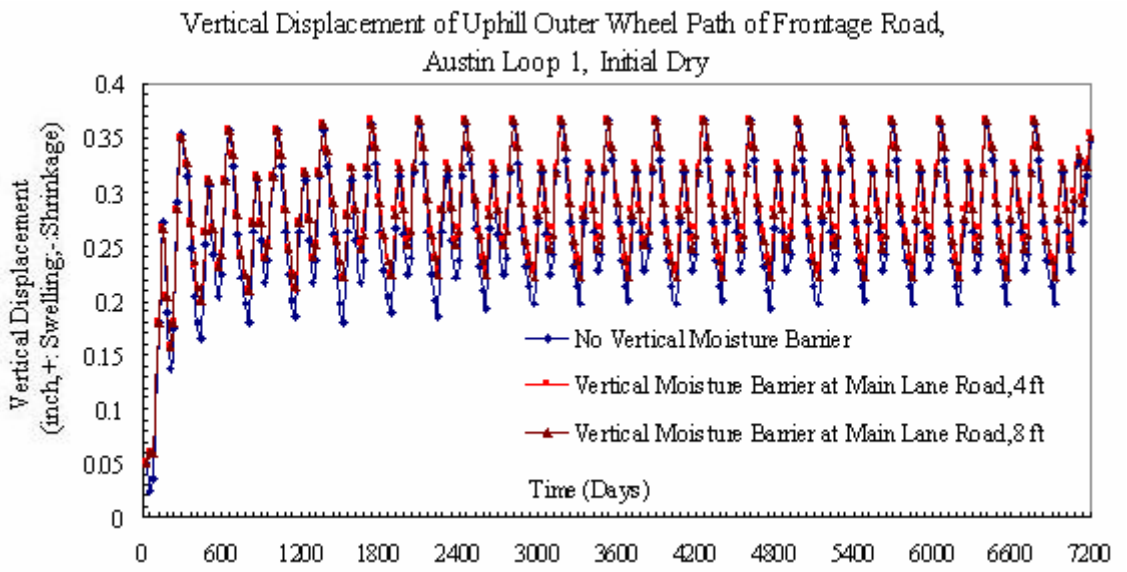

Figure 71. Vertical Displacement Measures at Uphill Outer Wheel Path of Frontage Road with Various Depths of Vertical Moisture Barrier Built at Main Lane, Austin Loop 1 (Initial Dry).

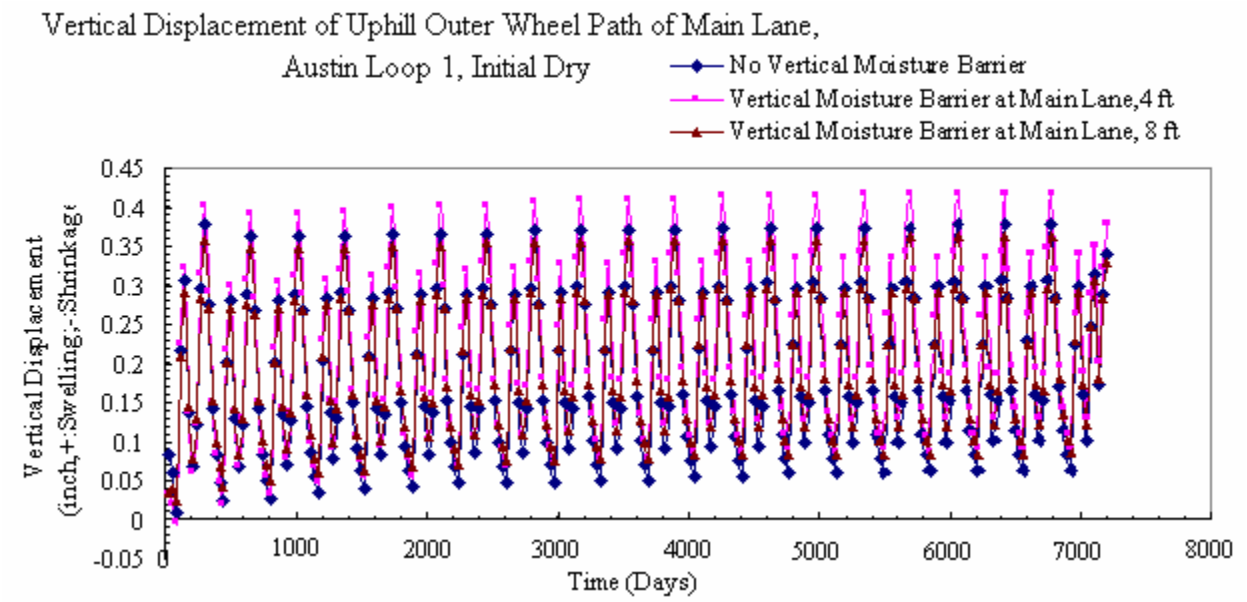

Figure 72. Vertical Displacement Measures at Uphill Outer Wheel Path of Main Lane with Various Depths of Vertical Moisture Barrier Built at Main Lane, Austin Loop 1 (Initial Dry).

Effects of the Paved Median

The effects of the paving median condition on vertical movement at the uphill outer wheel path of frontage road and main lane are illustrated in Figures 73 and 74.

Figure 73. Vertical Displacement Measures of Paving Conditions at Uphill Outer Wheel Path of Frontage Road, Austin Loop 1.

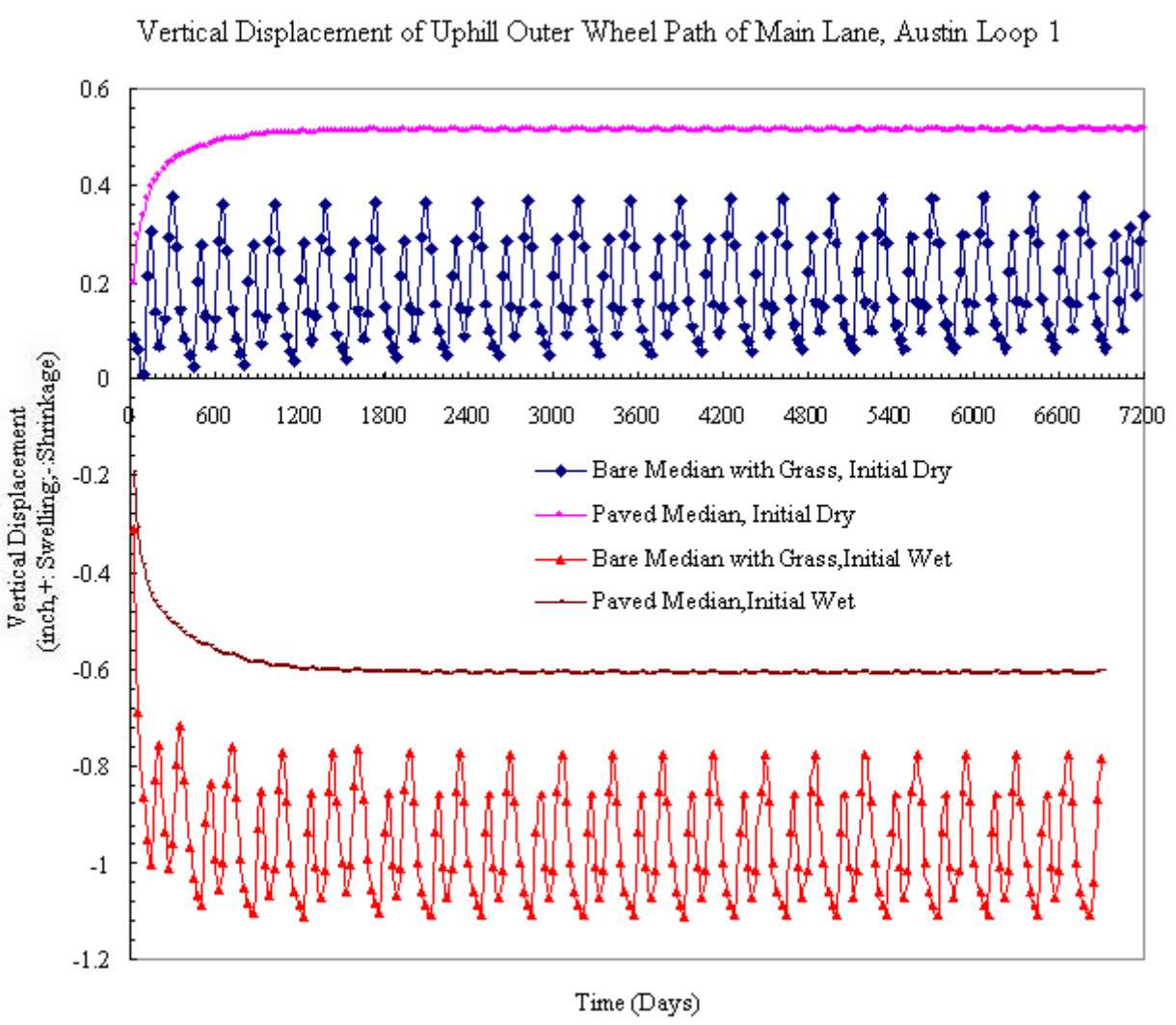

Figure 74. Vertical Displacement Measures of Paving Conditions at Uphill Outer Wheel Path of Main Lane, Austin Loop 1.

From Figure 73 and Figure 74, it can be indicated that the paved median condition has significant effect on reducing the vertical displacement measures at uphill outer wheel path of main lane. But the paved median condition has slight effect on the vertical displacement measures at uphill outer wheel path of frontage road.

CONCLUSIONS

From the results of the parameter studies at these four sites, the following conclusions can be drawn:

- The analysis program can simulate a 20 years' performance period in around one hour on a desktop computer of 1 GHZ CPU and is capable of analyzing both asphalt and concrete pavements on expansive soils. The lateral boundary conditions that may be used include drainage (ponded water of different depth in the roadside ditches) , grasses and trees.
- A vertical moisture barrier is normally an effective method to reduce the pavement surface total vertical movement. However, for the Austin site, due to the existence of an intact limestone layer, the effect of a vertical moisture barrier is not obvious; it may even increase the vertical movement at the outer wheel path.
- Paving the median can reduce the pavement surface shrinkage significantly compared with the bare median case; however, it doesn't have much effect on reducing the swelling value. The reason for this is that the grass usually existing in the bare median case dries out the underlying soil layers and thus causes a large soil shrinkage movement. With the median paved, the moisture evaporation is controlled. So the soil shrinkage value is decreased.
- Paving the shoulder is effective in decreasing the pavement surface displacements and reducing the vertical displacement change magnitude due to cyclic climatic conditions.
- Lime stabilization and "inert" material are both productive in reducing the pavement vertical movement. Lime stabilization thickness of 8 inches and 18 inches are employed in the analyses.

The value of the time step Δt is a very important factor in the analysis. In order to avoid the problem of numerical non-accuracy due to the high nonlinearity in the displacement analysis, a small time step value should be employed as a compromise with computational speed.

CHAPTER 6:
DESIGN OF NEW PAVEMENTS WITH REMEDIAL MEASURES

INTRODUCTION

The design analysis of three sites in Fort Worth, Atlanta, and Austin is performed using the program WinPRES with the data obtained from borehole logs, laboratory test results, climatic and drainage conditions, dimensions of road, and roughness and traffic information. All input data, output data, and figures of typical sections for the six study sections are presented in Appendix E.

The typical soil properties in each analysis section are constructed considering all data such as Atterberg Limits, particle size distribution, values of suction, and climatic and geometric conditions. The typical cross sections of the road for the six design sections are developed using the number of lanes and the width of shoulder. The pavement sections of both flexible and rigid pavement are estimated with different structural numbers (SN) and concrete thicknesses (D), respectively.

The typical values of the falling weight deflectometer modulus of the subgrade soil of 10,000 psi are used for the flexible pavement. A 28-day compressive strength of the concrete of 4000 psi, mean modulus of rupture of concrete of 620 psi, drainage coefficient of 1.0, modulus of subgrade of 515 pci, and load transfer coefficient of 3.2 for the rigid pavements are used as input parameters. A mean modulus of rupture of concrete of 650 psi was used in this analysis. A value that is more commonly used in design is 620 psi. A value of the subgrade modulus of 515 pci and a value of the load transfer coefficient of 3.2 were used in this report. Values that are more commonly used in design are 300 pci and 2.9, respectively. The trends of the predicted IRI and PSI shown in the figures will show a slower rate of deterioration of riding quality due to traffic than is commonly used in design.

The average daily traffic in one direction and the total 18 kip single axle loads in the traffic analysis period of 30 years for the three sites are assumed based on traffic information provided by the Fort Worth and Atlanta Districts. The initial serviceability index for flexible and rigid pavement are assumed to be 4.2 and 4.5, respectively. Generally, the minimum acceptable

serviceability index after 30 years is considered as 2.5. The regression equation between the international roughness index and the serviceability index is used.

The traffic distribution used in this report was 0.16, 0.16, 0.20, and 0.32 of the total traffic traveling in the five lanes starting from the inside lane for the study sections of Fort Worth site. The total of these fractions adds to 1.00. A more common used design approach is to make the design traffic distribution add to three times the total traffic in a given direction, which, in effect is to increase the design reliability for traffic. Approximately 60 percent of the roughness predicted in this report is due to expansive soil and the remaining 40 percent is due to traffic.

The following explanation of reliability was taken from the textbook Pavement Analysis and Design by Huang[34]. Reliability is a means of incorporating some degree of certainty into the design process to ensure that the various design alternatives will last the analysis period. The level of reliability to be used for design should increase as the volume of traffic, and public expectation of availability increase. The following table presents recommended levels of reliability for various functional classes.

Table 23. Suggested Levels of Reliability for Various Functional Classifications.

Functional Classification	Recommended Level of Reliability	
	Traffic	Expansive Soil
For Prediction	50%	50%
For Design		
Interstate and other freeways	85 – 99.9 %	80 – 99.9 %
Principal arterials	80 – 99.0 %	75 – 95.0 %
Collectors	80 – 95.0 %	75 – 95.0 %
Local	50 – 80.0 %	50 – 80.0 %

The 50 percent reliability level is used for prediction and the reliability levels of 90 percent and 95 percent are used for the design of flexible pavement and rigid pavement, respectively. The 50 percent reliability level that is used for prediction uses the equation (77) with standard normal deviate, Z, set equal to zero in predicting the expected value of the riding quality or roughness, without taking into account the variability of the input data. A 90 % level of reliability was used for all flexible pavements for both expansive soil and traffic-related roughness. A more commonly used reliability for traffic-related roughness is 95 %. Prior to this study no level of reliability was used for design with expansive clay roughness.

The typical results are obtained using the program WinPRES for the six sections (three sections at the Fort Worth site, one section at the Atlanta site, and two sections for main lanes and frontage road lanes at the Austin site). The program output provides the suction profile with depth, total vertical movement swelling plus shrinkage at the edge of the pavement and at the outer wheel path, serviceability index, and international roughness index with time. The wet and dry suction envelopes in the cases when no moisture control is used and when a stabilized soil layer is present are generated within the program. The design analysis is performed with flexible and rigid pavements with vertical moisture barriers, and lime stabilized and inert soil layers, and different thicknesses of asphalt concrete and Portland cement concrete. The various design alternatives for all case study sections are performed to provide acceptable predicted performance for a period of 30 years. However, they do not represent current practice.

FORT WORTH NORTH LOOP IH 820 SECTION A

One-Dimensional Model

Figure 75 shows the suction profile developed up to the depth of the moisture active zone, which is shown to be 15 ft. The initial suction for wetting at the surface is estimated using the climatic data, the Thornthwaite moisture index and the drainage condition at the site. The equilibrium suction of 2.58 pF, which was obtained from lab tests of the soil sample, is attributed to a water table being near the depth of 17 ft and yields only a small amount of heaving. In the stabilized soil layer, the suction envelope for wetting may not exceed the equilibrium suction or 3.5 pF [35], whichever is smaller (Figure 76).

Total vertical movements calculated at the edge of the pavement and at the outer wheel path are 1.46 inches and 0.61 inches, respectively (Table 24). The result shows that a negligible heave, 0.07 inch, is caused by a low equilibrium suction, which results in little change of suction in the wetting side. However, the expected shrinkage due to difference between the equilibrium suction and the suction of drying side is 1.39 inches. By adding a stabilized soil layer, it is found that the reduction of vertical movement in the outer wheel path is about 15 percent. The total vertical movements calculated at the edge of the pavement and at the outer wheel path for the case of adding a stabilized soil layer are 1.39 inches and 0.52 inches, respectively.

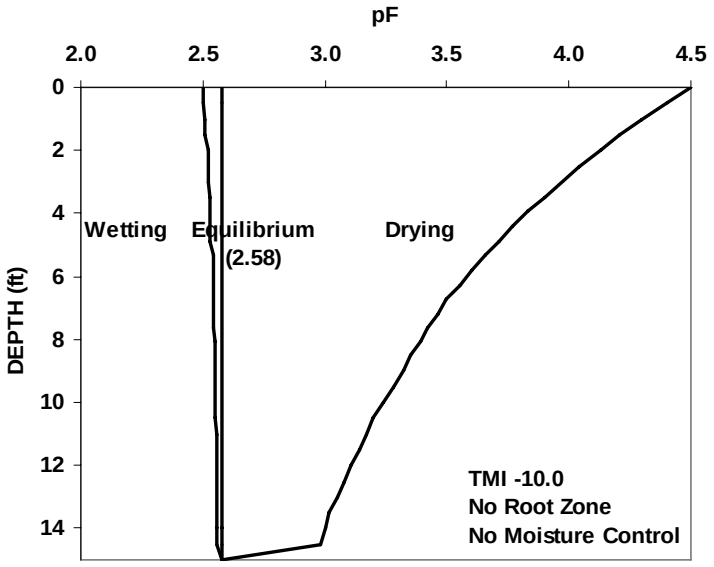

Figure 75. Suction Profile versus Depth for the Case of No Moisture Control, Fort Worth North Loop IH 820, Section A.

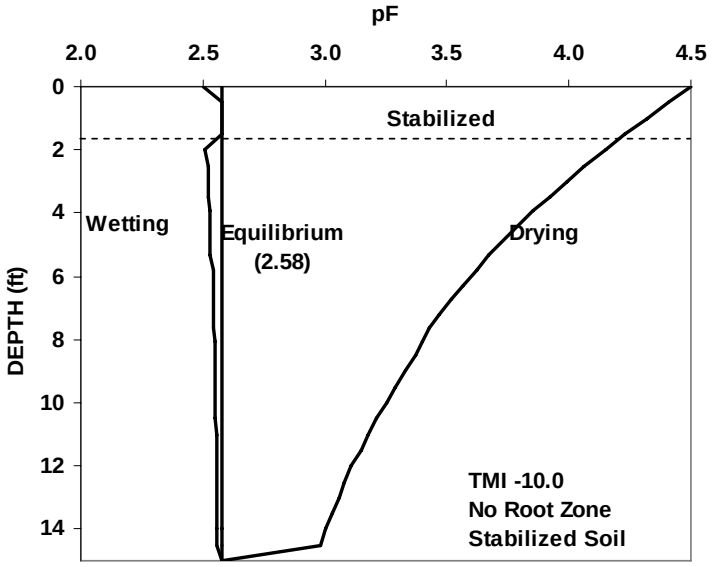

Figure 76. Suction Profile versus Depth with Adding Stabilized Layer, Fort Worth North Loop IH 820, Section A.

Table 24. Vertical Movement at the Edge of Pavement and at the Outermost Wheel Path, Fort Worth North Loop IH 820, Section A.

Systems of Pavement	At the Edge of the Pavement (inches)			At the Outermost Wheel Path (inches)
	Swelling	Shrinkage	Total	
No moisture control	0.07	1.39	1.46	0.61
Stabilized soil (1.5 ft)	0.04	1.26	1.39	0.52

Performance of Various Pavement Systems

The input parameters for the structural properties of both flexible and rigid pavements and the traffic data are shown in Table 25. For flexible pavements with alternative treatments including a vertical moisture barrier and stabilized layers, the loss of serviceability and the increase of international roughness index versus time at a level of reliability of 50 percent are shown in Figures 77 and 78, respectively. The results show that the serviceability index increases and the international roughness index decreases after 30 years, as the structural number increases. Both figures also show that for this site, a vertical barrier is less effective than stabilized layers in controlling roughness.

Table 25. Input Parameters for Structural Properties of Pavement and Traffic Data at the Fort Worth Site.

Flexible Pavement	Rigid Pavement
Reliability : 50% and 90% Falling Weight Deflectometer Modulus of Subgrade Soil : 10,000 psi Initial Serviceability Index : 4.2 Initial International Roughness Index : 75.2 in/mile	Reliability : 95% Modulus of Subgrade Soil : 515 pci (k =FWD/19.4) 28-day Compressive Strength of Concrete : 4,000 psi Mean Modulus of Rupture of Concrete : 650 psi Drainage Coefficient : 0.9 or 1.0 Load Transfer Coefficient : 3.2 Initial Serviceability Index : 4.5 Initial International Roughness Index : 65.4 in/mile
Distribution of Traffic for Five Lanes in One Direction (inner to outer): 0.16, 0.16, 0.16, 0.20, and 0.32 Average Daily Traffic of Outer Lane : 13,712 (T=0 yr), 21,744 (T=30 yr) Total W_{18} of Outer Lane (T=30 yr) : 8,415,520 Width of Pavement : 83.0 ft	Distance from the Center of Pavement : 27.0 ft

Figures 79 and 80 show the loss of SI and the development of IRI at a reliability of 90 percent for several different flexible pavement systems. These design alternatives do not represent current practice but instead provide the effects of treatments for a period of 30 years. The SI after 30 years is increased by 15 percent by adding an inert soil layer 1.5 ft thick beneath flexible pavements with the same SN of 5.06. The pavement system with a stabilized soil layer of 2.5 ft and an inert soil of 1.5 ft is expected to perform better than the same pavement without an inert soil layer. The pavement systems with a Lime Treated Subgrade (LTS) of 2.5 ft have acceptable performance. The criterion that was used in selecting these minimally acceptable treatments was for the pavement riding quality to remain above a PSI of 2.5 for the entire 30-year period without requiring any rehabilitation such as overlaying.

In the design analysis of rigid pavements, the systems with a concrete thickness of 11.5 inches and a stabilized soil layer of 8.0 inches (=0.67 ft) have unacceptable performance (Figures 81 and 82). A stabilized soil layer in this rigid pavement system with a concrete thickness of 12 inches has little effect. This is the result of using the AASHTO Design Equation for the traffic on rigid pavements. The concrete layer thickness term has an exponent of 7.35 in the design Equation (93) and influences significantly the predicted roughness of a rigid pavement on moderate expansive clay.

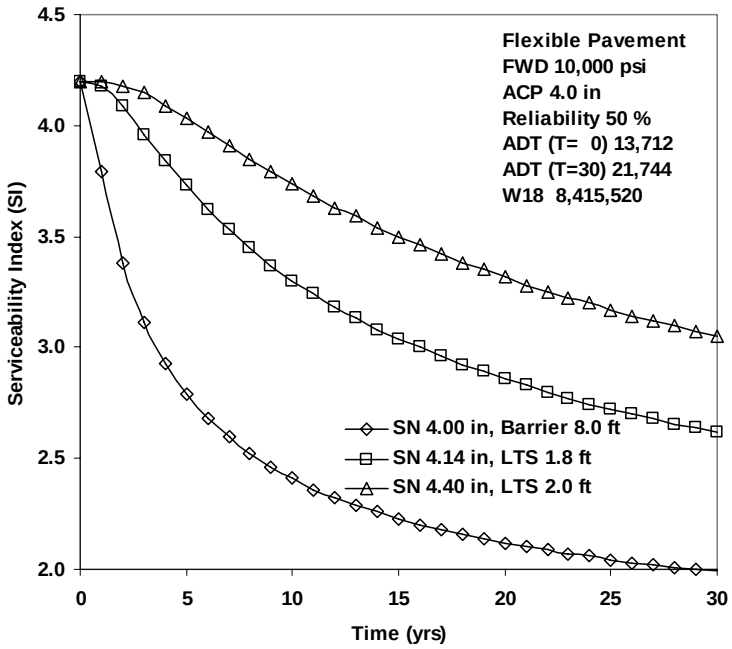

Figure 77. Serviceability Index versus Time for Several Different Pavement Systems with Reliability 50% in the Flexible Pavement, Fort Worth North Loop IH 820, Section A.

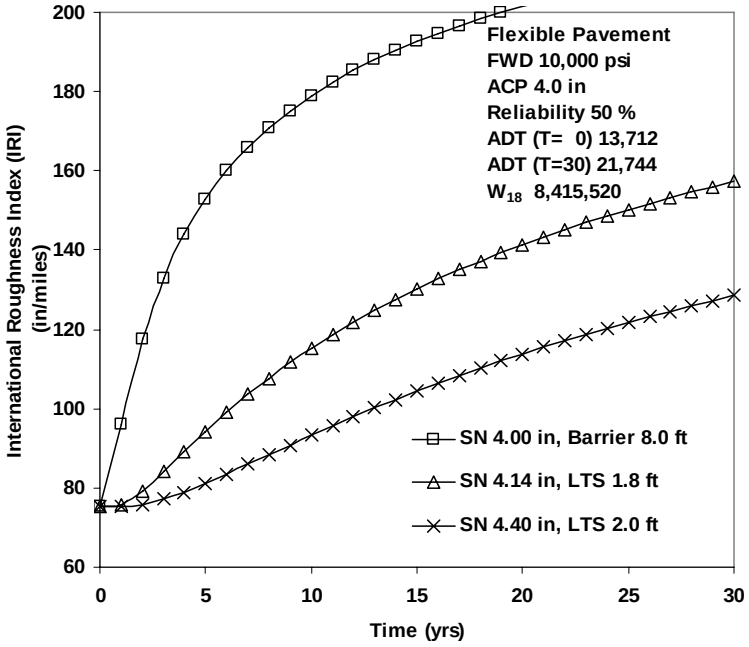

Figure 78. International Roughness Index versus Time for Several Different Pavement Systems with Reliability 50% in the Flexible Pavement, Fort Worth North Loop IH 820, Section A.

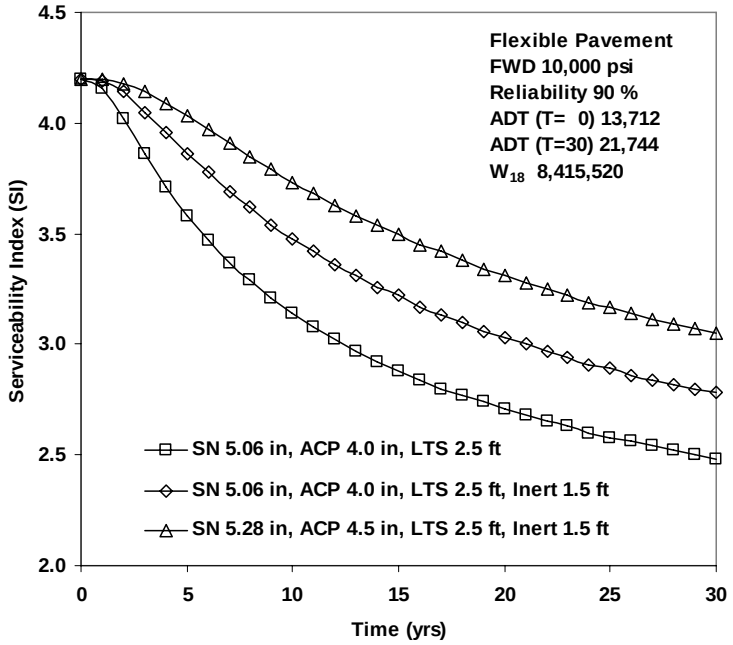

Figure 79. Serviceability Index versus Time for Several Different Pavement Systems with Reliability 90% in the Flexible Pavement, Fort Worth North Loop IH 820, Section A.

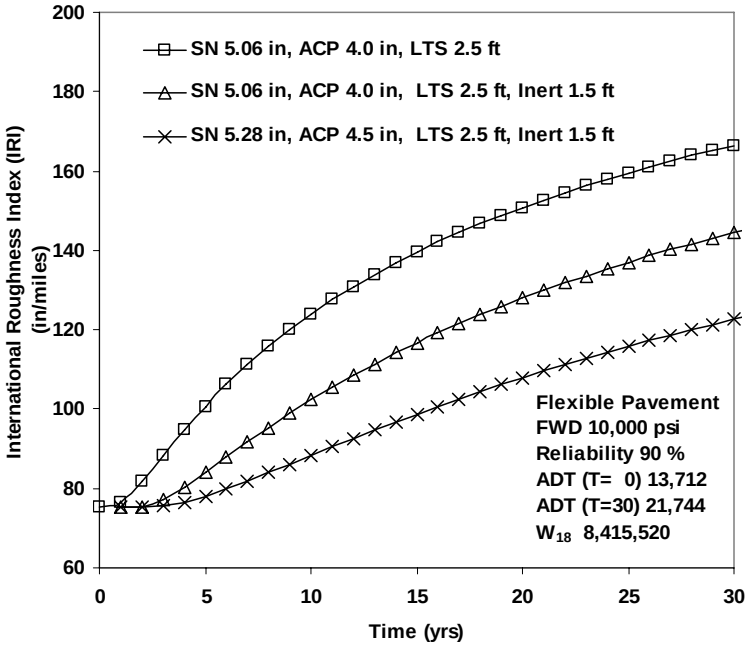

Figure 80. International Roughness Index versus Time for Several Different Pavement Systems with Reliability 90% in the Flexible Pavement, Fort Worth North Loop IH 820, Section A.

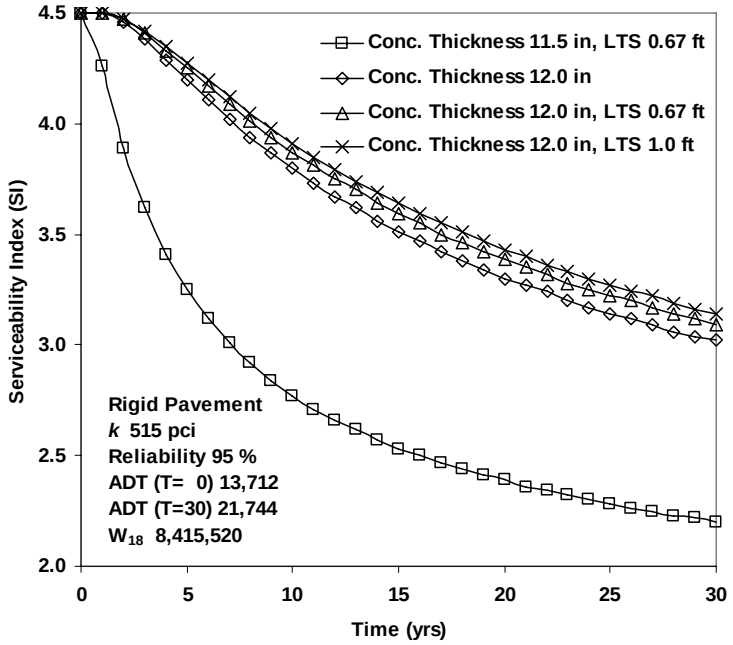

Figure 81. Serviceability Index versus Time for Several Different Pavement Systems with Reliability 95% in the Rigid Pavement, Fort Worth North Loop IH 820, Section A.

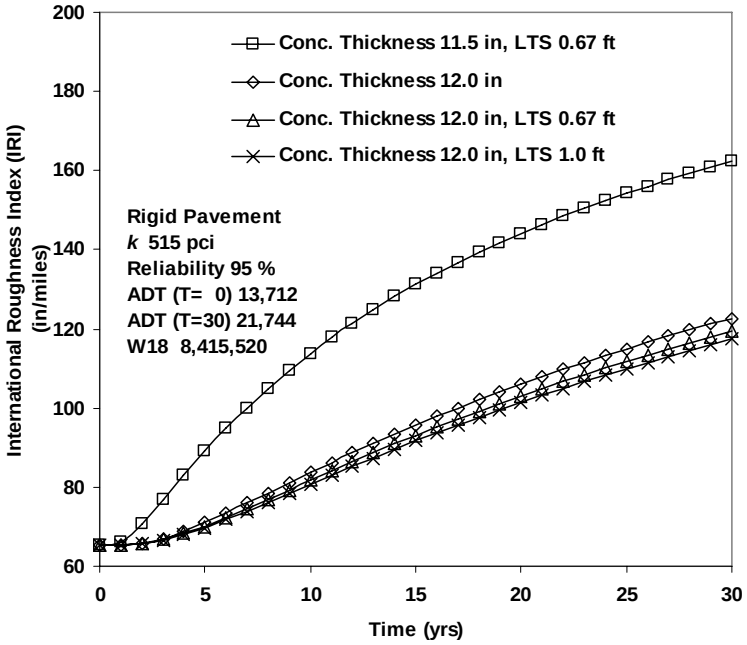

Figure 82. International Roughness Index versus Time for Several Different Pavement Systems with Reliability 95% in the Rigid Pavement, Fort Worth North Loop IH 820, Section A.

FORT WORTH NORTH LOOP IH 820 SECTION B

One Dimensional Model

The suction profile at this location is developed with the equilibrium suction of 3.45 pF; the limiting surface suction of 2.5 pF for wetting and 4.5 pF for drying is illustrated in Figure 83. Figure 84 shows that the wet suction caused by the effect of the stabilized layer is controlled by the equilibrium suction. A total vertical movement of 4.68 inches is calculated in the natural soil with no moisture control and it may be reduced to 3.03 inches with a stabilized soil layer of 1.5 ft. The vertical movement in the outer wheel path can be reduced as much as 0.6 inch with a stabilized soil layer (Table 26).

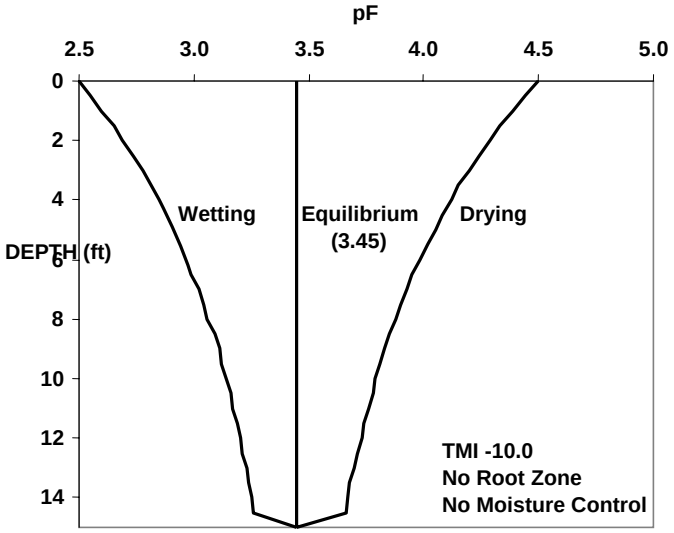

Figure 83. Suction Profile versus Depth for the Case of No Moisture Control, Fort Worth North Loop IH 820, Section B.

Table 26. Vertical Movement at the Edge of Pavement and at the Outermost Wheel Path Fort Worth North Loop IH 820, Section B.

Systems of Pavement	At the Edge of the Pavement (inches)			At the Outermost Wheel Path (inches)
	Swelling	Shrinkage	Total	
No moisture control	3.19	1.49	4.68	1.80
Stabilized soil (1.5 ft)	1.83	1.20	3.03	1.21

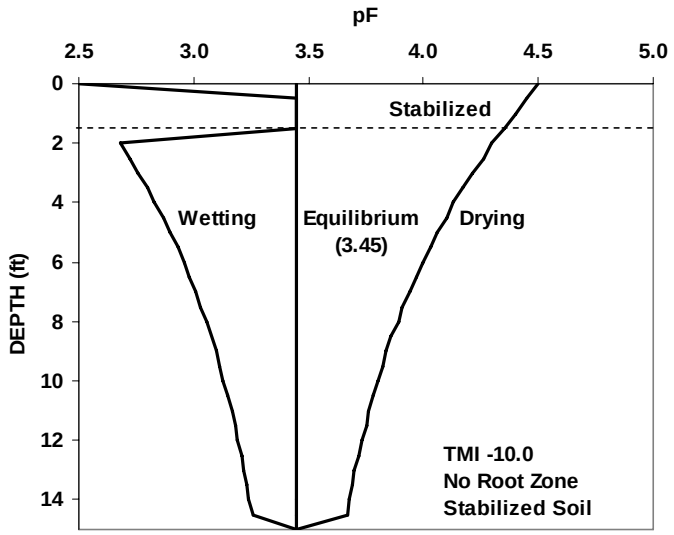

Figure 84. Suction Profile versus Depth with Adding Stabilized Layer, Fort Worth North Loop IH 820, Section B.

Performance of Various Pavement Systems

In the design analysis with a reliability of 50 percent, the structural number ranges between 4.40 and 5.06 inches (Figures 85 and 86). The results show that the effect of a stabilized soil layer of 0.2 ft greater thickness is greater than that of an inert soil layer of 1.5 ft. The serviceability indices calculated after 30 years for the pavement systems with a LTS of 2.0 ft and an inert soil of 1.5 ft, and with a LTS of 2.2 ft are 2.68 and 2.75, respectively.

In the design analysis with a reliability of 90 percent, the flexible pavement system with a stabilized soil layer of 2.5 ft, an inert soil of 1.5 ft, and an asphalt thickness of 5.0 inches will provide acceptable performance (Figures 87 and 88). The results show that the depth of the stabilized soil layer that is required is over 2.5 ft to control the total vertical movement of 4.68 inches at the edge of the pavement.

For the rigid pavement, at a reliability of 95 percent, the pavement system with a slab thickness of 12.0 inches and a stabilized soil layer of 8.0 inches thick could produce acceptable performance when the minimum SI after 30 years is set at 2.5 (Figures 89 and 90). The results show that the 30-year SI can be increased by 17 percent by adding a stabilized soil layer up to 1.0 ft. The expected total movements beneath the outer wheel paths for the pavements that produce the minimally acceptable predicted performance are 0.7 inches and 1.44 inches in the flexible and rigid pavements, respectively.

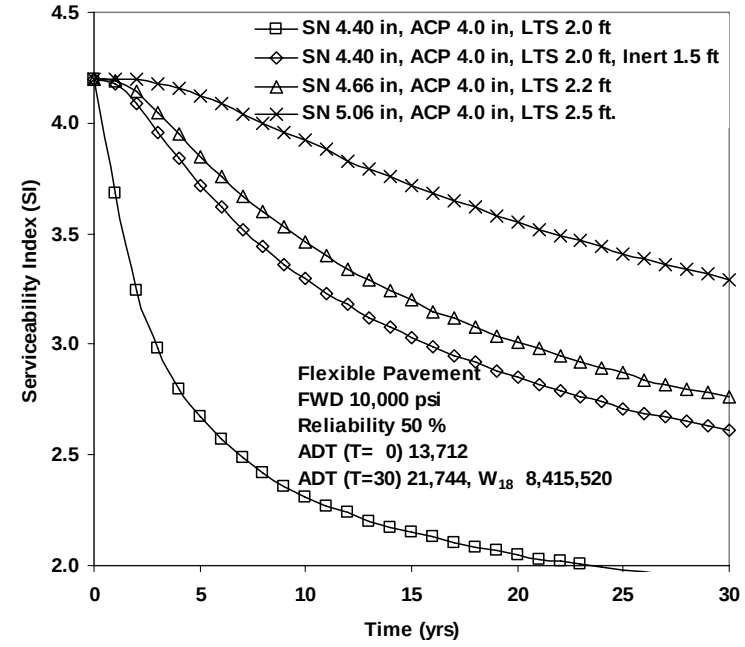

Figure 85. Serviceability Index versus Time for Several Different Pavement Systems with Reliability 50% in the Flexible Pavement, Fort Worth North Loop IH 820, Section B.

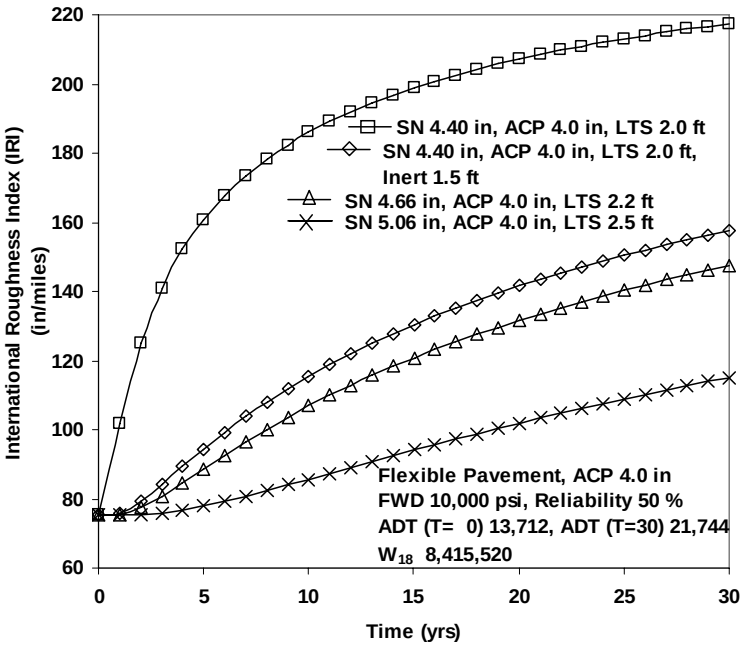

Figure 86. International Roughness Index versus Time for Several Different Pavement Systems with Reliability 50% in the Flexible Pavement, Fort Worth North Loop IH 820, Section B.

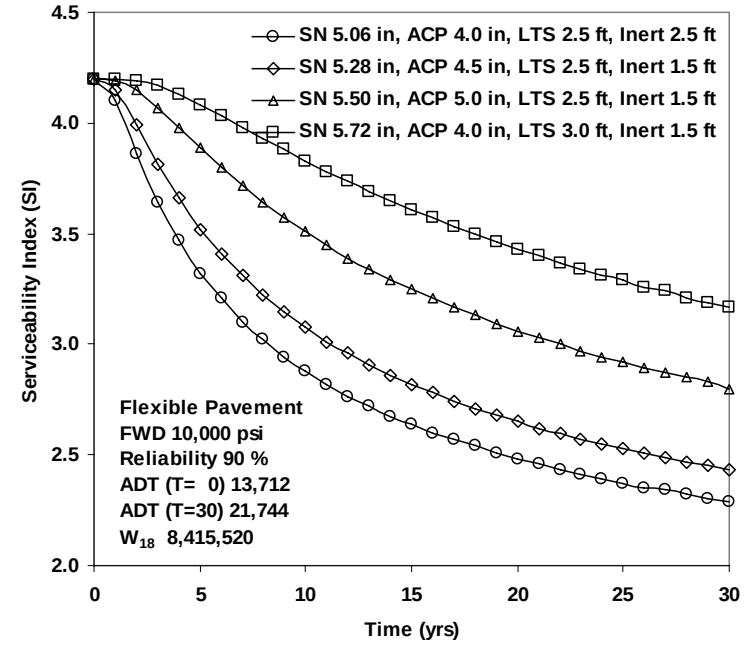

Figure 87. Serviceability Index versus Time for Several Different Pavement Systems with Reliability 90% in the Flexible Pavement, Fort Worth North Loop IH 820, Section B.

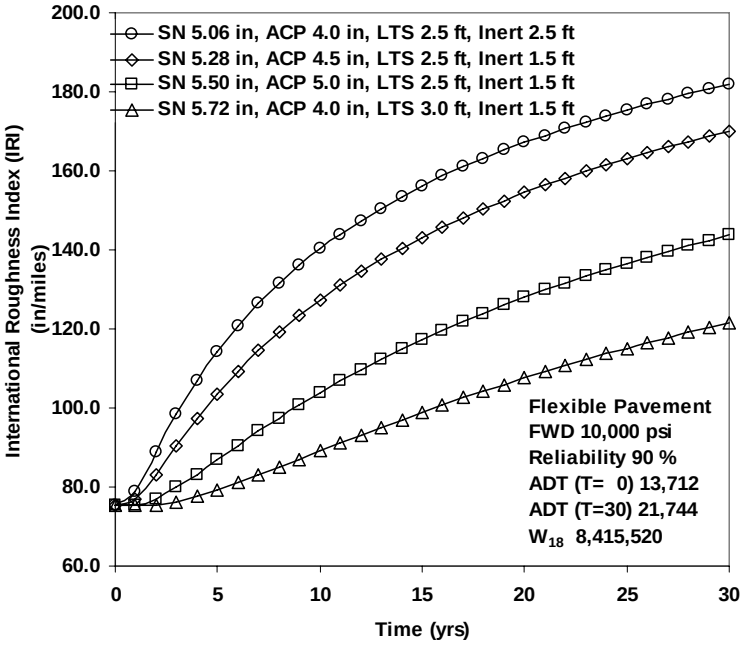

Figure 88. International Roughness Index Versus Time for Several Different Pavement Systems with Reliability 90% in the Flexible Pavement, Fort Worth North Loop IH 820, Section B.

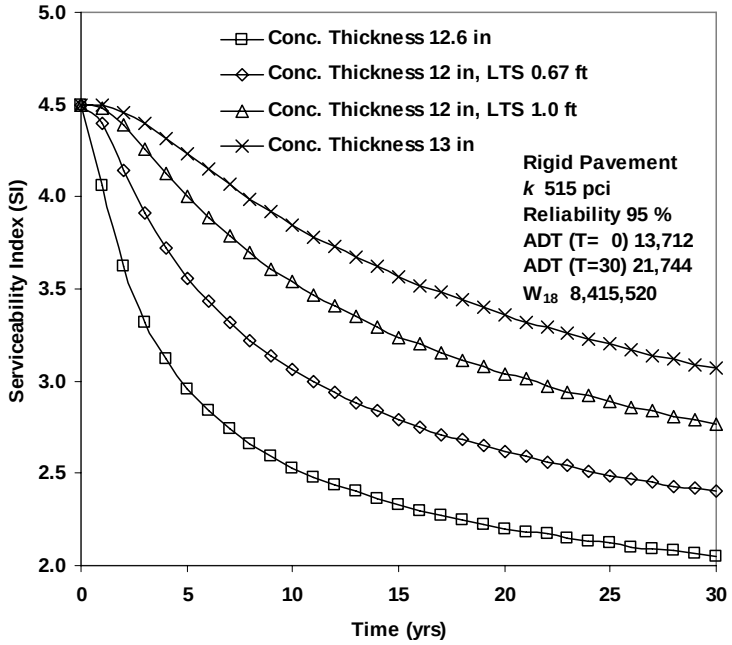

Figure 89. Serviceability Index Versus Time for Several Different Pavement Systems with Reliability 95% in the Rigid Pavement, Fort Worth North Loop IH 820, Section B.

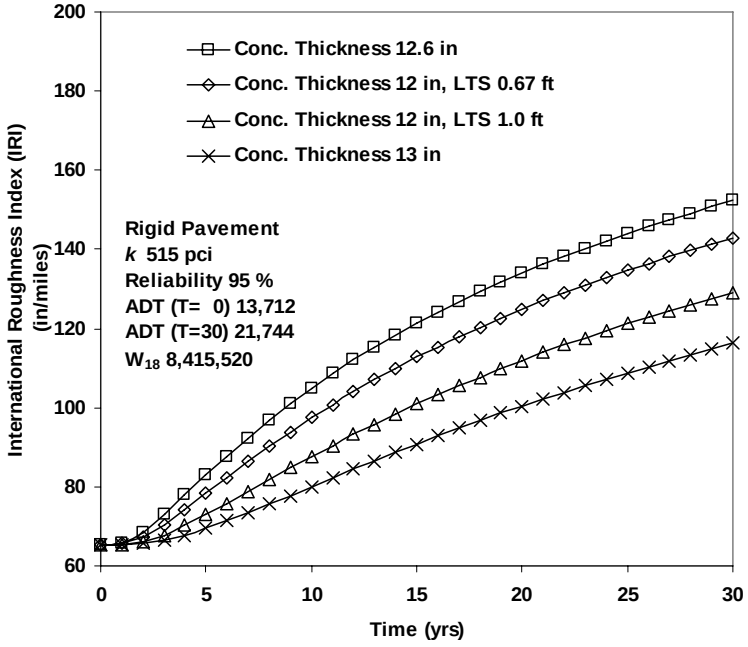

Figure 90. International Roughness Index Versus Time for Several Different Pavement Systems with Reliability 95% in the Rigid Pavement, Fort Worth North Loop IH 820, Section B.

FORT WORTH NORTH LOOP IH 820 SECTION C

One-Dimensional Model

The suction envelopes for the case of the natural soil with no moisture control and for the case with a stabilized soil layer 1.5 ft thick are shown in Figures 91 and 92, respectively. The limiting surface suctions of 2.5 pF for wetting and 4.5 pF for drying are illustrated with the equilibrium suction obtained from lab tests of soil sample. The vertical movements at the edge of the pavement and in the outermost wheel path are presented in Table 27. The swelling and shrinkage movements calculated in the natural soil without moisture control are 2.58 inches and 1.33 inches, respectively. The results show that the vertical movement of 1.62 inches in the wheel path can be reduced to 1.13 inches by adding a stabilized soil layer 1.5 ft thick.

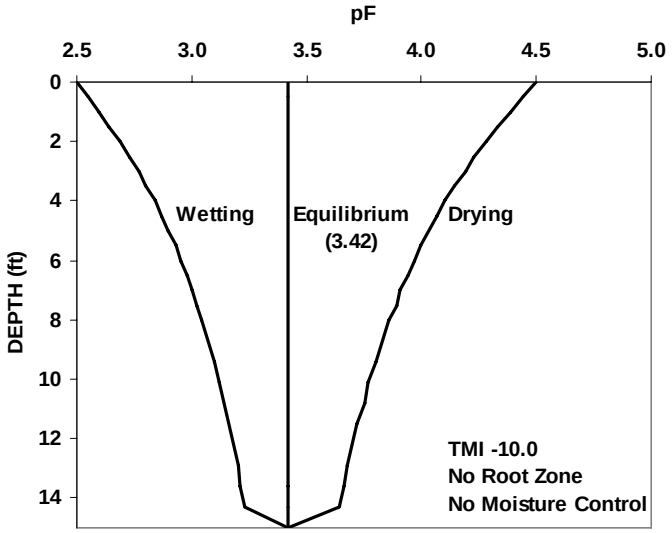

Figure 91. Suction Profile Versus Depth for the Case of No Moisture Control, Fort Worth North Loop IH 820, Section C.

Table 27. Vertical Movement at the Edge of Pavement and at the Outermost Wheel Path Fort Worth North Loop IH 820, Section C.

Systems of Pavement	At the Edge of the Pavement (inches)			At the Outermost Wheel Path (inches)
	Swelling	Shrinkage	Total	
No moisture control	2.58	1.33	3.91	1.62
Stabilized soil (1.5 ft)	1.62	1.11	2.73	1.13

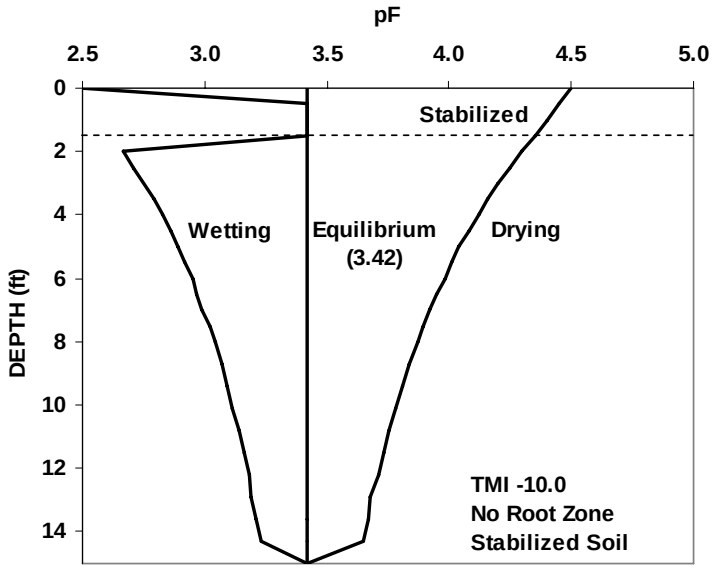

Figure 92. Suction Profile versus Depth with Adding Stabilized Layer, Fort Worth North Loop IH 820, Section C.

Performance of Various Pavement Systems

In the design analysis with a reliability of 50 percent for the flexible pavement, the effect of increasing the thickness of the stabilized soil layers is shown in Figures 93 and 94. The SI predicted at 30 years with stabilized soil layers of 2.0 ft, 2.2 ft, and 2.5 ft are 2.22, 2.88, and 3.35, respectively.

With a reliability of 90 percent, various structural numbers are used to estimate the serviceability and roughness (Figures 95 and 96). The results show that as the asphalt thickness increases from 4.0 inches to 4.5 inches, in the pavement systems with a stabilized soil of 2.5 ft and inert soil 1.5 ft, the 30-year SI increases by 23 percent, from 2.2 to 2.7. The pavement systems with a LTS of 2.5 ft, an inert soil of 1.0 ft and a ACP of 4.5 inches have acceptable predicted performance. The total movements calculated in this pavement at the edge of pavement and at the outer wheel path are 1.70 inches and 0.70 inches, respectively.

For the rigid pavement with a reliability level of 95 percent, the concrete pavement system with a slab thickness of 12.0 inches and a stabilized soil layer 1.5 ft thick will produce acceptable performance (Figures 97 and 98).

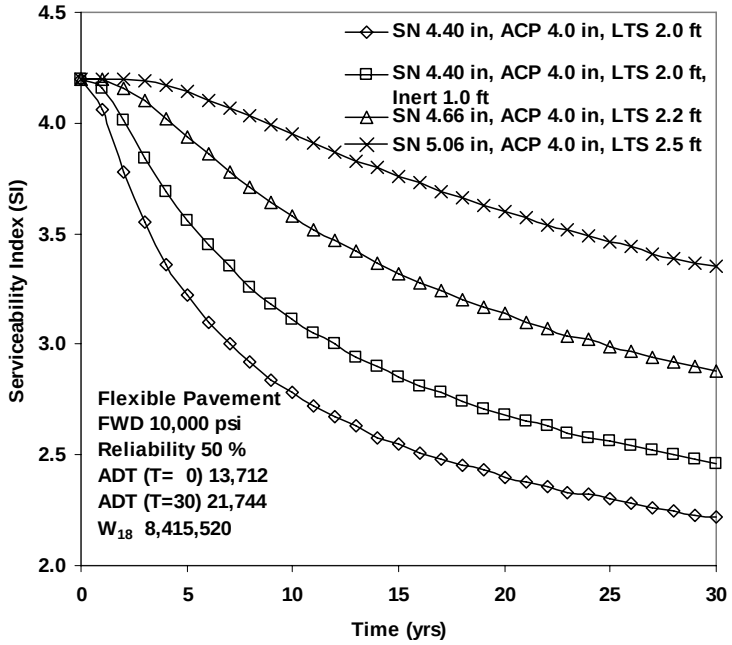

Figure 93. Serviceability Index versus Time for Several Different Pavement Systems with Reliability 50% in the Flexible Pavement, Fort Worth North Loop IH 820, Section C.

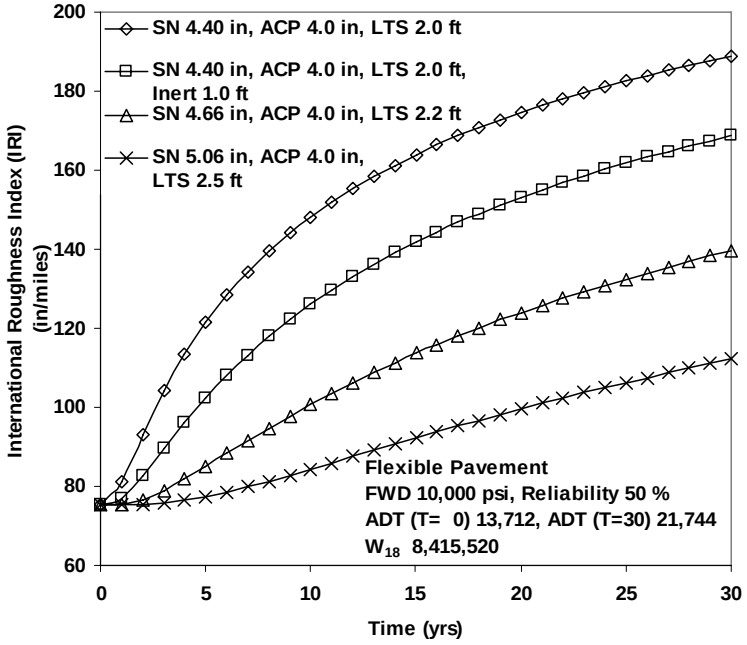

Figure 94. International Roughness Index versus Time for Several Different Pavement Systems with Reliability 50% in the Flexible Pavement, Fort Worth North Loop IH 820, Section C.

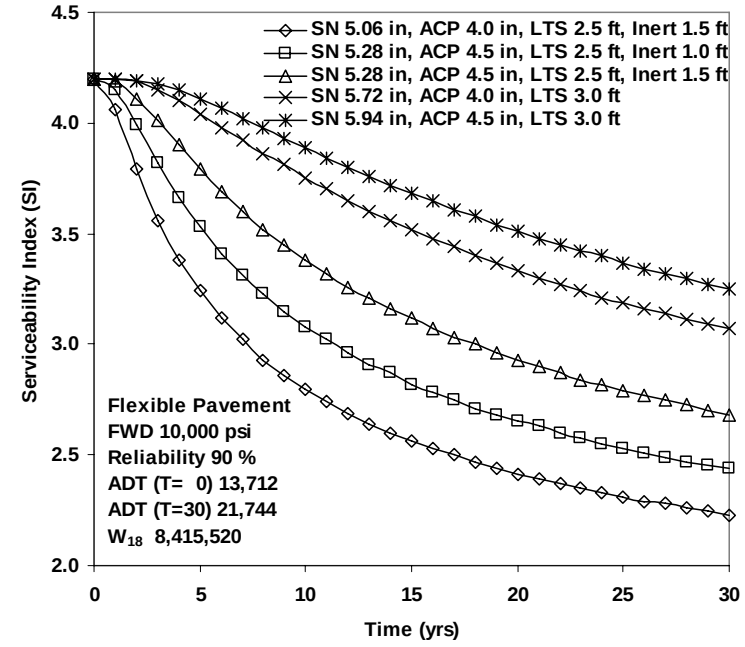

Figure 95. Serviceability Index versus Time for Several Different Pavement Systems with Reliability 90% in the Flexible Pavement, Fort Worth North Loop IH 820, Section C.

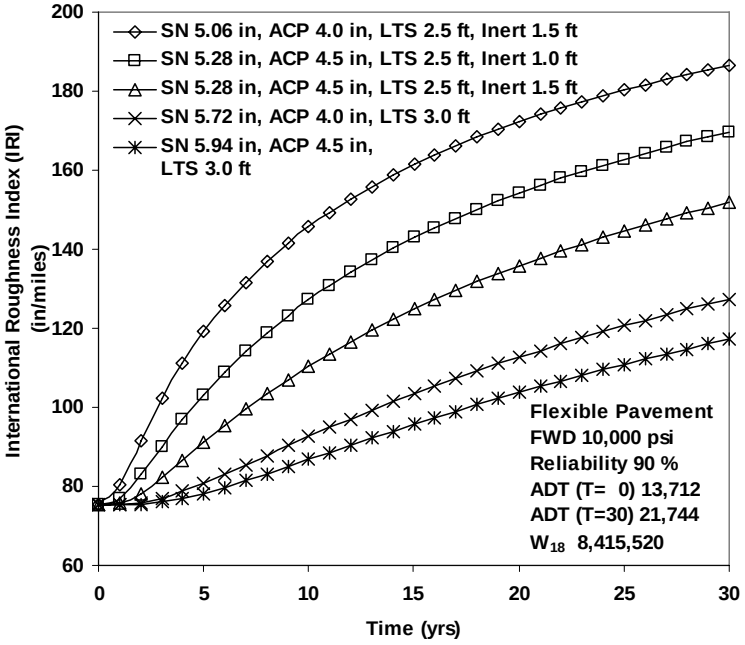

Figure 96. International Roughness Index versus Time for Several Different Pavement Systems with Reliability 90% in the Flexible Pavement, Fort Worth North Loop IH 820, Section C.

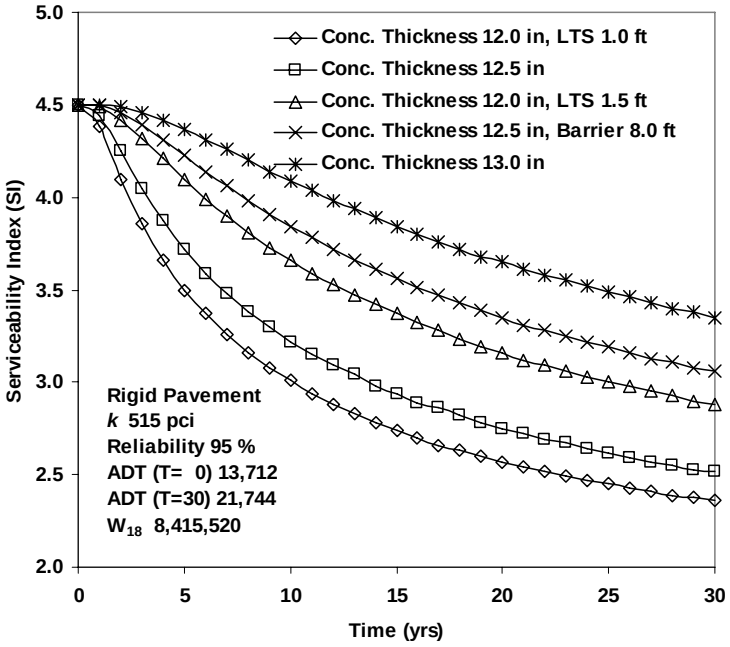

Figure 97. Serviceability Index versus Time for Several Different Pavement Systems with Reliability 95% in the Rigid Pavement, Fort Worth North Loop IH 820, Section C.

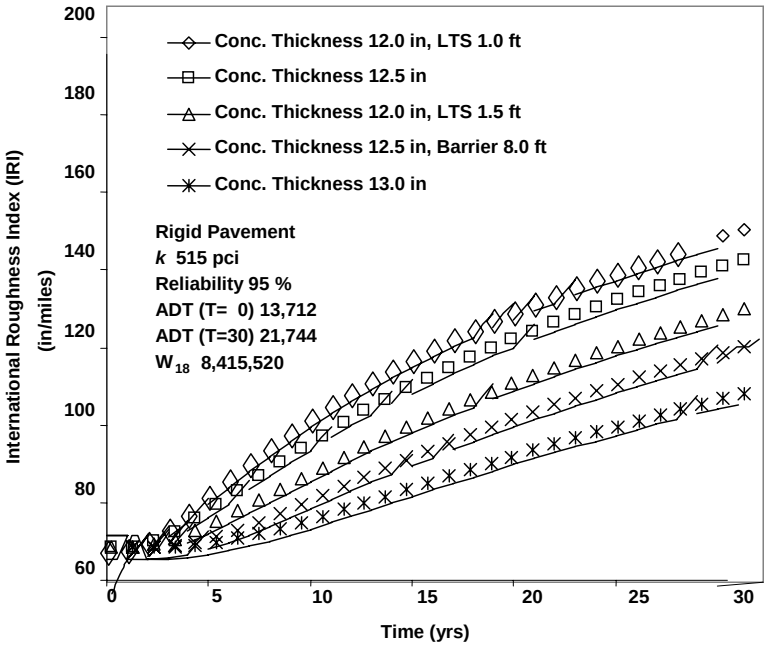

Figure 98. International Roughness Index versus Time for Several Different Pavement Systems with Reliability 95% in the Rigid Pavement, Fort Worth North Loop IH 820, Section C.

ATLANTA US 271

One-Dimensional Model

The suction profile at the edge of the pavement at the site in the Atlanta District along US 271 is generated with a root zone of 11.0 ft (Figures 99 and 100) based on the root fibers found in the boring log. The total vertical movement of 1.72 inches at the edge of the pavement is the sum of the heave of 0.68 inch and the shrinkage of 1.04 inches (Table 28). Generally, the swelling calculated is greater than the shrinkage because of consideration of the effect of lateral confinement within a possible upper crack zone. However, a large change between the equilibrium suction and the suction on the dry side provides more shrinkage movement than swelling movement. The total vertical movement of 1.34 inches is calculated at the outer wheel path in the natural soil without moisture control and it may be reduced to 1.09 inches by adding a stabilized soil layer of 1.5 ft.

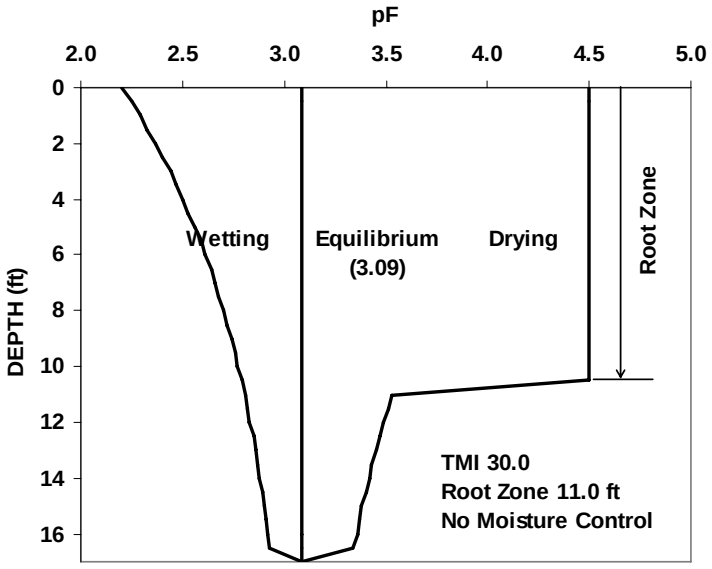

Figure 99. Suction Profile versus Depth for the Case of No Moisture Control, Atlanta US 271.

Table 28. Vertical Movement at the Edge of Pavement and at the Outermost Wheel Path, Atlanta US 271.

Systems of Pavement	At the Edge of the Pavement (inches)			At the Outermost Wheel Path (inches)
	Swelling	Shrinkage	Total	
No moisture control	0.68	1.04	1.72	1.34
Stabilized soil (1.5 ft)	0.37	1.00	1.37	1.09

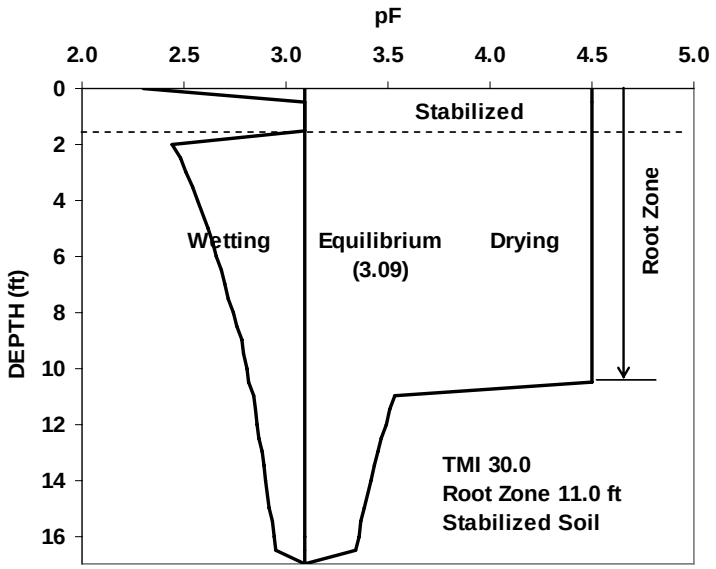

Figure 100. Suction Profile versus Depth with Adding Stabilized Layer, Atlanta US 271.

Performance of Various Pavement Systems

Input parameters for the structural properties of pavement and traffic data at the site in the Atlanta District along US 271 are assumed (Table 29). There is one lane in one direction with the width of pavement of 44.0 ft including the shoulder. The distance from the center of the pavement to the outer wheel path of interest is 9.0 ft. The average daily traffic and the total 18 kip ESALs in 30 years are assumed as 10,000, 20,000, and 2,500,000, respectively.

Table 29. Input Parameters for Structural Properties of Pavement and Traffic Data at the Atlanta US 271 Site.

Flexible Pavement	Rigid Pavement
Reliability : 50% and 90% Falling Weight Deflectometer Modulus of Subgrade Soil : 10,000 psi Initial Serviceability Index : 4.2 Initial International Roughness Index : 75.2 in/mile	Reliability : 95% Modulus of Subgrade Soil : 515 pci (k =FWD/19.4) 28-day Compressive Strength of Concrete : 4,000 psi Mean Modulus of Rupture of Concrete : 650 psi Drainage Coefficient : 1.0 Load Transfer Coefficient : 3.2 Initial Serviceability Index : 4.5 Initial International Roughness Index : 65.4 in/mile
Average Daily Traffic (T= 0 yr) : 10,000 Total W_{18} (T= 30 yr) : 2,500,000 Width of Pavement : 44.0 ft	Average Daily Traffic (T=30 yr) : 20,000 Number of Lanes : 1 Distance from the Center of Pavement : 9.0 ft

In the design analysis with a reliability of 50 percent, the SI and IRI predicted after 30 years with a structural number of 3.72 inches are 2.42 and 173 inch/mile (Figures 101 and 102). The results show that the SI after 30 years increases up to 2.84 from 2.42 if a moisture barrier 8.0 ft deep is installed.

Figures 103 and 104 show the effects of different asphalt layer thicknesses and thicknesses of stabilized soil layers in the design analysis with a reliability of 90 percent. A stabilized soil layer 2.2 ft thick is required in the pavement system with an ACP layer 4.0 inches thick when the SI after 30 years is required to be 2.5. The results show that as the stabilized soil layer thickness increase from 2.2 ft to 2.5 ft, the 30-year SI increases by 29 percent, from 2.4 to 3.1.

In the design analysis with a reliability of 95 percent, the various thicknesses of concrete slab, 10.5, 11.0, and 12.0 inches are applied for the rigid pavement design (Figures 105 and 106). Under design conditions with modulus of subgrade reaction of 515 pci, a 28-day compressive strength of 4000 psi and a mean modulus of rupture of 650 psi, a concrete thickness of 10.5 inches is expected to produce acceptable performance. The results show that just increasing the concrete layer thickness of 0.5 inches results in a considerable improvement in performance. The concrete layer thickness term in the AASHTO design equation has an exponent of 7.35 and influences significantly the predicted roughness of a rigid pavement on a moderate swell-shrink potential site.

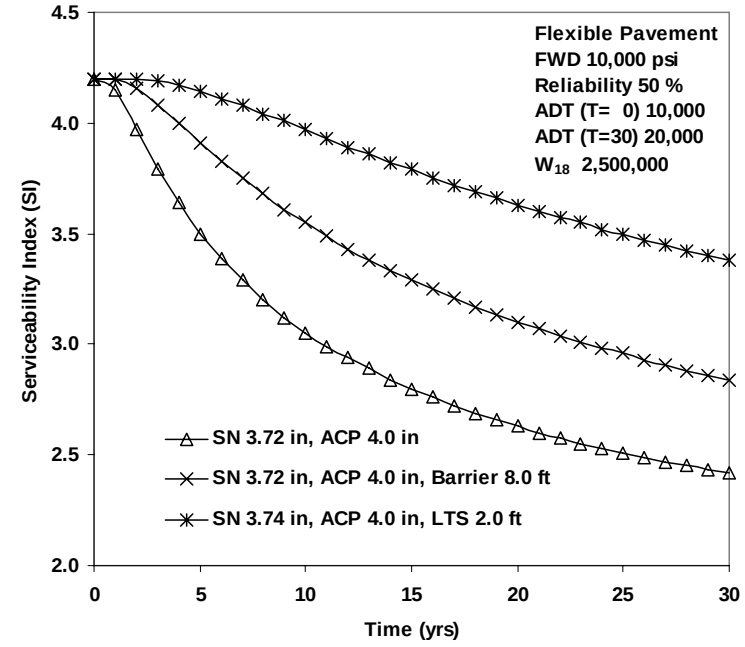

Figure 101. Serviceability Index versus Time for Several Different Pavement Systems with Reliability 50% in the Flexible Pavement, Atlanta US 271.

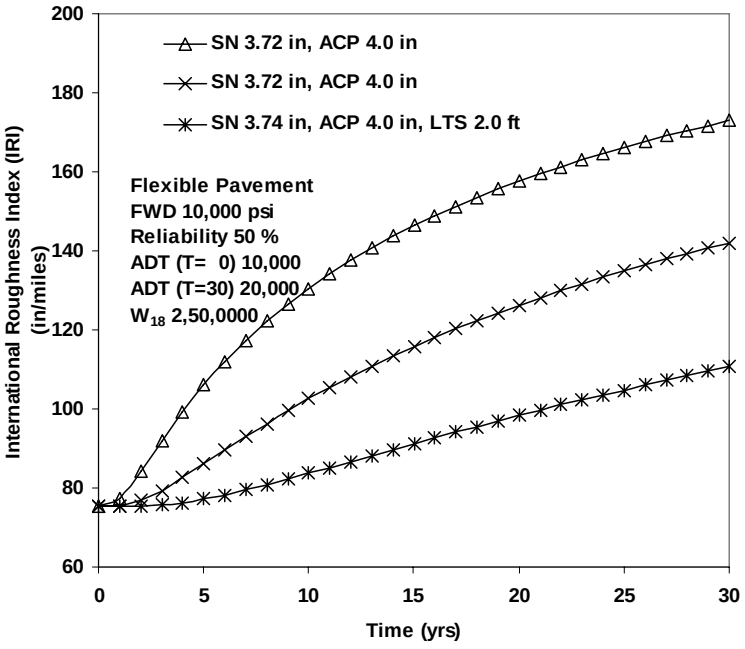

Figure 102. International Roughness Index versus Time for Several Different Pavement Systems with Reliability 50% in the Flexible Pavement, Atlanta US 271.

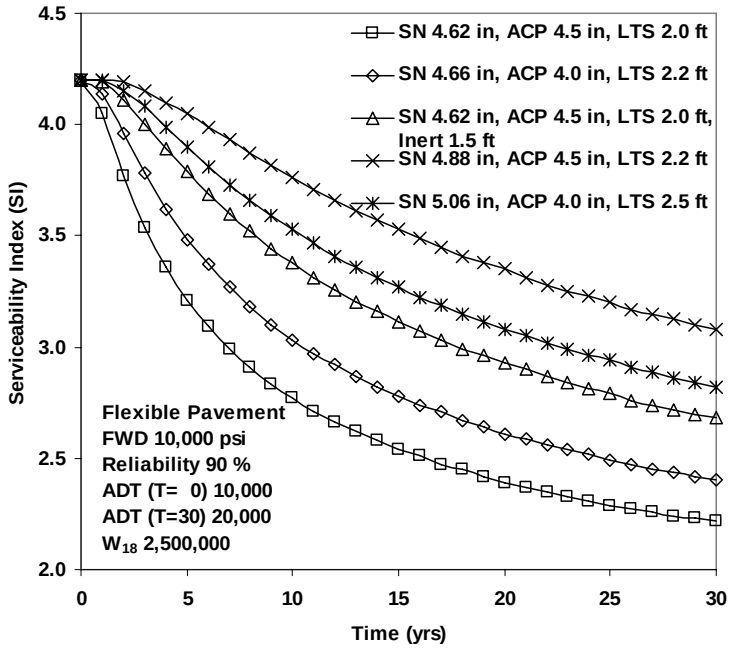

Figure 103. Serviceability Index versus Time for Several Different Pavement Systems with Reliability 90% in the Flexible Pavement, Atlanta US 271.

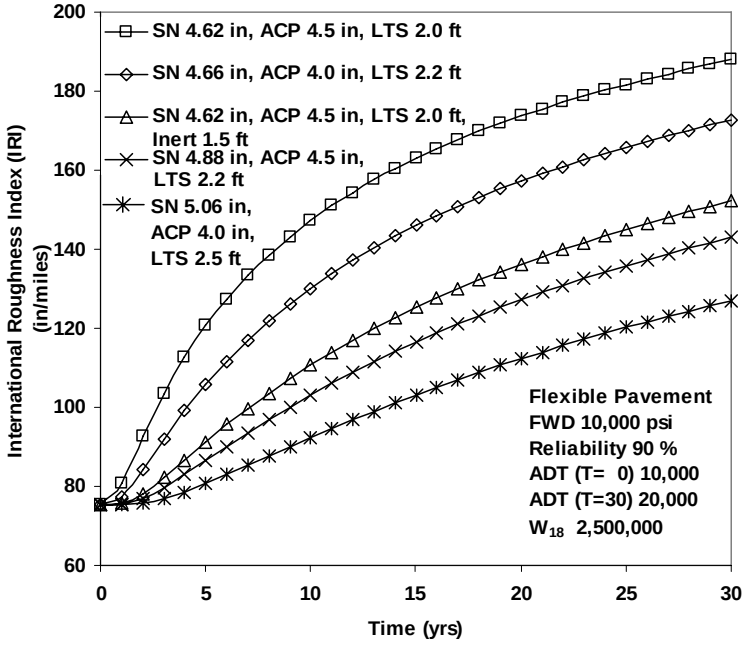

Figure 104. International Roughness Index versus Time for Several Different Pavement Systems Conditions with Reliability 90% in the Flexible Pavement, Atlanta US 271.

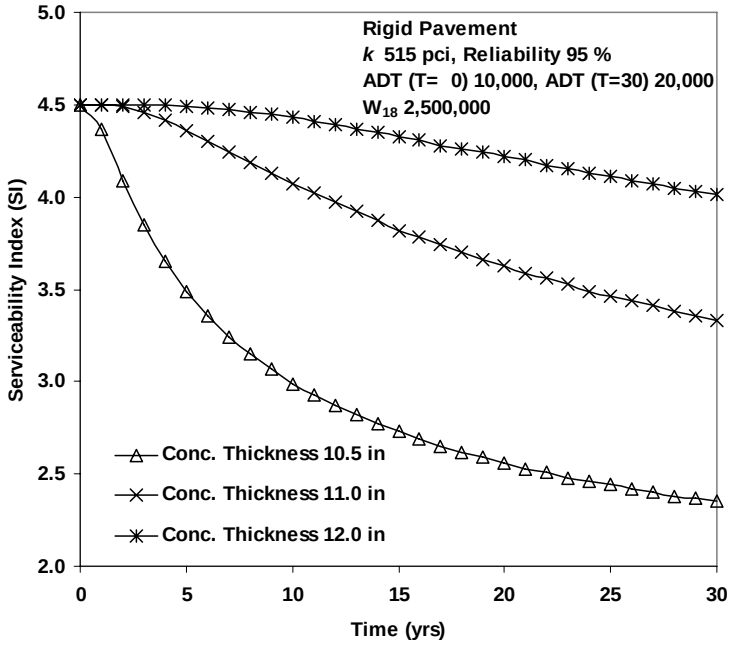

Figure 105. Serviceability Index versus Time for Several Different Pavement Systems with Reliability 95% in the Rigid Pavement, Atlanta US 271.

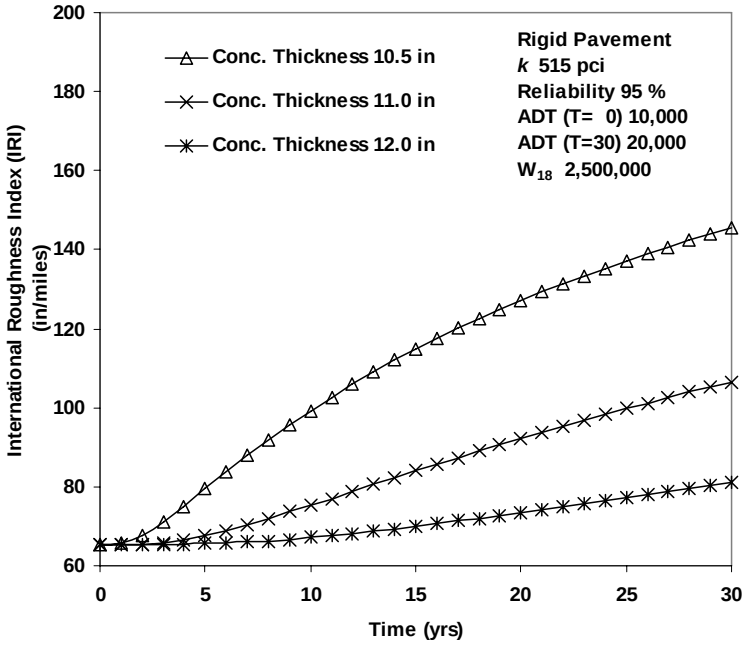

Figure 106. International Roughness Index versus Time for Several Different Pavement Systems with Reliability 95% in the Rigid Pavement, Atlanta US 271.

AUSTIN LOOP 1

One-Dimensional Model

The suction profiles with equilibrium suction of 3.45 pF in the natural soil with no moisture control and in the stabilized soil layer 1.5 ft thick are illustrated in Figures 107 and 108, respectively. Based on the data obtained from laboratory tests and three boring logs located in the frontage road, the typical section for the design analysis is constructed (Appendix E). The main lanes are about 20 ft higher than the frontage road and there is a deep grass-covered median between the northbound and southbound main lanes. The soil profile for analysis at the main lane is assumed as the same due to insufficient data. The swelling and shrinkage movements calculated in the natural soil without moisture control are 2.03 inches and 0.98 inches, respectively. The total vertical movement at the edge of the pavement and the predicted movement in the outer wheel path at a distance of 15.0 ft from the center of the pavement are 2.46 inches and 1.21 inches (Table 30). The total vertical movement in the outer wheel path can be reduced by 50 percent by adding stabilized soil layer of 1.5 ft thick.

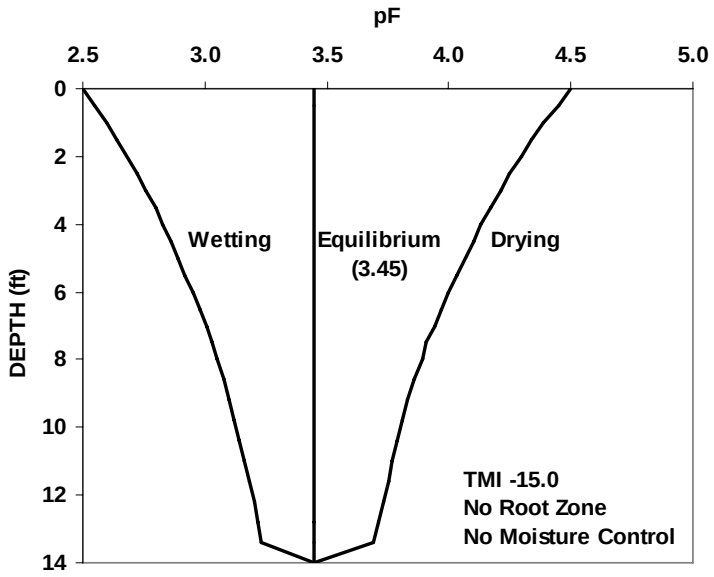

Figure 107. Suction Profile versus Depth for the Case of No Moisture Control, Austin Loop 1.

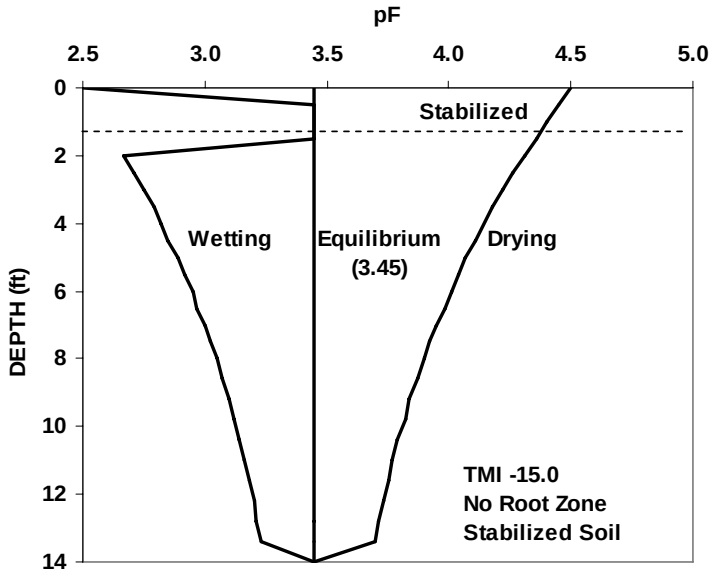

Figure 108. Suction Profile versus Depth with Adding Stabilized Layer, Austin Loop 1.

Table 30. Vertical Movement at the Edge of Pavement and at the Outermost Wheel Path, Austin Loop 1.

Systems of Pavement	At the Edge of the Pavement (inches)			At the Outermost Wheel Path (inches)
	Swelling	Shrinkage	Total	
No moisture control	2.03	0.98	3.01	2.46
Stabilized soil (1.5 ft)	1.21	0.82	2.03	1.21

Performance of Various Pavement Systems

Table 31 shows the input parameters for the pavement and traffic data of the main lanes. The main roadway has four lanes in one direction, and the width of the pavement is 62.0 ft. The input ADT and the total 18-kip ESALs in 30 years are assumed to be the same as the Fort Worth North Loop IH 820 sections with 38 percent of the total traffic being applied to the outer lane.

Table 31. Input Parameters for Structural Properties of Pavement and Traffic Data at the Austin Loop 1 Site, Main Lane.

Flexible Pavement	Rigid Pavement
Reliability : 50% and 90% Falling Weight Deflectometer Modulus of Subgrade Soil : 10,000 psi Initial Serviceability Index : 4.2 Initial International Roughness Index : 75.2 in/mile	Reliability : 95 % Modulus of Subgrade Soil : 515 pci (k =FWD/19.4) 28-day Compressive Strength of Concrete : 4,000 psi Mean Modulus of Rupture of Concrete : 650 psi Drainage Coefficient : 1.0 Load Transfer Coefficient : 3.2 Initial Serviceability Index : 4.5 Initial International Roughness Index : 65.4 in/mile
Distribution of Traffic for Four Lanes in One Direction (inner to outer): 0.19, 0.19, 0.24, and 0.38 Average Daily Traffic of Outer Lane : 16,283 (T=0 yr), 25,821 (T=30 yr) Total W_{18} of Outer Lane (T=30 yr) : 9,993,430 Width of Pavement : 62.0 ft Distance from the Center of Pavement : 21.0 ft	

In the design analysis with a reliability of 50 percent, three different pavement systems with stabilized soil layers 2.2 to 2.5 ft thick and an inert soil layer 1.0 to 1.5 ft thick are analyzed and the SI and IRI are predicted (Figures 109 to 110). The pavement systems with an ACP layer 4.0 inches thick, a stabilized soil layer 2.8 ft thick, and an inert soil layer 1.5 ft thick will produce acceptable performance with a reliability of 90 percent (Figures 111 and 112). The expected total movement beneath the outer wheel path in this pavement system is 0.93 inches. The results show that the pavement systems with an ACP of 4.0 inches will produce better performance by adding a LTS of 0.2 ft thick from LTS of 2.8 ft thick than by adding an inert soil layer of 1.5 ft thick.

For the rigid pavement design analysis with a reliability of 95 percent, the various pavement treatments applied are following: concrete thickness of 12.0 and 12.5 inches, stabilized soil layer 2.0 ft thick, inert soil layer 1.5 ft thick, and vertical moisture barrier of 10 ft and 13 ft (Figures 113 and 114). The results show that the loss of SI with time or the increase of international roughness index is practically the same in the pavement with concrete thickness of 12.0 inches and a vertical moisture barrier of 13.0 ft and the pavement with a stabilized soil layer of 2.0 ft thick. The SI after 30 years in these pavements is 2.4, which is nearly acceptable performance for that period of time.

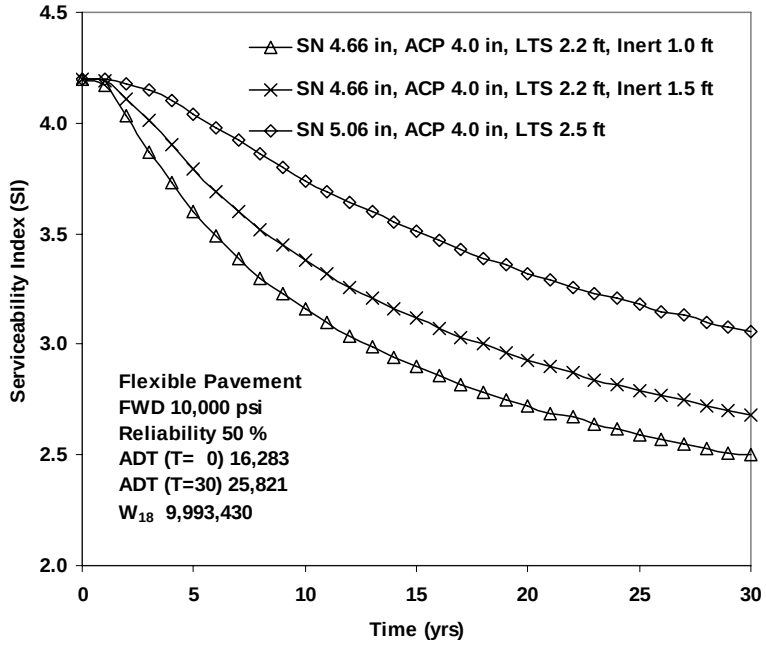

Figure 109. Serviceability Index versus Time for Several Different Pavement Systems with Reliability 50% in the Flexible Pavement, Austin Loop 1, Main Lane.

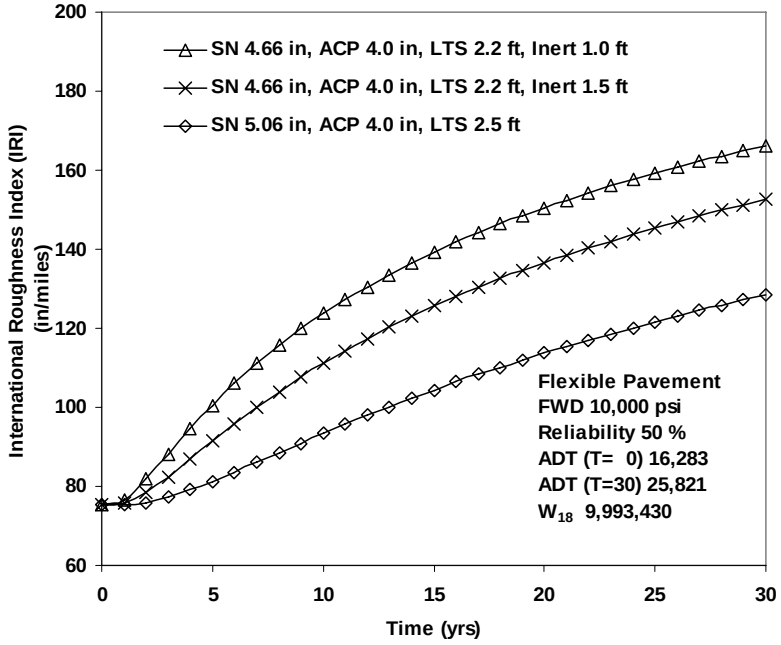

Figure 110. International Roughness Index versus Time for Several Different Pavement Systems with Reliability 50% in the Flexible Pavement, Austin Loop 1, Main Lane.

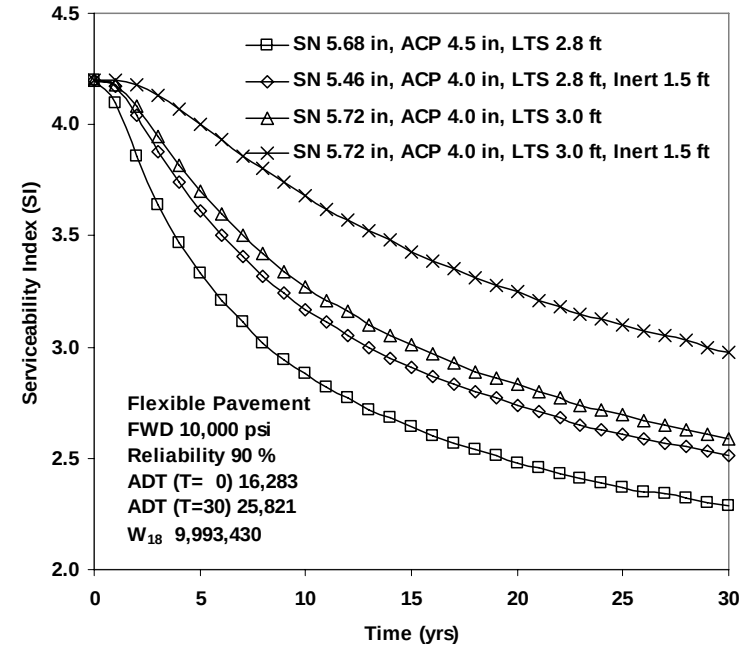

Figure 111. Serviceability Index versus Time for Several Different Pavement Systems with Reliability 90% in the Flexible Pavement, Austin Loop 1, Main Lane.

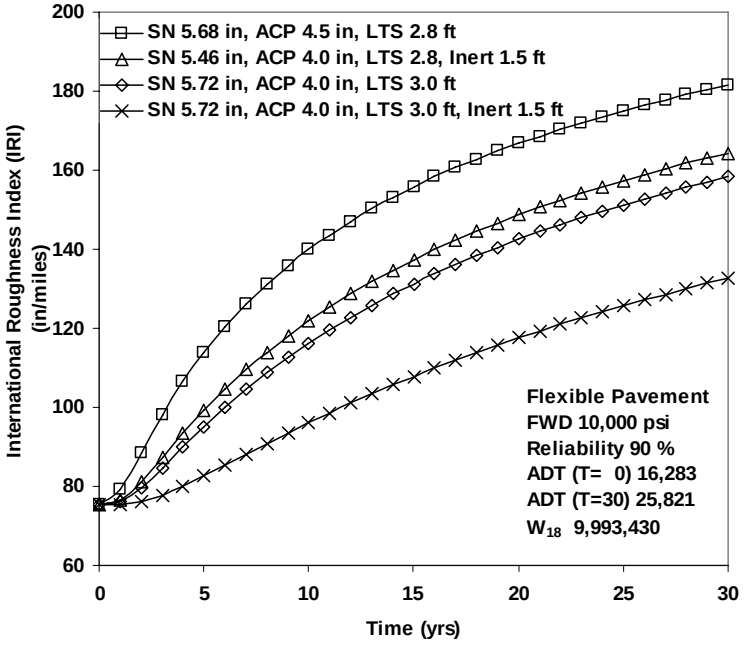

Figure 112. International Roughness Index versus Time for Several Different Pavement Systems with Reliability 90% in the Flexible Pavement, Austin Loop 1, Main Lane.

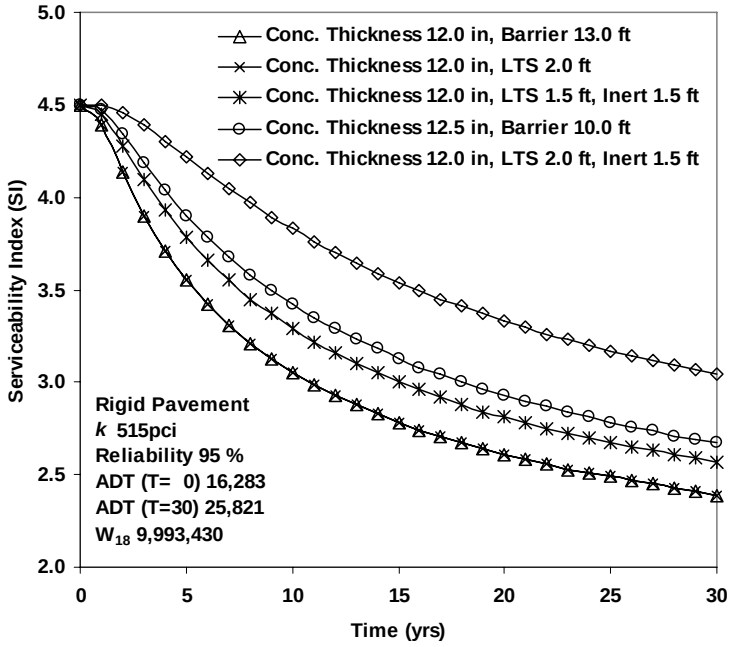

Figure 113. Serviceability Index versus Time for Several Different Pavement Systems with Reliability 95% in the Rigid Pavement, Austin Loop 1, Main Lane.

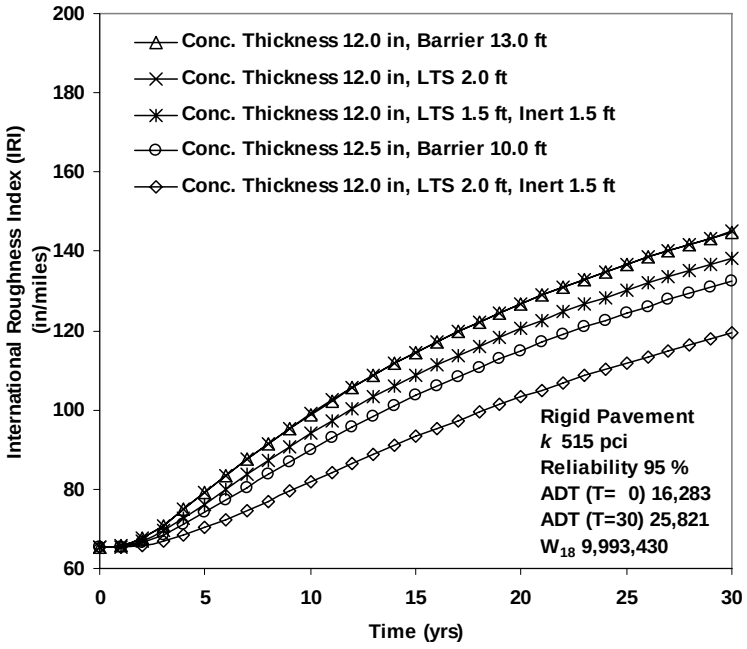

Figure 114. International Roughness Index versus Time for Several Different Pavement Systems with Reliability 95% in the Rigid Pavement, Austin Loop 1, Main Lane.

The volume of traffic in the frontage road is assumed to be 10 percent of the main lanes. The frontage road has three lanes in one direction and width of pavement of 50.0 ft. The distance from the center of the pavement to the outer wheel path is estimated as 15.0 ft. The input parameters for the frontage road are presented in Table 32.

Table 32. Input Parameters for Structural Properties of Pavement and Traffic Data at the Austin Loop 1 Site, Frontage Road.

Flexible Pavement	Rigid Pavement
Reliability : 50 % and 90% Falling Weight Deflectometer Modulus of Subgrade Soil : 10,000 psi Initial Serviceability Index : 4.2 Initial International Roughness Index : 75.2 in/mile	Reliability : 95 % Modulus of Subgrade Soil : 515 pci (k =FWD/19.4) 28-day Compressive Strength of Concrete : 4,000 psi Mean Modulus of Rupture of Concrete : 650 psi Drainage Coefficient : 0.9 Load Transfer Coefficient : 3.2 Initial Serviceability Index : 4.5 Initial International Roughness Index : 65.4 in/mile
Distribution of Traffic for Three Lanes in One Direction (inner to outer): 0.20, 0.33, and 0.47 Average Daily Traffic of Outer Lane : 4,028 (T=0 yr), 6,837 (T=30 yr) Total W_{18} of Outer Lane (T=30 yr) : 2,472,059 Width of Pavement : 50.0 ft Distance from the Center of Pavement : 15.0 ft	

In order to predict the SI and IRI for the frontage road, several pavement treatments in the design analysis with a reliability of 50 percent are used: LTS of 1.5 ft to 1.8 ft, inert soil layer of 1.5 ft, and a vertical moisture barrier of 8.0 ft (Figures 115 and 116). The pavement system including a LTS of 1.8 ft will produce acceptable performance when the SI after 30 years is required to be 2.5. In the design analysis with a reliability of 90 percent for the frontage road, stabilized soil layers 2.0 to 2.5 ft thick and inert soil layers 1.5 to 2.5 ft thick are used to design the flexible pavement (Figures 117 and 118). The pavement system with an asphalt thickness of 4.0 inches, a stabilized soil layer 2.0 ft thick, and an inert soil layer 2.5 ft thick will produce acceptable performance. The predicted serviceability index and international roughness index after 30 years in this pavement system are 2.42 and 130 in/miles. The total vertical movements expected at the edge of pavement and in the outer wheel path are 1.25 inches and 0.93 inches, respectively.

Three different concrete thicknesses 11.0, 11.5, and 12.0 inches are used to estimate the loss of SI and the development of IRI in the rigid pavement (Figures 119 and 120). The pavement system with a slab thickness of 11.0 inches could produce acceptable performance.

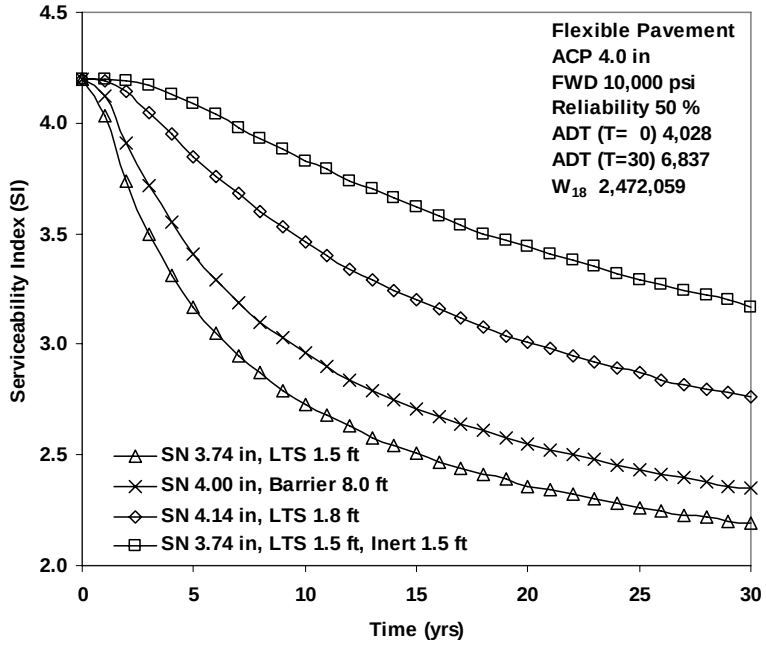

Figure 115. Serviceability Index versus Time for Several Different Pavement Systems with Reliability 50% in the Flexible Pavement, Austin Loop 1, Frontage Road.

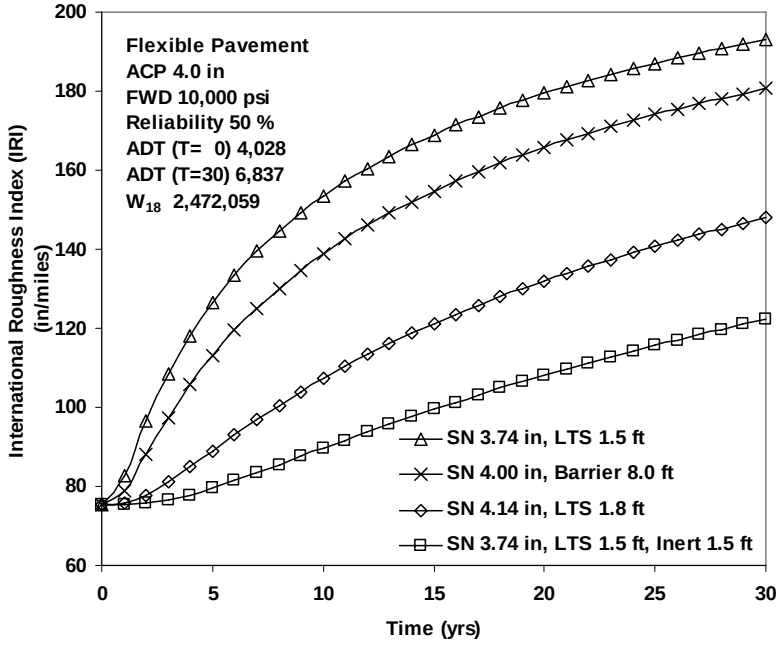

Figure 116. International Roughness Index versus Time for Several Different Pavement Systems with Reliability 50% in the Flexible Pavement, Austin Loop 1, Frontage Road.

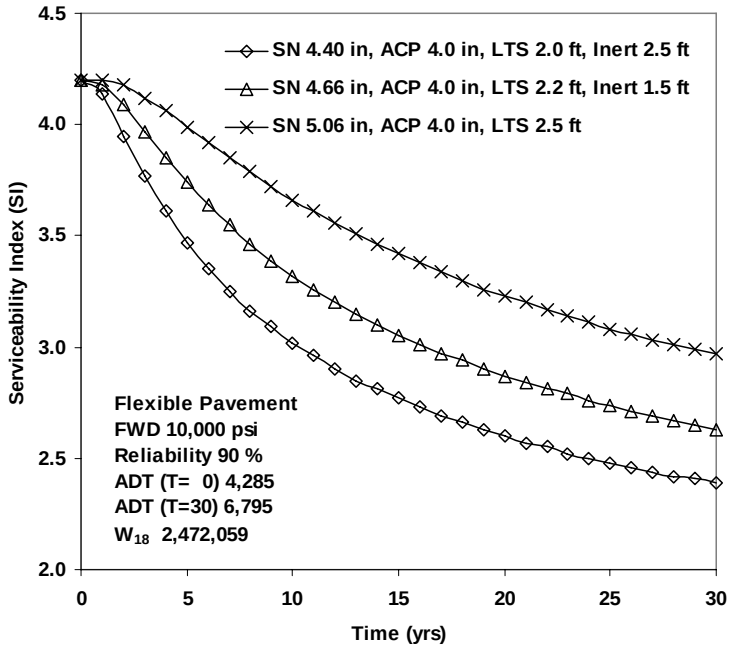

Figure 117. Serviceability Index versus Time for Several Different Pavement Systems with Reliability 90% in the Flexible Pavement, Austin Loop 1, Frontage Road.

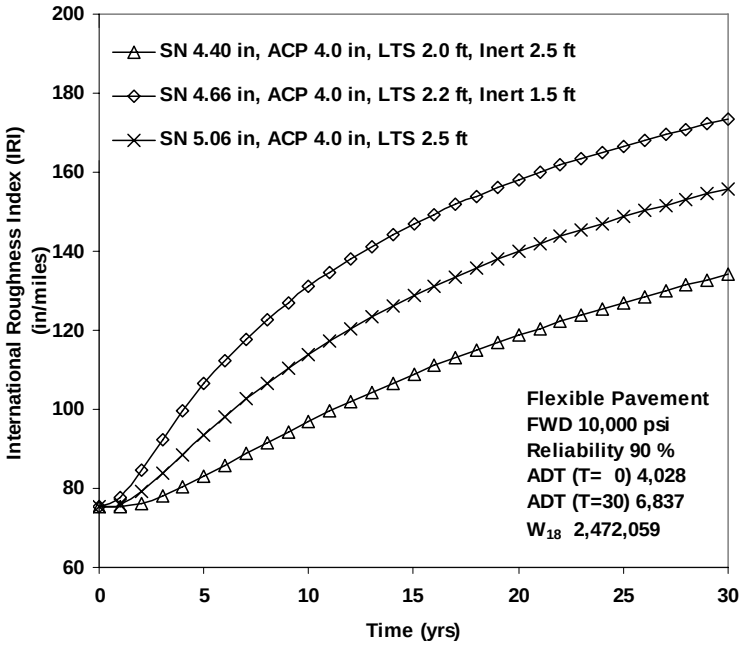

Figure 118. International Roughness Index versus Time for Several Different Pavement Systems with Reliability 90% in the Flexible Pavement, Austin Loop 1, Frontage Road.

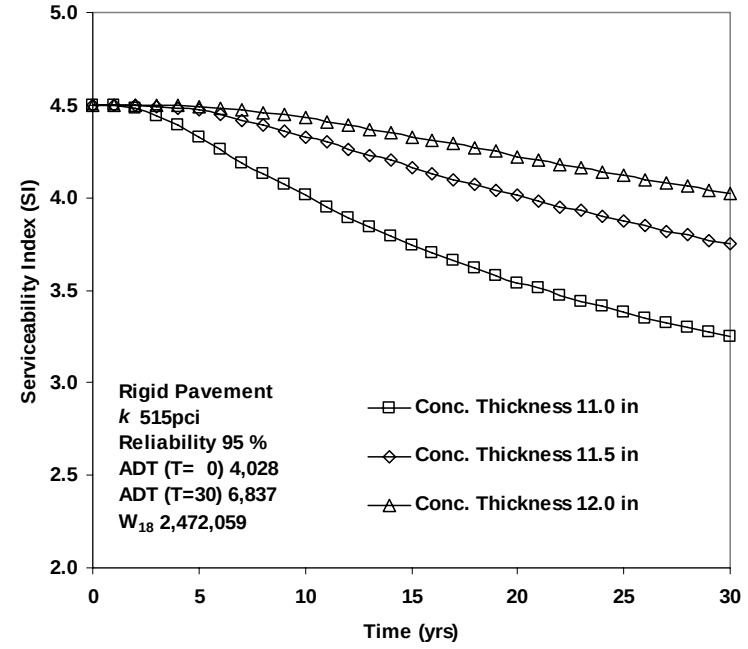

Figure 119. Serviceability Index versus Time for Several Different Pavement Systems with Reliability 95% in the Rigid Pavement, Austin Loop 1, Frontage Road.

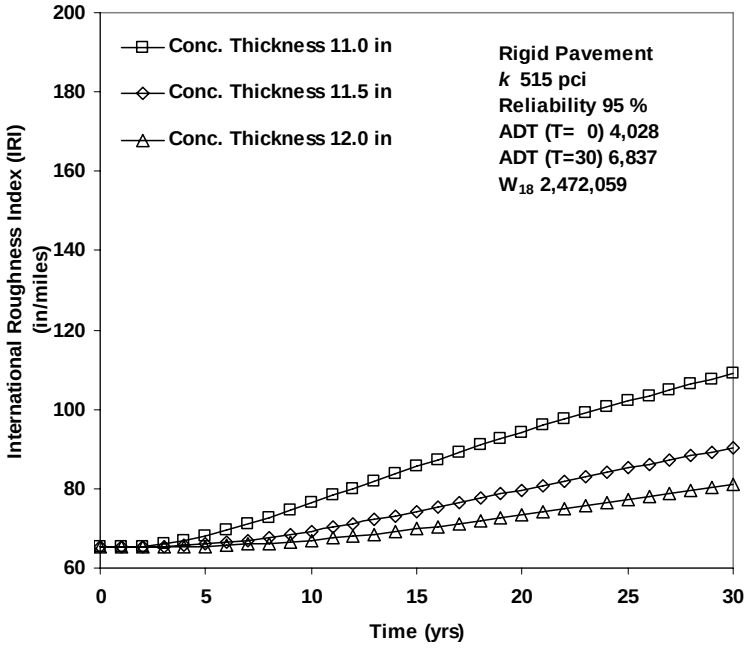

Figure 120. International Roughness Index versus Time for Several Different Pavement Systems with Reliability 95% in the Rigid Pavement, Austin Loop 1, Frontage Road.

CHAPTER 7:
COMPARISON OF PVR DESIGN CRITERIA WITH CASE STUDY RESULTS

The potential vertical rise computed for a given site is currently used in pavement design to determine what depth of the natural soil must be removed and replaced with a more inert soil or modified in place in order to reduce the computed PVR to 1 inch, 1.5 inches, or 2 inches dependent upon the highway facility (1″ for IH/US, 1.5″ for SHs, and 2″ for FMs). In this chapter, the amount of movement that is predicted both at the edge of the pavement and beneath the outer wheel path by the method described in this report is compared to the calculated PVR for the same cases. Contrary to the way the PVR is calculated, the predicted vertical movement is the sum of both shrinkage and swelling movements. The purpose of the comparison is to determine whether the previously used PVR criterion is conservative when compared to the movements that are calculated by the methods of this report. **A secondary purpose is to illustrate with the case studies the design advantages that are provided by having an estimate of both shrinking and swelling movements.**

The new method of predicting the vertical movement uses this information to predict the accumulation of pavement roughness with time and traffic. It was discovered in the course of the analysis of the field monitoring data that were collected for a period of over 20 years in some cases that the total movement in the subgrade beneath a given wheel path governs the *rate of increase* of roughness rather than the level of roughness itself. Roughness is predicted as a decrease of present serviceability index (PSI) as well as an increase of the international roughness index (IRI). The computed results are found in Tables 33 through 39. The case studies are discussed one cross section at a time for pavements with no treatment of the expansive subgrade soil (Tables 33 through 35). Then the reduced movements, calculated both by the new method and by the PVR method, due to treatments applied to the subgrade are compared. The treatments that are used for the comparisons were shown in Chapter 6 to provide a minimum acceptable predicted performance over 30 years with 90 percent reliability on flexible pavements and 95 percent reliability on rigid pavements (Tables 36 through 39).

FORT WORTH NORTH LOOP IH 820 CASE STUDY

Three cross sections were used as separate case studies along the IH 820 Loop north of Fort Worth. Cross sections A and B were embankment sections with Cross Section A being unusually wet and Cross Section B being closer to the normally expected moisture level. Cross Section C had an embankment on the north side of the roadway and was at grade on the south side. It, too, was at a more normally expected moisture level for the Fort Worth climatic zone. Table 33 shows the calculated vertical movements for each of the cross sections as they were predicted by the new method and also by the PVR method. The predictions were made at two locations: at the edge of the pavement where the soil movement is not affected by the weight of the pavement and beneath the outer wheel path where the weight of the pavement will restrain the vertical movement to some extent. The new method predicts both a swelling and a shrinkage vertical movement and a total movement, which is the sum of the two. The swelling vertical movement is the figure to be compared to the PVR.

Table 33. Subgrade Movements Compared with PVR (TEX-124-E) for the Pavement with No Treatment, Fort Worth North Loop IH 820.

Case Study Location	Pavement Location	Swelling (inches)	Shrinkage (inches)	Total (inches)	PVR (inches)
Cross Section A	Edge	0.07	1.39	1.46	2.22
	Outer Wheel Path	0.03	0.58	0.61	1.87
Cross Section B	Edge	3.19	1.49	4.68	3.07
	Outer Wheel Path	1.23	0.57	1.80	2.39
Cross Section C	Edge	2.58	1.33	3.91	2.38
	Outer Wheel Path	1.07	0.55	1.62	1.70

The swelling that is expected in Cross Section A is very small because of the moist condition of the embankment, but the expected shrinkage is very large. The new method shows that not much additional swelling is to be expected in Cross Section A, but a large amount of shrinkage is expected. The shrinkage figure is important because it is an indicator of future longitudinal shrinkage cracking along the edge of the pavement. The PVR for the same section is roughly in the same range as the total movement predicted by the new method, but it is considerably larger than the swelling that is predicted. The movement beneath the outer wheel path reflects the effect of the weight of the pavement in the case of the PVR calculation but also indicates the added effect of the diffusion of moisture from the edge of the pavement in the case

of the new method predictions. The new method expects to have less movement beneath the outer wheel path than does the PVR method.

In Cross Section B, the swelling expected at the edge of the pavement using the new method is fairly close to the calculated PVR. However, the total movement is larger than the PVR because it includes the expected shrinkage. Once more, the movement beneath the outer wheel path predicted by the new method is less than is expected by the PVR method.

In Cross Section C, the new method predicts a swelling that is roughly equal to that of the PVR at the edge of the pavement. The addition of the shrinkage makes the total movement expected by the new method considerably larger than the PVR. The weight of the pavement makes the PVR about equal to the new method total movement beneath the outer wheel path.

In all three cross sections, the new method predicted about the same amount of vertical shrinkage movement beneath the outer wheel path, indicating that longitudinal shrinkage cracks can be expected along the edge of the pavement in all of the cross sections. This shrinkage can be reduced by controlling the moisture influx and efflux beneath the edge of the pavement with the use of a vertical moisture barrier or wide paved shoulder.

ATLANTA DISTRICT US 271 CASE STUDY

The subgrade soil beneath the pavement at the Atlanta District case study site was not very expansive but there were trees growing within the right of way along the entire length of the case study site. The trees had extracted moisture from beneath the pavement and had caused a considerable amount of longitudinal shrinkage cracks. In the boring log taken beside the pavement in the roadside ditch, root fibers were logged at a depth of 13 ft. The predicted movements using the new method showed that more shrinkage should be expected at this site than at the Fort Worth site, which had even more expansive subgrade soil. So the longitudinal cracking that was observed at this case study site could have been expected using the new method. The calculated vertical movements by the new method and the PVR method are shown in Table 34.

Table 34. Subgrade Movements Compared with PVR (TEX-124-E) for the Pavement with No Treatment, Atlanta District, US 271.

Case Study Location	Pavement Location	Swelling (inches)	Shrinkage (inches)	Total (inches)	PVR (inches)
US 271	Edge	0.68	1.04	1.72	1.62
	Outer Wheel Path	0.53	0.81	1.34	1.16

The table shows that the PVR predicts more swelling than is expected by the new method both at the edge of the pavement and beneath the outer wheel path. The total movement is close to the calculated PVR. The presence of a tree root zone to a depth of 13 ft in close proximity to the edge of the pavement is what accounts for the vertical shrinkage movement predicted by the new method being larger than the predicted swelling. Once more, as in the Fort Worth District case studies, the swelling predicted by the new method beneath the outer wheel path are smaller than the PVR, which accounts for the weight of the pavement.

AUSTIN DISTRICT LOOP 1 CASE STUDY

The case study site in the Austin District was a sloping site in which the main lanes of Loop 1 were at a higher elevation than the frontage road. The frontage road had been overlaid several times to correct for the expansive clay roughness that had developed over time. There was a deep, grass-covered median between the main lanes.

The calculated PVR is greater than the swelling vertical movement predicted by the new method, but the total movement, which includes the shrinkage movement, is nearly the same as the PVR. Because the same composite boring profile was used in computing the movements beside and beneath the main lanes and the frontage road, the movements predicted by both methods are the same for both cross sections. The calculated movements are shown in Table 35.

Table 35. Subgrade Movements Compared with PVR (TEX-124-E) for the Pavement with No Treatment, Austin District, Loop 1.

Case Study Location	Pavement Location	Swelling (inches)	Shrinkage (inches)	Total (inches)	PVR (inches)
Main Lanes	Edge	2.03	0.98	3.01	2.97
	Outer Wheel Path	1.42	0.68	2.10	2.37
Frontage Road	Edge	2.03	0.98	3.01	2.97
	Outer Wheel Path	1.42	0.68	2.10	2.37

While the total movement predicted by the new method is nearly equal to the calculated PVR, the predicted swelling is only two-thirds of the total amount both at the edge of the pavement and beneath the outer wheel path for both the main lanes and the frontage road.

PAVEMENT TREATMENTS WITH ACCEPTABLE PREDICTED PERFORMANCE

Chapter 6 shows the results of the application of a number of alternative treatments to each of the six cross sections in the case studies. These alternatives included different pavement layer thickness, vertical moisture barriers, lime-treated subgrade layers, and removal and replacing of subgrade with a layer of a more inert soil. The design program WinPRES allows the designer to try a wide variety of alternative treatments to see which ones can provide acceptable performance at a reasonable cost and construction effort. Some of these alternatives work better than others as can be seen in each of the figures in Chapter 6. In this chapter, which compares the predicted results using the new method with the PVR method, it is important to compare the predicted movements at the edge of the pavement and beneath the outer wheel path for both the PVR method and the new method to determine whether and to what extent the PVR criterion of 1 inch is conservative. The pavement treatments in Table 36 do not represent current practice but instead were those found in chapter 6 to provide minimally acceptable predicted performance for a period of 30 years. Both flexible and rigid pavements are shown in that table. The criterion that was used in selecting these minimally acceptable treatments was for the pavement riding quality to remain above a PSI of 2.5 for the entire 30-year period without requiring any rehabilitation such as overlaying. This performance was to be maintained at a reliability level of 90 percent for the flexible pavements and 95 percent for the rigid pavements.

Table 36 shows the treatments that were found in the design case studies to provide minimally acceptable performance at the required level of reliability. A review of the relevant figures in Chapter 6 will reveal how these treatments were selected. The predicted movements by the new method and by the PVR both at the edge of the pavement and beneath the outer wheel path will be compared for the purpose of evaluating whether the PVR design criterion is too conservative.

Table 36. Pavement Treatments with Acceptable Predicted Performance.

Case Study Site	Case Study Location	Type of Pavement	Design Reliability	Treatment for Acceptable Performance*
Fort Worth North Loop IH 820	Cross Section A	Flexible Rigid	90 % 95 %	ACP 4.0 in, LTS 2.5 ft CRCP 12.0 in
	Cross Section B	Flexible Rigid	90 % 95 %	ACP 5.0 in, LTS 2.5 ft, Inert 1.5 ft CRCP 12.0 in, LTS 8 in
	Cross Section C	Flexible Rigid	90 % 95 %	ACP 4.5 in, LTS 2.5 ft, Inert 1.0 ft CRCP 12.0 in, LTS 1.5 ft
Atlanta District US 271		Flexible Rigid	90 % 95 %	ACP 4.0 in, LTS 2.2 ft CRCP 10.5 in
Austin District Loop 1	Main Lanes	Flexible Rigid	90 % 95 %	ACP 4.0 in, LTS 2.8 ft CRCP 12.0 in, LTS 2.0 ft
	Frontage Road	Flexible Rigid	90 % 95 %	ACP 4.0 in, LTS 2.0 ft, Inert 2.5 ft CRCP 11.0 in

* LTS–Lime-Treated Subgrade; ACP–Asphalt Concrete Pavement;
CRCP–Continuously Reinforced Concrete Pavement; Inert–Inert Soil Layer.

The title of this project was "Re-evaluate Current Potential Vertical Rise (PVR) Design Procedures". The objective of this study was not to duplicate the design practice commonly used in the districts in which the case studies were conducted. Instead, it was to develop a way of objectively comparing the new method of design accounting for expansive clay roughness with the previously used PVR method. Finding a pavement design that provided minimally acceptable riding quality over thirty year period with a high level of reliability and a realistic traffic estimate was the first step in the comparison. The second step was to find the PVR that such a pavement would produce and then determine whether the PVR-design criterion would be met with this pavement.

SUBGRADE MOVEMENTS FOR ACCEPTABLE PERFORMANCE: FORT WORTH NORTH LOOP IH 820

Table 37 shows the results of the design calculations in the three case studies along the IH 820 route in the Fort Worth District. The table shows for each of the cross sections, A, B, and C, which of the treatments provided the minimally acceptable predicted performance for both flexible and rigid pavements. The next three columns show how much swelling and shrinkage and total movement was calculated at the edge of the pavement using the new method. The next column gives the amount of total movement that is expected beneath the outer wheel path using the new method. The amount of upward and downward movements that add up to this total are in the same proportion as with the movements at the edge of the pavement. The next two columns

give the calculated values of the PVR both at the edge of the pavement and beneath the outer wheel path. Because the PVR is a calculated amount of swelling, the values in these columns should be compared only with the swelling movements that are calculated with the new method.

Table 37. Subgrade Movements Compared with PVR (TEX-124-E) for the Pavement Design with Acceptable Predicted Performance, Fort Worth North Loop IH 820.

Case Study Location	Type of Pavement	Acceptable Pavement Design*	Movements at the Edge of Pavement (in)			Movements in Outer Wheel Path (in)	PVR (in)	
			Swelling	Shrinkage	Total	Total	Edge	Outer+
Cross Section A	Flexible	ACP 4.0 in LTS 2.5 ft	0.02	1.16	1.19	0.46	1.77	1.62
	Rigid	CRCP 12.0 in	0.07	1.39	1.46	0.61	2.22	1.87
Cross Section B	Flexible	ACP 5.0 in LTS 2.5 ft Inert 1.5 ft	0.90	0.77	1.67	0.70	2.02	1.55
	Rigid	CRCP 12.0 in LTS 8.0 in	2.29	1.33	3.62	1.44	2.69	2.06
Cross Section C	Flexible	ACP 4.5 in LTS 2.5 ft Inert 1.0 ft	0.96	0.74	1.70	0.70	1.19	0.95
	Rigid	CRCP 12.0 in LTS 1.5 ft	1.90	1.21	3.11	1.29	1.99	1.64

* LTS–Lime-Treated Subgrade; ACP–Asphalt Concrete Pavement; CRCP–Continuously Reinforced Concrete Pavement; Inert–Inert Soil Layer.
+ Outer Wheel Path.

Cross Section A was unusually wet and the calculated swelling using the new method was small, less than 0.1 inch, at the edge of the pavement. By way of contrast, the PVR values at the same location were 1.77 and 2.22 inches beneath the flexible and rigid pavements, respectively. In this case, the PVR greatly overpredicts the expected amount of swelling movement. A similar imbalance is seen between the expected swelling beneath the outer wheel path as calculated by the new method and by the PVR method. This imbalance would normally lead to the selection by the designer of an overly conservative treatment to restrain the development of roughness due to expansive clay. Instead, the new method alerts the designer that shrinkage, and not swelling, will be the major problem at this cross section. This will result in longitudinal cracking at the edge of the pavement and possibly in some transverse and random cracking in the pavement surface.

Cross Section B has a more typical moisture distribution in the embankment materials beneath the pavement. The new method shows that much larger movements, both swelling and shrinking, may be tolerated by the rigid pavement than by the flexible pavement that produces the minimally acceptable predicted performance. The expected total movements beneath the

outer wheel paths are 0.70 and 1.44 inches in the flexible and rigid pavements, respectively. The corresponding swelling movements calculated by the PVR method are 1.55 and 2.06 inches beneath the outer wheel path in the flexible and rigid pavements, respectively. Both of these are greater than the 1-inch criterion that is presently used for the design of interstate highway pavements on expansive clay. As with the previous section, the PVR method overpredicts the amount of swelling in the outer wheel path and would lead to an overly conservative treatment to restrain the development of roughness due to expansive clay.

Cross Section C is nearly at grade and has a moisture level that is similar to that of Cross Section B. The new method calculates expected movements at the edge of the pavement that are larger than the calculated value of the PVR. In this case, however, the values of the swelling movement calculated with the new method are close to the calculated values of the PVR at the edge of the pavement. The total movements of the subgrade beneath the outer wheel paths are 0.70 and 1.29 inches in the flexible and rigid pavements, respectively, while the amounts of swelling predicted by the PVR method are 0.95 and 1.64 inches beneath the same outer wheel paths. Although the flexible pavement treatment meets the 1-inch PVR criterion, the rigid pavement treatment does not and would require a more conservative treatment. In both cases, the PVR, a calculated amount of swelling movement, overpredicts the total movement that is calculated by the new method.

In each of the three cross sections, the PVR, which is a calculated vertical swelling movement, overpredicts the amount of total movement beneath the outer wheel path, which includes both swelling and shrinkage movements. A substantial amount of shrinkage movement, as is the case with all three cross sections, is a warning to the designer that some provision must be made to retain moisture beneath the pavement by use of a wider shoulder or a vertical moisture barrier in order to avoid longitudinal shrinkage cracking from reflecting through to the pavement surface. The treatments that are compared in this table are those that would work well on this site, providing an acceptable predicted performance with at least a 90 percent level of reliability. The use of the PVR method in choosing a treatment of these pavements to restrain the development of roughness due to expansive clay will prove to be more conservative than these.

SUBGRADE MOVEMENTS FOR ACCEPTABLE PERFORMANCE: ATLANTA DISTRICT, US 271

Table 38 shows the movements at the edge of the pavement and beneath the outer wheel path as calculated by both the new method and the PVR method. The Atlanta case study site is in northeast Texas in a wet climate where trees are growing along the roadside within the right of way. Because of these site conditions, a certain amount of shrinkage is expected and is predicted by the new method. Root fibers were logged at a depth of 13 ft in the boring taken in the roadside ditch. The soil is not particularly expansive but the presence of the tree roots so close to the paved surface leads to the expectation that shrinkage cracking will be found in both the shoulder and the traveled lanes. Photographs of this site revealed longitudinal cracks along the edge of the pavement, as expected.

Table 38. Subgrade Movements Compared with PVR (TEX-124-E) for the Pavement Design with Acceptable Predicted Performance, Atlanta District, US 271.

Case Study Location	Type of Pavement	Acceptable Pavement Design*	Movements at the Edge of Pavement (in)			Movements in Outer Wheel Path (in)	PVR (in)	
			Swelling	Shrinkage	Total	Total	Edge	Outer+
US 271	Flexible	ACP 4.0 in LTS 2.2 ft	0.30	0.97	1.27	1.02	1.21	0.91
	Rigid	CRCP 10.5 in	0.58	1.03	1.61	1.26	1.62	1.16

* LTS–Lime-Treated Subgrade; ACP–Asphalt Concrete Pavement; CRCP–Continuously Reinforced Concrete Pavement; Inert–Inert Soil Layer.
+ Outer Wheel Path.

The swelling movements calculated at the edge of the pavement by the new method were 0.30 and 0.58 inch for the flexible and rigid pavements, respectively. As a contrast, the swelling movements calculated by the PVR method were 1.21 and 1.62 inches, respectively, for the same pavements. The vertical shrinkage movements at the pavement edge were calculated to be 0.97 and 1.03 inches, respectively, indicating that much more shrinkage can be expected at this cross section than heaving. The total movements beneath the outer wheel paths were 1.02 and 1.26 inches beneath the flexible and rigid pavements, respectively. These total movements compare well with the calculated swelling movement using the PVR method at the same location. However, these PVR movements are swelling, which are not expected to be the major problem at this location. The flexible pavement treatment meets the 1-inch PVR criterion beneath the outer wheel path but the rigid pavement treatment does not. The presence of the trees drawing moisture from beneath the pavement and shoulder makes the shrinkage much more than it would be if the tree were not present. In the absence of the tree, the total movements that would be

predicted by the new method would be less than 1 inch. With this level of predicted shrinkage, the designer is alerted to the fact that the pavement surface must be protected from the reflection of shrinkage cracks in the subgrade due to the drying influences of the trees. The PVR criterion of 1 inch will require a more conservative treatment beneath the concrete pavement than the one that is predicted to provide acceptable performance at a level of reliability of 95 percent.

SUBGRADE MOVEMENTS FOR ACCEPTABLE PERFORMANCE: AUSTIN DISTRICT, LOOP 1

Table 39 shows the movements that were calculated beneath the edge and outer wheel paths for both flexible and rigid pavements and for both the main lanes and the frontage road along the southbound Loop 1, the MoPac Freeway in Austin. This is a sloping site that is underlain by a sloping bed of limestone. A creek travels parallel to the frontage road and at about a 40 ft lower elevation. The main lanes are about 20 ft higher than the frontage road and there is a deep grass-covered median between the northbound and southbound main lanes. There has been a considerable amount of differential movement along the frontage road, which has been corrected periodically by a sequence of asphalt concrete overlays. The subgrade soil is a moderately active expansive clay. The table shows the amounts of movement that are expected in the future starting from its current condition, and the treatments that will provide for an acceptable predicted performance at a 90 percent level of reliability for the flexible pavement and at a 95 percent level of reliability for the rigid pavement.

Table 39. Subgrade Movements Compared with PVR (TEX-124-E) for the Pavement Design with Minimum Acceptable Predicted Performance, Austin, Loop 1.

Case Study Location	Type of Pavement	Acceptable Pavement Design*	Movements at the Edge of Pavement (in)			Movements in Outer Wheel Path (in)	PVR (in)	
			Swelling	Shrinkage	Total	Total	Edge	Outer+
Main Lanes	Flexible	ACP 4.0 in LTS 2.8 ft	0.78	0.66	1.44	0.93	2.40	1.93
	Rigid	CRCP 12.0 in LTS 2.0 ft	1.03	0.76	1.79	1.19	2.54	2.10
Frontage Road	Flexible	ACP 4.0 in LTS 2.0 ft Inert 2.5 ft	0.71	0.54	1.25	0.93	2.08	1.76
	Rigid	CRCP 11.0 in	2.03	1.00	3.03	2.28	2.97	2.37

* LTS–Lime-Treated Subgrade; ACP–Asphalt Concrete Pavement; CRCP–Continuously Reinforced Concrete Pavement; Inert–Inert Soil Layer.
+ Outer Wheel Path.

The new method shows that somewhat more swelling is expected than is shrinkage movement at the edge of the pavement. The PVR method predicts more than twice as much swelling at this site than does the new method except for the rigid pavement on the frontage road. The PVR also predicts more swelling beneath the outer wheel path than the *total* movement predicted by the new method.

Both of the total movements predicted by the new method beneath the outer wheel path of the flexible pavement are within the 1-inch criterion used with the PVR. However, none of the PVR values predicted for these acceptable treatments are within the 1-inch criterion. The PVR method would, in both the main lanes and the frontage road, require a more conservative treatment than the ones predicted by the new method to provide acceptable performance.

SUMMARY OF COMPARISONS

Vertical movements calculated by the new method, including both the swelling and shrinking, were compared with the swelling movement predicted by the PVR method for each of the six case study cross sections. Pavement treatments had been selected to provide an acceptable predicted performance at high levels of reliability, and the vertical movements were calculated both at the edges of the pavements and beneath the outer wheel paths using both the new method and the PVR method. A major purpose of the comparisons of the movements was to evaluate the PVR method in light of the new method, which was based upon many years of monitoring of pavements in several locations across Texas and careful modeling of the measured pavement roughness. Of concern was to determine from these case studies whether the 1-inch PVR criterion, which has been used by the TxDOT in the past, required treatments to restrain the development of pavement roughness due to the expansive clay that were unnecessarily conservative. The case studies included a wide variety of traffic levels, site conditions, and soil activities.

The results of the case studies are that in every case, the PVR criterion of 1-inch proved to be unnecessarily conservative. The PVR overpredicts the swelling movement that can be expected using the new method both at the edge of the pavement and beneath the outer wheel path. Furthermore, the PVR does not provide a means of anticipating subgrade shrinkage that will result in longitudinal cracking along the edge of the pavement. In addition, both transverse and random cracks may reflect upward from shrinkage cracks in the subgrade.

The design criterion of lowering the PVR to 1-inch by removing and replacing the native soil with a more inert soil is conservative to differing degrees depending largely upon how wet the subgrade soil is at the time of construction. The wetter soils will not swell much but will shrink, and the pavement resting on them will get rougher than is estimated with the 1-inch PVR criterion. Also, if the soil is drier at the time of construction, it will swell substantially unless moisture control measures such as vertical and horizontal moisture barriers and stabilized and inert layers are used to control the moisture and the subsequent development of roughness. The new method shows that these control measures are more effective than is presently anticipated by the PVR method.

The design calculations with the new method have shown a total movement beneath the outer wheel path ranging between 0.46 to 1.02 inches for flexible pavements that had acceptable performance at a reliability level of 90 percent. On the same sites, rigid pavements were predicted to have acceptable performance at a 95 percent level of reliability when the total vertical movement beneath the outer wheel path ranged between 0.61 and 2.28 inches. This leads to the conclusion that neither the swelling movement, as in the PVR method, nor the total movement, as in the new method, is a reliable indicator of likely acceptable performance. Instead, all of these case studies show that it is important to use the predicted history of the present serviceability index and the international roughness index as the proper design guideline for an acceptable treatment of the subgrade of an expansive soil.

CHAPTER 8:
SUMMARY, CONCLUSIONS, AND RECOMMENDATIONS

SUMMARY OF DEVELOPMENTS IN THIS PROJECT

This report has accomplished several important results in the course of evaluating the PVR method that is described in the TxDOT Test Method Tex-124-E. The results are in the areas of laboratory testing, development of and testing by the project panel of Beta versions of design and analysis software, and the use of these developments in case studies in three districts of TxDOT: Fort Worth, Atlanta, and Austin Districts. The case studies were based upon detailed site information, boring logs taken at each of the three sites, and sample testing that was done in the laboratories of Texas A&M University. The project has successfully determined the shortcomings of the presently used method and has made several advances that overcome these disadvantages. The results of this project, when properly implemented, will provide designers with tools that are capable of evaluating the effectiveness of a variety of treatments that may be applied to restrain the development of roughness due to expansive clay beneath highway pavements. The treatments include lime-or cement-stabilized layers, removal and replacement with inert layers, and vertical and horizontal moisture barriers. The effects of sulfate swelling are not included in either the design or the analysis software. The designer may use the design software to design either asphalt or concrete surfaced pavements at any selected level of reliability while accounting for the effects of both traffic and expansive clay subgrade activity on the development of pavement roughness. In the brief paragraphs below, each of these developments are described and summarized.

Field Investigation

In this project, borings were advanced at all sites to a depth of 20 ft. This provided sufficient information to make realistic analytical and design studies at all sites. While other sites may require deeper borings, the 20 ft depth should be considered a minimum in all future design or forensic investigations. Samples should be taken from each distinct soil layer. A detailed knowledge of site conditions is important, including the longitudinal and lateral slopes, vegetation along the roadway such as grass and trees, width of shoulder, and the characteristic weather patterns.

Laboratory Testing

The ASTM and AASHTO standard tests that were run on the soil samples were the Atterberg Limits, the percent of soil particles passing the #200 sieve, the percentage of soil particles finer than 2 microns, and unit weight. The tests to determine the suction components, both matric and total suction, were made with filter paper and are improvements on the ASTM D5298 specifications for those tests. The unsaturated diffusivity tests were made with a testing apparatus and analytical software that were designed and built at Texas A&M University. Test protocols for the suction tests and the diffusivity measurements were written in the standard TxDOT specification format, and instructional CDs were prepared to show step-by-step how the samples are prepared and the tests are done. The repeatability and accuracy of these test results are considered to be excellent. Both the analysis and design case studies relied upon the test data generated to arrive at the results that have been presented in this report.

Laboratory tests were made on samples taken from five borings on each of three cross sections on the case study site in the Fort Worth District; three borings in the Atlanta District case study site; and three borings at the case study site in the Austin District. A complete set of the laboratory test results for all three case study sites has been put onto another CD and provided to TxDOT as part of the deliverables of the project.

Pavement Design Program

A pavement design program, named WinPRES, was written in Fortran and visual Basic and used for the design case studies that are presented in this report. The program name is an acronym for Windows-based Pavement Roughness on Expansive Soils. The design program permits the designer to consider both flexible and rigid pavements, traffic expressed in 18-Kip Equivalent Single Axle Loads, and multiple layers of subgrade soil all characterized by their Atterberg Limits, the percent of soil particles passing the #200 sieve, the percentage of soil particles finer than 2 microns, and unit weight. The designer can try different treatments for restraining the roughness due to expansive clay subgrade including lime-or cement-stabilized layers, removal and replacement with a more inert soil, and vertical and horizontal moisture barriers. The designer can specify the level of reliability at which it is desired to have the predictions made by the program and can designate several different wheel paths in which to evaluate the effectiveness of the treatment. The program runs very quickly, typically presenting

the results of the calculations graphically on the monitor screen within 10 seconds after starting the computational process. Both the present serviceability index and the international roughness index are calculated in each selected wheel path for a period of 30 years. The program also calculates the expected amount of vertical swelling and shrinkage movement beneath each selected wheel path that results in the predicted performance.

A user's guide for this program was prepared and was provided to the project panel for their use in running the program and for their comments, which were very helpful and constructive. Three rounds of editorial changes were incorporated in the user's guide. A similar number of revisions were made in the design program in order to make the input and output more user-friendly and to provide more information that is useful to the designer. The present version of the program may be considered to be an advanced Beta version and to be ready for implementation and further revisions to bring it into its final version.

Transient Analysis Program

The transient analysis program was developed by making improvements on the original program FLODEF, which was developed by Derek Gay (1994)[6] in his doctoral work at Texas A&M University. The program name indicates that within the program both moisture flow and its related elastic deformation are calculated. The program is a finite element program that sequentially couples an elasticity and a diffusion computation within each time step as it marches forward in time from its initial state to its future state some 5 to 20 years later. Typical time steps are one month for moisture movement and one day for elastic displacement. The elements that are used in the program are capable of handling large strains. The program takes the same input as the design program and generates the material properties that the program uses for its computations with empirical relations with the Atterberg Limits, the percent of soil particles passing the #200 sieve, the percentage of soil particles finer than 2 microns, and unit weight that have been reported in the technical literature. The program is set up to analyze a pavement cross section including its timewise response to external influences such as typical weather patterns, drainage, trees, and grass and internal influences such as the presence of the pavement structure, stabilized layers, inert layers, vertical and horizontal moisture barriers, sloping geologic layers, and zones of different soils. A typical analysis of a 20- year period requires about 45 minutes on a desktop computer. This program is very useful to determine the effects of unusual site features

such as a high water table and an extension of an embankment as was encountered in the Fort Worth District case studies, a sloping hard layer and a median such as was encountered in the Austin District case study, and trees and roadside ditches as was encountered in the Atlanta District case study. The program is useful to verify the expected results of the treatments that are selected in the design studies. The program was revised extensively from its original form to accommodate the conditions that were encountered in the case studies. The input and output to the program were also revised extensively to make the input very simple and user-friendly and to present the graphical output in very flexible and easily understood formats.

As with the design program, a user's guide was prepared for use with this program and was furnished to each member of the project panel. This guide was proofread and commented upon extensively by the members of the panel. Their comments and suggestions proved to be very helpful and constructive. This program is considered to be an important companion to the design program. It is not expected to be used by designers as much as the design program because of its longer running time. However, it is considered to be useful in verifying the calculated results generated by the design program on alternative treatments that have been shown to be cost effective and for which a final decision must be made. The present version of the program and its user's guide may also be considered to be an advanced Beta version that is ready for implementation, further improvement, and final revisions.

Evaluation of the PVR Method

The laboratory tests and the design and finite element analyses were used together in case studies at each of three sites in the Fort Worth, Atlanta, and Austin Districts. A total of six cross sections were analyzed, and the design case studies were used as a basis for comparing the PVR method with the new method presented in this report as a basis of design of pavements on expansive clays. An assessment of the results of these design studies is contained in Chapter 7. It showed that in all cases, the PVR overpredicted the swelling movements beneath the outer wheel path and did not provide a means to alert the designer to the likely distress due to shrinkage that will occur in the same pavement. The overprediction means that the use of the PVR method will consistently lead to design treatments of the expansive clay subgrade that are overly conservative. The use of the 1-inch maximum PVR, or in fact, any vertical movement criterion is inadequate to assure the designer of acceptable performance. Instead, the design should be based

upon the expected rate of development of pavement roughness such as PSI or IRI or both over an extended time horizon at a high level of reliability. The appropriate level of reliability for design is discussed in textbooks on pavement design and is summarized in Chapter 6 of this report that presents the design program.

CONCLUSIONS

The test methods developed in this project work very well, and are repeatable, efficient, and accurate. They are easy to learn and to apply using the protocols and specifications written in the TxDOT standard specification format. The instructional CDs that have been prepared to accompany the specifications are simple to use and provide step-by-step illustrations on how to run each of the tests. The tests and the data generated are capable of being used to make accurate predictions of the field behavior of the clay subgrades.

The predicted behavior using both the analysis and the design programs matched the observed differential movements in the field in all of the case studies. The differential movements were observed as the difference in the thickness of overlays that were placed to restore riding quality and the shrinkage cracking that was observed in those pavement sections in which a substantial amount of shrinkage movement was predicted. The close correspondence of the predicted and the observed behavior shows the importance to design of not only the expansive nature of the subgrade soil, but also the initial moisture condition, the presence of roadside vegetation including grass and trees, and slopes and drainage.

Both the design and the analysis programs are user-friendly, flexible, and capable of a wide variety of design tasks. They allow the designer to consider a wide variety of treatment options: stabilized layers, inert layers, moisture barriers, drainage, roadside vegetation, local weather patterns and extremes, the effects of traffic, and asphalt and concrete pavements. These programs and their user's guides are ready to be employed in an implementation effort.

The analysis and design studies showed that the PVR method is generally too conservative. Acceptable performance can be achieved at a high level of reliability with both flexible and rigid pavements while using smaller amounts of subgrade treatment than are required by the presently used PVR criterion. The use of the predicted PSI or IRI or both is a more reliable indicator of acceptable performance and is shown in this report to be related to the total movement beneath the pavement, including both the swelling and shrinking movement,

rather than the swelling movement alone. The design program of this report uses the total movement and predicts both the PSI and the IRI in any selected wheel path and allows the designer to select the desired level of reliability. As such, it constitutes a substantial improvement in the design of pavements on expansive clay subgrades.

The soil acquisition, testing and data analysis conducted in this project also required the development of new equipment and analytical software, a process which required the full term of this project. When TxDOT implements these processes into standard practice, it is estimated that the soil testing, data analysis, and reporting can be completed in a two week period once the borings have been made and samples taken. The only soil tests that are required as input are Atterberg Limits, (–#200) sieve analysis and (–2 micron) hydrometer analysis.

RECOMMENDATIONS

The test methods, their instructional CDs, and the design and analysis programs and their user's guides are ready to be implemented in other TxDOT districts in addition to the Fort Worth, Atlanta, and Austin districts that provided the case studies of this report. The urban districts of Beaumont, Bryan, Corpus Christi, Dallas, El Paso, Houston, Pharr, San Antonio, and Waco would benefit from having training schools on the testing, analysis, and design methods developed in this project. Their experience with actual case studies in their districts and their suggestions will help to refine the test protocols, design methods, and the user's guides and provide TxDOT with sound methods for designing effective treatments of pavements on expansive soils.

There are other recommendations that have emerged from the experience of this project. One is a caution that the effect of sulfate swelling is not included in the analysis or the design method of this report. Designers in Texas are well aware of the problems that are caused by the growth of the expansive minerals that result from the combination of lime, soluble sulfates, and clay minerals in the subgrade. It is believed to be possible to represent the expansion that is a result of this crystalline growth in both of these programs but that will require further development of testing procedures, theory, and software that is capable of representing the effects accurately. At present, it should be sufficient to use these design and analysis programs as they are intended, and that is under the assumption that no sulfate swelling potential is present in the subgrade soil.

Another recommendation is related to the treatment of the stabilized layers in both of the programs. The prediction of the reduced swelling and shrinking potential of both lime-and cement-stabilized soils is based upon a limited number of laboratory tests that were run on stabilized soils that were tested in previous projects. It is recommended that the computational rules that are used in the analysis and design programs to estimate the swelling and shrinking characteristics of these soils should be verified and perhaps modified by the results of further testing.

The analysis program can be enhanced further by providing a wider variety of annual surface suction variations that are characteristic of at least each of the Texas districts instead of the nine choices that designers have in the present version. This can be done as part of an implementation project in which these programs are put to use in other districts in addition to those that have cooperated with this project effort.

A final recommendation concerns the FLODEF analysis program. The program predicts not only the vertical movement of every point of the subgrade surface beneath the pavement, but it predicts the horizontal movement, as well. This analysis program predicts both vertical and horizontal shrinkage movements, which are responsible for the shrinkage cracks that appear at the pavement surface. The program also has the capability that was programmed into it but not used in this report to generate shrinkage cracks when the stress in the subgrade exceeds the tensile strength of the soil. This leads to the recommendation that this capability should be further enhanced to predict the reflection of shrinkage cracks in the subgrade up through the pavement. In view of the importance of this type of pavement distress to maintenance and rehabilitation planning and costs, especially in areas where the subgrade is volumetrically active, this capability may prove to be a valuable addition to the pavement designer's tool box.

REFERENCES

1. Texas Department of Transportation (1999). "Method for Determining the Potential Vertical Rise, PVR," Manual of Testing Procedures, Chapter 1-Soils, Section 23, Tex-124-E, pp. 1-171 to 1-185.
2. Jayatilaka,R., Gay, D.A., Lytton, R.L.,and Wray, W.K. (1993), "Effectiveness of Controlling Pavement Roughness Due To Expansive Clays With Vertical Moisture Barriers", Texas Transportation Institute Research Report 1165-2F, May.
3. McDowell, C. (1956). "Interrelationship of Load, Volume Change, and Layer Thickness of Soils to the Behavior of Engineering Structures," Proceedings of the Highway Research Board, No. 35,754-772.
4. Lytton, R.L. (1977). "The Characterization of Expansive Soils in Engineering," Presentation at the Symposium on Water Movement and Equilibria in Swelling Soils, American Geophysical Union, San Francisco, California.
5. Mitchell, P.W. and Avalle, D.L. (1984). "A Technique to Predict Expansive Soil Movements," Proceedings, 5th International Conference on Expansive Soils, Adelaide, South Australia.
6. Gay, D.A. (1994). "Development of a Predictive Model for Pavement Roughness on Expansive Clay," Doctoral Dissertation, Texas A&M University, College Station, Texas.
7. Jayatilaka, R. (1999). "A Model to Predict Expansive Clay Roughness in Pavements with Vertical Moisture Barriers," Doctoral Dissertation, Texas A&M University, College Station, Texas.
8. Lytton, R.L. (1994) "Prediction of movement in expansive clay," Vertical and Horizontal Deformations of Foundations and Embankments, Publication No. 40, Yeung, A.T., and Felio, G.Y. ed. ASCE, New York, NY, Vol. 2, pp. 1827-1845
9. Lytton, R. (1997) "Engineering structures in expansive soils," *Keynote Address, Proceedings 3rd Intl. Symposium on Unsaturated Soils*, Rio de Janeiro, Brazil.
10. Mitchell, P.W. (1979), "The Structural Analysis of Footings on Expansive Soil" Kenneth W. G. Smith and Associates Research Report No. 1, (1st Edition), Newton, South Australia.

11. Mitchell, P. W. (1980) "The structural analysis of footings on expansive soils," Proc. 4th International Conference on Expansive Soils, ASCE, Vol. 1, pp. 438-447.
12. Covar, A.P. and Lytton, R.L. (2001). "Estimating Soil Swelling Behavior Using Soil Classification Properties," ASCE Geotechnical Special Technical Publication No. 115.
13. Covar, A.P. and Lytton, R.L. (2001). "Estimating Soil Swelling Behavior Using Soil Classification Properties," Houston National ASCE Convention, October 2001.
14. Casagrande, A. (1948). "Classification and Identification of Soils," Transactions ASCE, Volume 113, No. 2, pp 901-930.
15. Osman, M.A. and Sharief, A.M.E. (1987). "Field and Laboratory Observations of Expansive Soil Heave," Proceedings, 6th International Conference of Expansive Soils, New Delhi, India.
16. Dhowian, A., Erol, A.O., and Youssef, A. (1987). "Assessment of Oedometer Methods for Heave Prediction," Proceedings, 6th International Conference of Expansive Soils, New Delhi, India.
17. Juarez-Badillo, E. (1986). "General Theory of Consolidation for Clays," Consolidation of Soils: Testing and Evaluation, ASTM STP 892, R.N. Yong and F.C. Townsend, Eds. American Society of Testing Materials, Philadelphia, pp.137-153.
18. Juarez-Badillo, E. (1987+), "Mechanical Characterization of Mexico City Clay," Journal. Unknown (Personal Copy). pp.65-69.
19. Holtz R.D. and Kovacs W.D. (1981). An Introduction to Geotechnical Engineering, Prentice Hall, Englewood Cliffs, New Jersey.
20. McKeen, R.G. (1981). "Design of Airport Pavements on Expansive Soils," Report No. DOT/FAA-RD-81-25, Federal Aviation Administration, Washington, D.C.
21. Mojeckwu, E.C. (1979). "A Simplified Method for Identifying the Predominant Clay Mineral," Master of Science Thesis, Texas Tech University, Lubbock, Texas.
22. Mason, J.G., Ollayos, C.W., Guymo, G.L., and Berg, R.L. (1986). User's Guide for the Mathematical Model of Frost Heave and Thaw Settlement in Pavements, U.S. Army Cold Region Research and Engineering Laboratory, Hanover, New Hampshire.
23. www.dfwmaps.com
24. http://maps.e-pages.com/texas/tx_j.html
    A. (www.e-pages.com. ©2001 www.e-pages.com)

25. http://www.ci.austin.tx.us/help/austinmap.htm
26. "ASTM D4318 Test Methods for Liquid Limit, Plastic Limit, and Plasticity Index of Soils," Annual Book of ASTM Standards, Sec. 4, Vol. 04.08, Soil and Rock; American Society for Testing and Materials, 2001.
27. "ASTM D1140-00 Test Method for Amount Finer Than the No. 200 (75μm) Sieve," Annual Book of ASTM Standards, Sec. 4, Vol. 04.08, Soil and Rock; American Society for Testing and Materials, 2001.
28. "ASTM D422-63 (1998) Test Method for Particle-Size Analysis of Soils," Annual Book of ASTM Standards, Sec. 4, Vol. 04.08, Soil and Rock; American Society for Testing and Materials, 2001.
29. Mitchell, P.W. (1979). The Structural Analysis of Footings on Expansive Soils, Research Report No. 1, K.W.G. Smith and Assoc. Pty. Ltd, Newton, South Australia.
30. Bulut, R., Lytton, R.L, and Wray, W.K. (2001). "Soil Suction Measurement by Filter Paper." ASCE Geotechnical Special Technical Publication No. 115.
31. Jayatilaka, R. and Lytton, R.L. (1999) "Prediction of expansive clay roughness in pavements with vertical moisture barriers," Research Report No. FHWA/TX-98/197-28F, Texas Transportation Institute.
32. Mitchell, P.W. (1980). The Concepts Defining the Rate of Swell of Expansive Soils. Proc., Fourth International Conference on Expansive Soils, Denver, Colorado,1, ASCE, pp. 106-116.
33. AASHTO (1993). AASHTO Guide for Design of Pavement Structures. American Association of State Highway and Transportation Officials, Washington, D.C.
34. Huang, Y.H. (1993). Pavement Analysis and Design, Prentice Hall 1st Edition, pp.568-572.
35. Rajendran, D. and Lytton, R.L. (1997), "Reduction of Sulfate Swell in Expansive Clay Subgrades in the Dallas District", Texas Transportation Institute Research Report 3929-1, September.